Numerical simulation and operating strategy of a wind-powered electricity and freshwater production system

The case study of Agios Efstratios island in Greece

Angeliki-Chrysoula Pytharouliou

TUDelft

Delft University of Technology

Faculty of Mechanical, Maritime and Materials Engineering
MSc Offshore and Dredging Engineering

Numerical simulation and operating strategy of a wind-powered electricity and freshwater production system

The case study of Agios Efstratios island in Greece

By

Angeliki-Chrysoula Pytharouliou

Student Number: 5600308

in partial fulfilment to obtain the degree of

Master of Science

at the Delft University of Technology,
to be defended publicly on Tuesday, June 27, 2023.

Thesis Committee:	Dr. ir. A. Jarquin Laguna,	TU Delft, Chairman-Daily Supervisor
	MSc. F. Greco,	TU Delft, Daily Supervisor
	Dr. ir. M.B. Zaayer,	TU Delft, External Committee Member
	Dr. ir. G.H. Keetels,	TU Delft, External Committee Member

TUDelft

DOT

Acknowledgements

Having reached the end of my thesis, I would like to thank everyone who contributed to its completion. First of all, I would like to sincerely thank my university supervisor Dr. ir. Antonio Jarquin Laguna for his unwavering guidance and insightful advice. Your expertise and interest in the topic led to intriguing and beneficial discussions which brought solutions to the questions that arose. Additionally, I wish to express my gratitude to my daily supervisor, MSc. Francesca Greco, for her continuous support and assistance, valuable criticism and feedback during my bi-weekly progress meetings. Thank you both for your constant support and trust in me, which significantly affected the completion of this thesis.

Secondly, I would like to thank Roberto and Dries for their effort in explaining and guiding me through the DOT500 PRO concept. Your knowledge and work on this project provided insightful and decisive information that allowed my research to flourish. You encouraged me to express my questions and doubts without hesitation and welcomed me into the DOT family wholeheartedly. I also want to thank all personnel from DOT and DOB for rendering the Academy an excellent place to work, which encouraged my daily presence in the office to complete my research. You set the working environment standards high and I am more than thankful to have met you all!

Furthermore, I want to express my gratitude to Posidonia Exhibitions SA for granting me a scholarship through the Union of Greek Shipowners, which supported my studies at the Delft University of Technology. Without you, this journey of knowledge and experience would not have been possible and for that, I am deeply grateful.

Last, but not least, I want to sincerely thank my friends for their support during the entire length of my studies in Delft. Special thanks to my friends, with whom we decided to do this journey together, which otherwise would not have been as thrilling and enjoyable. I also want to express my gratitude to my family and especially to my parents, Niko and Anna, for their endless support and confidence in me that kept me focused on achieving my goals. Thank you from the bottom of my heart for giving me the strength to chase my dreams!

Thank you all,

Angelina Pytharouliou

Delft, June 2023

Abstract

The rapid increase in global population and rising demands have resulted in a shortage of clean water, depleting several of the Earth's reservoirs, especially those that reserve fresh water. Just 0.007% of the water on Earth is used to hydrate and feed billions of people, as determined by the water balance of the planet. Water-stressed nations are now desalinating salty ocean water to produce fresh water for use in their homes, industries, and fields. Among the processes used to produce freshwater, reverse osmosis (RO) is the most reliable technique for seawater desalination due to the high energy efficiency of the membranes and low desalination-associated costs. The major disadvantage of this technology is its high energy consumption, which is mostly derived from conventional sources like fossil fuels. Therefore, with a view to a sustainable future, renewable energy sources must be integrated to power the reverse osmosis systems.

All conventional wind systems convert mechanical energy into electricity, which is used to power the desalination units. Delft Offshore Turbine (DOT) aims to replace the conventional drivetrain with a hydraulic transmission system that uses seawater as a hydraulic transfer medium. The examined DOT500 PRO system consists of a wind turbine connected to a hydraulic positive displacement pump, which induces seawater flow under high pressure. A reverse osmosis unit can be used to desalinate saltwater using this high-pressure flow and a Pelton turbine generator can be used to produce electricity. The long-term objective of the DOT project is to lower complexity, mass, maintenance, and capital expense to make offshore wind a competitive source of electricity. To further reinforce the concept's techno-economic components, the future strategy calls for the centralized production of electricity.

This study aims to develop an operating strategy for the DOT500 PRO system for freshwater production at an offshore location. The viability of using such a system in a place with offshore wind conditions and predetermined freshwater demand was investigated using a constant operating scheme of a single spear valve. A numerical model is developed in Python to deliver the appropriate desalination unit size under offshore wind conditions in order to cover the water requirements of a given location. The model is applied to a case study of Agios Efstratios in Greece and can be used as a tool to investigate possible applications using the associated datasets. This research has yielded the following results:

1. A simple and robust system operating strategy for maximum water production that will ensure stable turbine function, while active control is used to maintain the system at constant operation when its limits are reached.

2. The direct influence of the spear valve position and reverse osmosis unit size on the system's rated conditions and a reduced rated wind speed by 21.3% from the one utilized conventionally on the reference wind turbine.

3. The minimum required number of RO pressure vessels and membranes according to site-specific offshore wind profile and freshwater demand, as well as options for reducing the RO unit size.

Table of Contents

Nomenclature

Abbreviations

Abbreviation	Definition
DOT	Delft Offshore Turbine
DUWIND	Delft University Wind Energy Research Institute
ERD	Energy Recovery Device
IDA	International Desalination Association
L	Leakage
LCOE	Levelized Cost of Electricity
LCOW	Levelized Cost of Water
MD	Membrane Distillation
NF	Nanofiltration
OF	Overflush
PRO	Pilot Reverse Osmosis
PX	Pressure Exchanger
RO	Reverse Osmosis
RPM	Round Per Minute
SWRO	Sea Water Reverse Osmosis
VM	Volumetric Mixing

Symbols

Symbol	Definition	Unit
α	Terrain roughness exponent of the power law	[-]
γ	Recovery rate	[-]
$\Delta\pi$	Osmotic pressure difference	[Pa]
Δp	Pressure difference	[Pa]
δ	Gas constant	[J/mol·K]
λ	Tip speed ratio	[-]

η	Efficiency	[-]
ρ	Density	[kg/m^3]
τ_P, τ_{HPP}	Torque on different system components	[Nm]
ω	Rotational speed	[rad/s]
A	Effective area	[mm^2]
C_d	Discharge coefficient	[-]
$C_{f,p,c,eff}$	Salt concentration	[ppm]
C_τ	Torque coefficient	[-]
C_P	Power coefficient	[-]
D	Diameter	[mm]
G	Gearbox ratio	[-]
J_w	Water flux	[kg/m^2·s]
K_w	Permeability coefficient	[s/m]
k	Runner speed-jet ratio	[-]
n	Number of ions in the fluid	[-]
M	Molarity of fluid	[g/mol]
P	Power	[W]
p	Pressure	[Pa]
Q	Flow rate	[m^3/s or l/min]
R_r	Rotor radius	[m]
R	Rejection rate	[-]
s	Spear valve opening	[mm]
T	Temperature	[Kelvin]
$U, \overline{U}_w$	Wind speed	[m/s]
U_{jet}	Water jet velocity	[m/s]
V	Volumetric displacement	[m^3/rad or l/rev]

List of Figures

List of Tables

Chapter 1

Introduction

The purpose of this Chapter is to introduce the problem that this thesis is going to address. Background information on the problem is stated, followed by the system that is going to be examined and the problem description. Finally, the objective of the project, research question and proposed methodology will be described.

1.1. Background on Desalination

The higher living standards and the significant rise in global population, industry and agriculture have increased water consumption per capita, which has resulted in a decline in high-quality freshwater resources. Freshwater makes up a very small fraction of the water available on the planet. Nearly 70% of the world is covered by water, from which only 2.5% is highly pure usable water while the rest is saline and ocean based. Of the usable water, just 1% is easily accessible, with much of it trapped in glaciers and snowfields. Therefore, only 0.007% of the Earth's water is available to fuel and feed billions of people [1]. Statistical forecasts have predicted that by 2050, more than half of the global population (57%) will live in areas that experience water scarcity for at least one month per year [2]. The challenge is to ensure that this critical point will not be reached.

Seawater desalination is a very effective technology that has gained popularity over the past few decades. It refers to a process that removes dissolved salts and minerals from seawater or brackish water, providing adequate freshwater quality for human consumption. According to the International Desalination Association (IDA), more than 20,000 desalination plants are installed worldwide, with a total capacity of around 130 million m^3 of freshwater daily [3]. The coasts of the Mediterranean Sea hold most of the desalination plants of Europe, due to better proximity to seawater abundance. Desalinated water is used by more than 300 million people worldwide to meet all of their daily needs [3]. This is mostly due to the limited supply of renewable freshwater resources, rapid population and economic expansion and significant lifestyle changes.

Among the processes used to produce freshwater, reverse osmosis is the most reliable technique for seawater desalination due to the high energy efficiency of the membranes and low desalination-associated costs [4]. However, its negative aspect is the high energy consumption compared to other technologies like filtration, sedimentation and distillation. While the energy use of conventional treatments for surface water ranges between 0.2 and 0.4 kWh per cubic meter of produced water, the theoretical specific energy consumption for a seawater reverse osmosis plant is approximately 3.5-4.5 kWh/m^3 [5]. This energy consumption includes the electricity requirements of the associated pre-treatment and post-treatment processes. According to a case study performed in Turkey [6], it was estimated that electricity consumption cost constitutes a total of 69% of the operating costs of a reverse osmosis unit. Currently, due to the low fuel costs, most of these plants use fossil fuels as their main

power source, thus emitting air pollutants and negatively contributing to climate change. The state-of-the-art desalination plants emit between 1.4 and 1.8 kg of CO_2 per cubic meter of produced water [7].

One of the key operating characteristics of reverse osmosis is the high feed flow pressure requirement at the inlet of the unit, which makes this desalination technique an energy-intensive process. The energy that is lost can be recovered from the concentrate flow (high salinity water, brine), which can be directed to a pressure exchanger (energy recovery device, ERD) to transfer its energy to low-pressure pumped seawater. The use of an ERD can significantly increase the efficiency of the desalination process.

1.1.1. Desalination Using Renewable Energy Sources

Over the last few years, the research on integrating renewable energy sources into desalination processes has significantly increased. Most nations with limited access to freshwater resources, such as those in the Middle East or Africa, have a considerable quantity of renewable energy resources. Several solar-powered small-scale desalination facilities have been installed, mostly in isolated and off-grid locations. Unfortunately, technological and economic barriers, such as the lack of skilled personnel and technological constraints make scaling up to large operations difficult.

Several renewable energy technologies have been investigated and assessed for their possible integration into desalination [8]. According to Mathioulakis et al. [8], several challenges have to be overcome for a full acceptance of renewable energy-powered desalination plants. Some of them include the intermittency of renewable energy sources, the energy storage availability and the control strategy for the operation and integration of the existing desalination methods with the energy technologies. Wind power is an interesting option for seawater desalination, especially for coastal areas with a significant availability of wind energy resources. The constantly growing wind farms have the potential to produce freshwater at a reasonable cost [8]. This technology is conventionally used to convert wind energy into electrical energy, which is then transferred and used to power desalination plants. This may lead to low efficiencies due to energy losses during conversion and transmission, while the system is less reliable since it requires more components to function [8].

Due to the requirement for high pressures to desalinate seawater, reverse osmosis has significant energy consumption. Energy recovery devices, or ERDs, are used to extract energy from the concentrate stream to increase the efficiency of the desalination process and to obtain high-pressure conditions. According to Moreno et al. [9], if a direct connection of a desalination plant with renewable energy can be accomplished, initial costs will significantly drop and the system as a whole will become more straightforward and feasible.

1.1.2. Wind-driven Desalination

All conventional wind systems convert mechanical energy to electricity, which is used to power the desalination units. In order to remove the intermediate conversion components and reduce the transportation-related losses, the electrical conversion step can be eliminated. This translates into a system of a wind turbine, mechanically and hydraulically connected to the desalination reverse osmosis plant [10].

The Delft Offshore Turbine (DOT), which was established in 2008 as a research project of TU Delft, utilizes the direct-driven wind power desalination concept. The long-term objective of the DOT project is to lower complexity, mass, maintenance and capital expense in order to make offshore wind a competitive source of electricity. The main idea of the project was to replace the conventional drivetrain

with a hydraulic transmission system that uses seawater as a hydraulic transfer medium [11]. The wind turbine drives a hydraulic pump that feeds pressurized seawater to a centralized hydraulic turbine combined with a generator. A subsequent adjustment to the system allowed for water production by connecting a reverse osmosis module in parallel to the electricity production unit. When the system is used to prioritize freshwater production, the energy that is not utilized by the reverse osmosis unit and is available in the system can be used to drive a Pelton turbine and generate electricity.

Figure 1-1: The conventional configuration of a drive-train wind turbine (left) compared to a configuration with hydraulic components (right). The advantage of mass and space reduction in the nacelle is self-evident [12]*.*

With a focus on the interaction between the hydraulic drive train and the rotor behaviour, Diepeveen et al. [13] developed this idea and thoroughly investigated the technical possibilities of putting this wind turbine concept into practice. A schematic depicted in Figure 1-2 perfectly describes the core of the concept and shows the most important components. The long-term plan is to centralize the power generation to further strengthen the techno-economic features of the concept. This would include constructing a hydroelectric power plant to which the hydraulic fluids of several DOT turbines within a wind farm would be connected to generate electricity in a centralized manner.
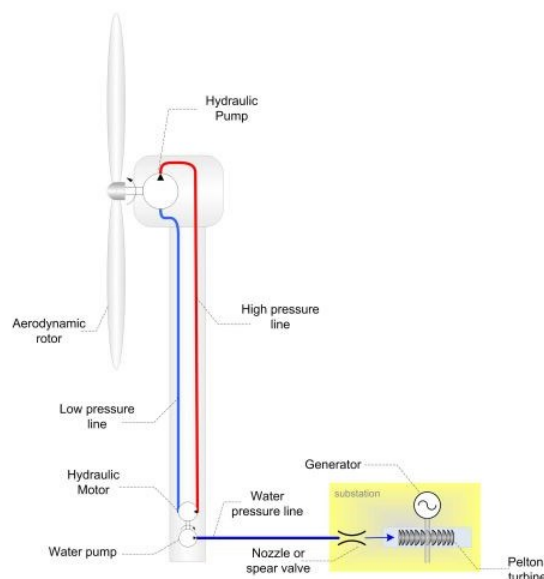
Figure 1-2: Initial hydraulic wind turbine concept [13]*.*

The components of the DOT concept have been designed and tested to define the system parameters and control. The combination of DOT with a RO unit coupled with a pressure exchanger and a Pelton turbine has been under research in order to define the controllability of the system for either maximum water production or maximum electricity generation [14]. The behaviour of the system under variable conditions of pressures and flows is known in order to set the constraints of the components. The most recent development of the system is the utilization of the nozzle of a spear valve as the only control action for system optimization [14].

1.2. Freshwater Demand in the Aegean Sea

The world's greenhouse emissions have significantly increased over the years due to the ongoing use of fossil fuels, having a negative effect on the climate. Climate change is causing more frequent extreme weather events, such as droughts, while the increase in population, agriculture and tourism impose the problem of freshwater scarcity. According to the latest statistics, about one in five people in the Mediterranean region suffer from freshwater shortage [15]. Water scarcity as a consequence of climate change poses a huge challenge for the whole world, but especially for islands and remote areas. Islands that lack freshwater resources depend on desalination plants or tanker ships to transport their water. Hence, the prices of electricity and transportation are the deciding factors for the cost of fresh water. Both options for supplying water to islands require fossil fuels, which is a power source that must be replaced.

This thesis is going to focus on the water scarcity of Greek islands, which exceed 2,500 in the Aegean Archipelagos, with only 7% of them being inhabited [16]. Due to the semi-arid climate, the freshwater shortage is a significant problem for both domestic and agricultural use for the vast majority of small and medium-sized islands in the Aegean Sea. Groundwater pollution is also an issue due to the increasing use of fertilizers or seawater intrusion, thus making the groundwater inappropriate for human consumption [17]. During the summer season, the average water demand compared to the winter demand doubles and, in some cases, triples due to blooming tourism.

One of the most important concerns regarding the water problem in Greek islands is the questionable quality of transportation of water from the mainland with tanker vessels. This problem, set the foundation for extended research on seawater desalination techniques, with reverse osmosis being the most reliable and the one adopted in most islands in the Aegean Sea. The implementation of reverse osmosis desalination plants in some islands raised the electricity demand from an average value of 2.5 kWh/m^3 to 7.5 kWh/m^3 [18]. Due to the combined effects of transportation and increasing fuel costs, renewable energy supply systems are a very promising solution.

Almost all islands located in the Aegean Archipelagos have great potential for renewable energy sources. In this context, the integration of seawater reverse osmosis desalination techniques with renewable energy can result in lower installation and operating costs and can reduce the environmental impact of using fossil fuels. In coastal areas with high availability of wind resources, wind power is a great option for powering a reverse osmosis desalination plant [19]. To integrate these systems, an operating strategy has to be implemented to the system to match the available wind power to the electricity requirements of the desalination, due to high variability in wind speeds [20]. Currently, the conventional implementation of such a system dictates that wind resources will directly cover the electricity requirements of RO units. However, a challenge that has recently been posed concerns the use of wind power for freshwater production and not only power generation, by replacing the intermediate electrical conversion with fluid power transmission [10].

1.3. Problem Definition

With the global freshwater sources depleting, desalination techniques are gaining ever increasing popularity. However, the high energy consumption that characterises these methods leads to the necessity of integrating sustainable solutions to power the desalination plants. Reverse osmosis units are widely used due to the high energy efficiency of the membranes. The conventional connection between wind turbines and reverse osmosis units requires several energy conversions steps, which are eliminated

in the DOT500 PRO concept. Although detailed study and system modelling has been made to control the system for either water or electricity production under discrete wind speeds, a study on the system operating strategy under realistic wind speed conditions is yet to be conducted. The behaviour of the system and its operation points are yet to be examined as a function of the wind climate in combination with water and electricity demands. Moreover, one of the system's main controllers enables its regulation through the unremitting alternation of a spear valve opening. The utilization of the spear valve, however, adds to the design and operational concerns of the system. Therefore, the influence of a constant spear valve opening under realistic wind conditions on the system's pressures and flows is yet to be determined, while an operating strategy accounting for that has to be developed. On top of that, the influence of the size of the desalination unit to the rated conditions and consequently to the operation of the system with a constant spear valve opening requires investigation. A tool that will estimate the minimum required reverse osmosis unit for a specific location under the associated wind speed and water demand is yet to be examined and developed.

1.4. Thesis Objective

Following a thorough literature review on the developments of wind-driven desalination and especially on the Delft Offshore Turbine, the thesis' objective and specific research question can be defined. This will make the goal of this research clear and will assist in the research endeavours regarding direct wind-driven desalination prospects. According to previously conducted studies, the methodology that the present thesis will follow will be provided. Finally, the expected results will be described and their future applicability to the Delft Offshore Turbine concept will be discussed.

The goal of this thesis is to assist in the research regarding the possibility of producing desalinated water using a wind turbine for supplying islands. This was done by focusing on the production of freshwater using the 500 kW DOT hydraulic drivetrain integrated with a reverse osmosis unit combined with an energy recovery device and a Pelton turbine generator. The aim of this study is to investigate the behaviour of the system under realistic offshore wind data, in order to define a robust operating strategy that will allow for maximum water production, using a constant spear valve opening. A single spear valve control will be utilized in order to maintain constant operation at rated conditions, which will be established according to the defined operating scheme. A numerical model will be developed to simulate the operation of the system and to deliver the minimum required reverse osmosis unit that can cover the water needs of the examined location under site-specific offshore wind data and predefined water demand.

This model will be applied to a case study of an island in Greece that faces water shortage and can be used as a tool to investigate possible applications using the associated datasets. The appropriate size of the reverse osmosis module will be found according to site-specific wind data and predefined demand for the year 2021 for a Greek island. The island considered for this research will be Agios Efstratios, which has no desalination facility and relies only on ever-decreasing groundwater for its drinking water requirements.

1.4.1. Research Question

The main research question that characterizes the thesis project is the following:

How can the DOT500 PRO hydraulic drive train be adjusted and operated to meet a standard water demand under the influence of an offshore wind climate?

To answer the research question, five sub-questions are stated:

1. *What is a simple and robust operating scheme for the system that allows for maximum water production while ensuring stable operation?*

2. *How does the spear valve position influence the pressures and flows in the RO unit?*

3. *What is the effect of the combinations of different spear valve positions and RO sizes on the operating conditions of the system?*

4. *How can the required RO unit size and spear valve position be obtained under a predetermined water demand and an offshore wind profile?*

5. *How can the system components be adjusted in order to reduce the required number of RO pressure vessels and membranes?*

1.4.2. Methodology

In order to answer the research questions, the following steps were determined and are listed below:

1. Conduction of the literature research to acquire fundamental information on the wind-driven desalination concept and its sub-systems.

2. Determination of the operating scheme that will select the appropriate spear valve opening for the whole operation according to the wind profile of the location and the water that can be produced. The range of spear valve positions that are in stable operation and respect the limits of the sub-systems will be considered and the ideal position for the location will be found. The combination of each spear valve position with different sizes of the desalination unit will be examined to raise conclusions regarding the system behaviour under various operating conditions.

3. Developing a numerical model in Python that solves the system under varying wind speed to provide a better understanding of the influence of wind climate on the system behaviour and rated conditions. The model will take as input the hourly wind data and will provide the amount of water that can be produced daily by utilising the previously established operating strategy. The system limits that have to be considered during operation include the pressures and flow rates of the hydraulic pump and the reverse osmosis unit.

4. Performing a case study for a Greek island (Agios Efstratios) that faces water shortage, to evaluate the applicability of the system in remote areas. The numerical model will be applied to a real-case scenario with certain site conditions and water demand. The system will be tested using historical wind data, and its capacity to meet the island's water needs given its variable wind profile will be determined. Finally, the reduction in the size of the desalination unit has to be examined by simulating additional ancillary components, as possible improvements to the system.

1.4.3. Expected Results

The resulting algorithm will be used by the DOT500 PRO concept to quantify the water production capacity of the system depending on the wind climate. As wind speed will vary hourly during the simulation time of one year, the operating points of the system are expected to change in every time

step, which refers to every hour of the one-year dataset. As regards the results that the algorithm is expected to produce, water production will be assessed and compared to the fixed demand. More specifically, the model will show the optimal spear valve opening and RO size that will produce the required water amount. For every time step of the wind dataset, water production will be found and added to the daily production of the system. To account for the daily variation of wind speeds and water production, a weekly basis will be set as a comparison tool for the generated and required freshwater. More precisely, the daily production will be converted to a weekly production and will be compared with the corresponding water requirement of Agios Efstratios. Finally, the developed control strategy could serve as a tool to predict the system performance by using forecast wind time series, with a view to evaluating the potential of installation. By utilizing this tool, the appropriate reverse osmosis size can be found for the desired location based on the water demand. For a better understanding, the following diagram presents the general methodology and the anticipated outcome.

MODEL TOOL METHODOLOGY

Constant parameters
- Reference components
- Working limitations

Field data
- Offshore wind data (hourly wind speeds for a year)
- Freshwater demand

Variables
- RO unit size
- Spear valve position

INPUT

Hydraulic system
- Pressure range
- Flow rate range

SYSTEM CONSTRAINTS

RO unit
- Pressure range
- Flow rate range

STEADY-STATE MODEL

Output
- Water production
- Electricity production
- Spear valve position
- Appropriate number of RO vessels and membranes
- Size of required storage tank

Figure 1-3: Diagram of the proposed methodology for the thesis.

1.5. Thesis Outline

In order to answer the research questions, the system has to be analysed and simulated in a steady state model. The following chapters contain the required information and steps that contributed to the final conclusion.

In Chapter 2 the offshore wind prospects and water shortage in the Aegean Sea are presented, while the islands with water deficit are defined. The possibility of applying DOT500 PRO on a Greek island is discussed by analysing the associated framework set by the Greek government. Comparing the wind characteristics and drinking water demand of each island, Agios Efstratios was selected for the application of the concept. A reduction in the wind data size was conducted based on the representative annual wind speed of the last ten years.

Chapter 3 describes the DOT500 PRO concept, as well as its technical progress in terms of its hydraulic components. The initial idea and vision are stated, which are complemented by the latest system updates and theoretical research regarding the control strategies. Finally, the reference system used in this thesis is presented in detail, including the components' sizes and their characteristics and capacities.

The numerical model is extensively analysed in Chapter 4, where the interconnection of the three main sub-systems is explained. The steady-state equations used to describe and simulate the system are presented while the conversion of the aerodynamic to hydraulic behaviour is described.

Chapter 5 presents the existing control scheme, as well as the theoretical control for maximum water production. A simple and robust operating strategy is proposed to regulate the system such that it can cover the water requirements for the given location under offshore wind conditions. In Chapter 6 the behaviour of the system under the proposed strategy is presented for different operating conditions.

In Chapter 7 the developed algorithm logic is analysed in detail. The application of DOT500 PRO on Agios Efstratios is assessed while a sensitivity study is performed in terms of reducing the required RO unit by implementing additional auxiliary components. Finally, conclusions and recommendations for future research are given in Chapter 8. A schematic overview of the structure and organization of this thesis is given in Figure 1-4.

Research Scope

> **Chapter 1:**
> Background, problem
> definition and thesis objective

Literature Study

> **Chapter 2:**
> Offshore wind and water
> situation in Greek islands

> **Chapter 3:**
> The Delft Offshore Turbine

Model Simulation

> **Chapter 4:**
> System model, steady-state
> equations and algorithm setup

Operating Strategy

> **Chapter 5:**
> Current, theoretical and
> proposed operating strategy

Simulation and Application Analysis

> **Chapter 6:**
> Simulation of the model

> **Chapter 7:**
> Agios Efstratios application
> and algorithm logic

Concluding Remarks

> **Chapter 8:**
> Conclusions and
> Recommendations

Figure 1-4: Schematic of the thesis' structure in chapters.

Chapter 2

Offshore Wind and Water Demand in Greek Islands

2.1. Offshore Wind Energy in Greece

Greece is a nation with exceptional wind resources that has 4.5 GW of installed onshore wind power at the moment. Offshore wind energy with both bottom-fixed and floating technologies has enormous potential. The development of offshore wind power in Greece was outlined in a high-level strategy and new law by the Hellenic Ministry of Environment and Energy, which was approved by the Greek parliament in July 2022 [21]. Greece hopes to construct more than 2 GW offshore wind turbine farms by 2030, most of which will be floating offshore wind farms due to the characteristics of Greek seas with water depths of more than 50 meters [22]. Several decrees and available offshore wind development regions will be legally defined by the Hellenic Ministry for Environment and Energy in the upcoming months. Following that, precise installation zones within these regions will be designated, along with each zone's specific terms for offshore wind development. Other social interests, such as those related to military, fisheries, tourism and shipping routes will be consulted when defining these zones [22].
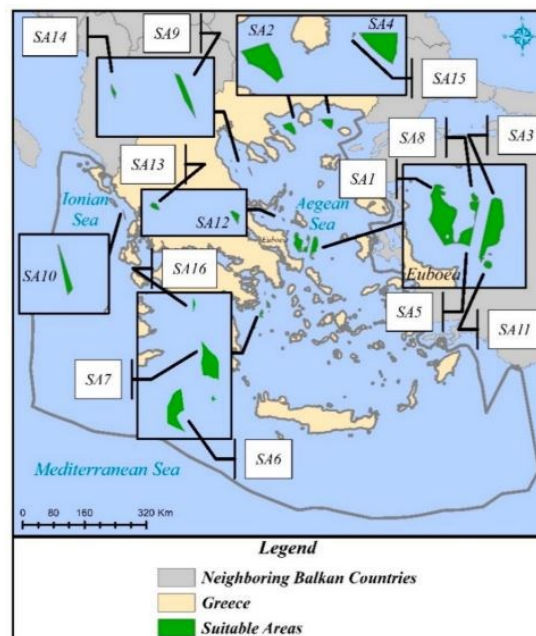
Figure 2-1: Initial planning of suitable areas for offshore wind farms in Greece [23].

Currently, the areas available for offshore wind project installations have not yet been legally defined. Figure 2-1 presents only a few of the final available areas that were defined in a preliminary stage, as they are away from major vessel routes. The Hellenic Ministry of Environment and Energy is still examining the regions that will be excluded as sensitive or shipping routes [22]. Thus, the selection of

the offshore location for the potential installation of the DOT500 PRO system will not be subject to the abovementioned limitations under evaluation but to criteria related to water shortage, wind climate and spatial conditions.

2.2. DOT Application in the Aegean Sea

2.2.1. Water Shortage in Islands

According to the most recent National Operational Plan for Drinking Water [24], the Aegean Sea is divided into the North and South Regions, for the definition of water quality and supply. The water needs of the Northern Aegean Region are mostly covered by underground water, secondarily by surface abstractions, while a small percentage of the needs is covered by desalination plants. The underground water is threatened by seawater intrusion, increased values of sulphate ions, as well as certain trace elements. The adequacy of water in the underground aquifer is significantly affected by the amount of rainfall that has been satisfactory in recent years but has become more uncertain due to climate change. Additionally, the age of the network that transports water to households has led to an increase in water transportation losses in the supply grid. However, the problem arises from the quantity of water available for human consumption rather than the quality. According to drinking water providers, the islands that will have to confront the water shortage problem soon are Agios Efstratios, Psara, Oinousses and Fourni, which are four of the smallest islands in the Northern Aegean Region.

As regards the South Aegean Region, the water demand is covered by underground wells, reservoirs, dams, desalination plants and water transport by trucks or tankers. In general, the quality of water for human consumption in the South Aegean Region is compatible with the requirements of the Hellenic Ministry of Health, while only small deviations of some indicative monitoring parameters have been reported. The main problem identified is the increased salt concentration of the region's underground water, with impacts on the available drinking water before treatment. This region has the highest number of desalination units among the other island regions, as some of the most touristic popular islands are located in the South Aegean Sea. In recent years, the problem of the islands' water supply sufficiency has worsened due to the pressure exerted by tourism, which increases the demand for water, as well as the large loss of transported water (more than 30%) in the water supply network, due to the age of the network. Finally, it should be noted that several cases of non-supply of water for human consumption have been reported. Specifically, water supply providers of the islands of Andros, Tinos and Mykonos reported the non-supply of water to about 50 communities (unserved population of up to 3,500 people in total).

According to the National Operational Plan for Drinking Water [24] that was conducted in 2022, immediate measures had to be taken to serve the needs for water adequate for human consumption in the regions of Greece. As regards the islands in North Aegean Region, a desalination unit has been constructed to serve the needs of the island of Oinousses with a capacity of 400 m^3/d, while a desalination unit with a capacity of 300 m^3/d started its operation in Fourni in 2022. It is expected that these desalination units combined with the underground water resources will be able to cover at least the permanent water demand of these islands for the near future. On the island of Agios Efstratios, there is no proposal for a desalination facility, but in Psara, the necessity for one has been emphasized for the local authorities to consider. The islands that are facing water shortage in the South Aegean Region are also included in the National Operational Plan for Drinking Water. The island of Mykonos has three desalination units that can cover up to 9000 m^3/d, while Tinos has two with a total capacity of 1500 m^3/d. However, these capacities are not enough during the touristic period that the number of residents

doubles or in some cases triples. Therefore, the operational plan has as a priority to support these needs with the construction of additional desalination plants in nine islands including Mykonos and Tinos. Moreover, in 2022, the Financial Committee of the Municipality of Andros assessed and accepted the financial offer for the supply of a portable saltwater purification and desalination unit with a minimum output of 48 m^3/h. This measure will provide a solution to the problem regarding the quality of water for human consumption that is faced in most of Andros' areas.

As can be seen, the national and local authorities are taking drastic measures to confront the water shortage problem for the islands in the Aegean Sea. The proposed projects, however, are a solution that will require additional support in the near future given the trend of increasing tourist activity in the majority of the Aegean islands. Therefore, it would be worthwhile to investigate the possibility of assisting an island with a wind-driven desalination project as it would ensure a "green" production of freshwater without relying on the island's power system. In order to select the island that will serve as the study area for the DOT PRO system installation, the characteristics of the islands have to be examined. These characteristics include the area, the number of residents, the permanent and seasonal water demand, as well as the available wind resources in the offshore area around the islands in question.

2.2.2. Island of Application

As mentioned above, seven islands on the Aegean Sea face the most severe problem regarding the water supply for human consumption (Agios Efstratios, Psara, Oinousses, Fourni, Mykonos, Tinos and Andros). Some of these islands are relatively big with a significant number of permanent residents, as well as seasonal population. The following table presents the area of the abovementioned islands and the number of permanent residents according to the latest population census.

Table 2-1: Area and population of the islands with the most significant water shortage [25], [26].

Island	Area (km2)	Permanent residents (National Census 2021)
Andros	380.0	8,883
Tinos	194.5	8,611
Mykonos	105.2	9,802
Psara	44.5	420
Agios Efstratios	43.3	257
Fourni	30.5	1,346
Oinousses	17.4	916

The selection of the island that will be examined for the potential of the DOT PRO concept installation will be conducted based on the offshore wind characteristics of each location and the supporting plans made by the government. The water demand will also be a deciding parameter as the concept will not be applied in an offshore wind farm but a single hydraulic wind turbine will serve the needs of the selected island. The wind turbine and certain system components will be scaled to meet the required water supply according to manufacturing and commercial limitations. Thus, the water demand of each island will be a major parameter in deciding the application location as the scaling constraints of the system limit the amount of water that can be produced by utilising a single hydraulic wind turbine.

The islands belonging to the South Aegean region (Andros, Tinos, Mykonos) are relatively big with a high number of residents, which almost doubles during the summer season. In the case of Mykonos,

touristic activity may triple the number of inhabitants and consequently their water demand. Therefore, for these three islands, a selection should be made on the portion of the water demand that could be covered by the DOT PRO system. This selection is dictated by the fact that only one wind turbine of 500kW will be utilised to drive the system and therefore it will not be able to fully cover the water needs of a big island. The research conducted by Greco et al. [27] concluded that the proposed system can desalinate water up to 25 m³/h at rated operating conditions, under its current configuration. This production range is not enough to adequately feed the water grid of the big islands of the South Aegean Sea.

However, it is of interest to examine whether the DOT system is capable of serving the needs of an entire island under the influence of its offshore climate by scaling the main components of its sub-systems within the allowable limits. The water demand of the island in question together with the offshore climate of the location will be the input to the model, which will find the appropriate scaling of the components to serve the required needs. Consequently, the location availability will be limited to the islands of the North Aegean Sea since their water demand is anticipated to be close to the attainable limits of the DOT500 PRO system.

Table 2-2: Water demand during winter and summer season for the islands of North Aegean Sea.

Island	Winter water demand (m³/d)	Summer water demand (m³/d)
Psara	100	400
Agios Efstratios	54	119
Fourni	306	514
Oinousses	550	850

The values for the permanent and seasonal water demand were acquired by communication with the municipalities and water services of the islands. The winter values correspond to six months between November and April, while the summer values correspond to the touristic period between May and October. The values for water demand presented in Table 2-2 were recorded for 2021.

The final selection will be made based on the offshore wind profile of the four islands of the North region. Time series of hourly wind vector components (u and v) in 10 m and 100 m were obtained from the ERA5 reanalysis for the desired offshore locations [28]. Using the rules of physics, reanalysis integrates model data with global observations to create a complete worldwide database [28]. The spatial resolution of the wind components is 0.28° × 0.28°, corresponding to a grid with sizes of around 31 km. The wind speed for each height can be calculated by:

$$U = \sqrt{u^2 + v^2}$$

<div align="right">(2.1)</div>

Where u and v correspond to the horizontal and vertical components of the wind. According to the sign of the vector components, the direction of the wind can be found for each time step of the dataset. In order to acquire the wind speed at the hub height of the DOT500 wind turbine (56 m), the power law was utilised to extrapolate the data that correspond to 10 m.

$$\bar{U}_w(z) = \bar{U}_w(z_r)\left(\frac{z}{z_r}\right)^a$$

<div align="right">(2.2)</div>

The exponent a depends on the roughness of the terrain and is typically equal to 0.14 for onshore and 0.12 for offshore locations. However, due to variations in the meteorological conditions, the power law

exponent varies over time and by assuming a constant value, the accuracy decreases [29]. Therefore, the wind speed was acquired at two different heights to estimate the power law exponent value for each time step with the following formula:

$$a = \frac{\log\left(\frac{U_{100}}{U_{10}}\right)}{\log\left(\frac{100}{10}\right)}$$

(2.3)

The values of a were obtained for the entire time series and were used in Equation (2.2). to find the hourly wind speed at hub height for the four locations. Having calculated the speed and direction of the wind, the wind roses for the islands were plotted in Figure 2-2, in order to examine the availability of the wind resource. From the wind roses, the range of available wind speeds, as well as the percentage of occurrence during the period examined can be seen. Having in mind that the rated wind speed of the wind turbine is 12 m/s, a rough estimate can be extracted from the following figure regarding the proximity of the offshore wind speeds to the rated conditions. For the island of Fourni, around 9% of the available wind is between 13.5 and 17.9 m/s. For Oinousses, 9% of the wind lies beneath the range of 12-16m/s, while in Psara 8% is between 14.2 and 18.9 m/s. Finally, 10% of the wind offshore Agios Efstratios is higher than 13m/s with a maximum of 17.4m/s
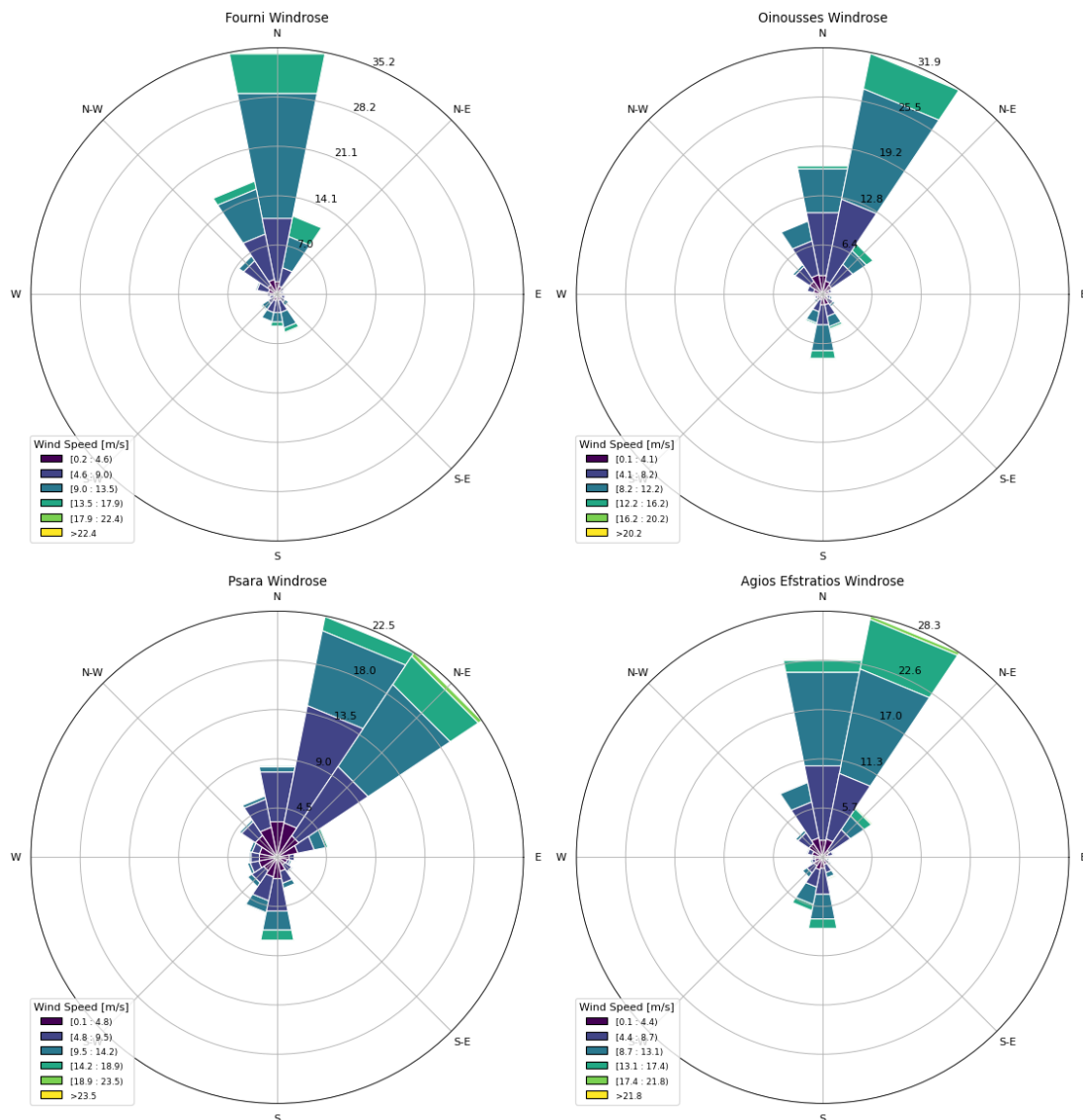
Figure 2-2: *Wind roses of the four examined islands in the Aegean Sea.*

According to a more detailed analysis, the percentage of wind speeds that exceed the cut-in and rated wind speed of the turbine were found, to establish the island that has the most potential for power and water production.

Table 2-3: Wind speed percentages above the cut-in and rated wind speeds of the DOT500 wind turbine.

Islands	Above cut-in 3 m/s [in %]	Above rated 12 m/s [in %]
Psara	84.62	15.54
Agios Efstratios	92.25	22.57
Fourni	89.35	18.58
Oinousses	87.11	9.16

As evident from Table 2-3, the turbine could extract power at all four locations for almost 90% of the year examined. The remaining 10% corresponds to wind speeds below 3 m/s, where the turbine is not producing electricity. Moreover, the island of Agios Efstratios presents the highest operating percentage within the rated region of the wind turbine. The wind percentage of occurrence can also be translated into probability function in order to be plotted and compared with the power curve of the wind turbine used in the DOT500 PRO project.
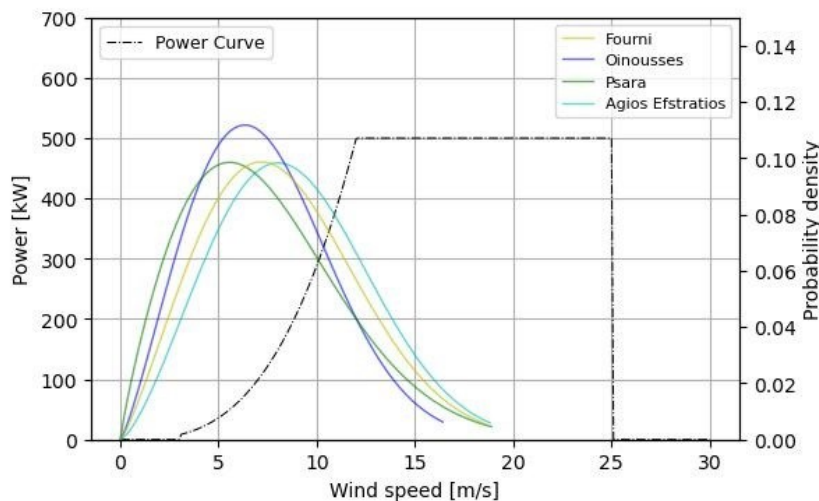
Figure 2-3: Power curve of the DOT500 PRO and probability density function of the islands' wind speeds.

As expected from the values of Table 2-3, the probability density function of Agios Efstratios island is shifted towards higher wind speeds compared to the probability density functions of the other islands. This translates into higher probabilities of occurrence of wind speeds within both the operational and rated range of the wind turbine. Therefore, Agios Efstratios island seems to be the most promising in terms of wind availability during the year.

2.3. Agios Efstratios Case

Agios Efstratios island is located in the Northern Aegean Region, and there is only one island in the immediate vicinity, allowing for the wind profile to develop around the island with no terrain obstacles (see Figure 2-4). The wind availability of the location led the Greek government set the initiative for rendering Agios Efstratios energy-autonomous. An onshore RES station, consisting of wind turbines and solar PVs, is planned for construction to meet the energy requirements of the island [30]. The application of the DOT500 PRO project in Agios Efstratios would enhance the vision for energy

transition and autonomy of the island by introducing wind-driven desalination. Hence, this would make it independent of both the energy grid and the cost of water transportation in the case of underground water shortage.
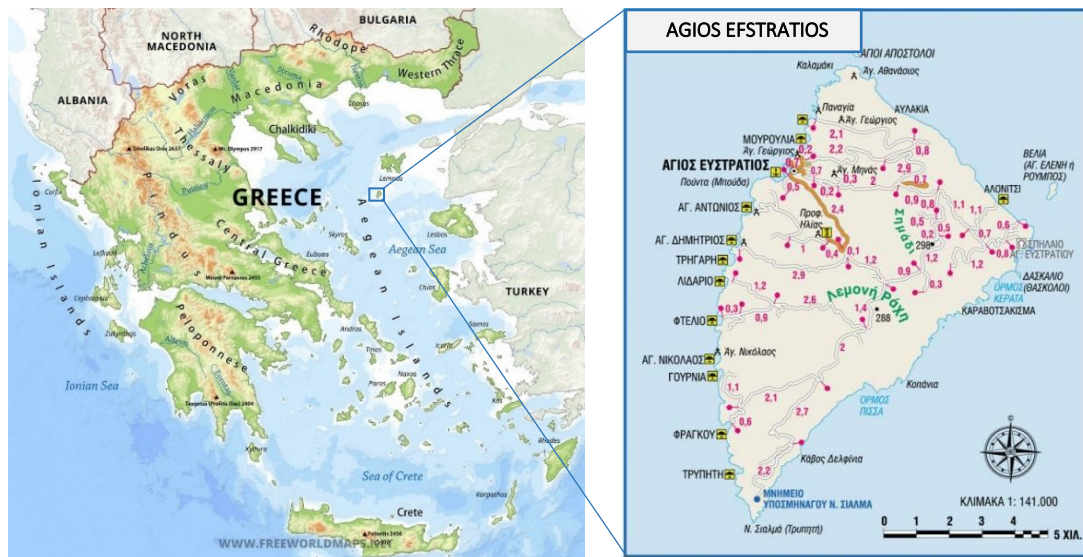
Figure 2-4: Location of the Agios Efstratios island [31],[32].

Agios Efstratios was chosen for the DOT500 PRO application based on its characteristics for offshore wind speed, water scarcity, and demand. Agios Efstratios appeared to have the highest wind resource availability of all the places initially investigated when the wind speeds over the previous ten years were compared for each site. In order to assess the possibility of applying the DOT500 PRO concept with the proposed operating strategy, the representative wind speed over ten years has to be established and used as input to the algorithm. The only limitation regarding the extent of the wind speed data used for the system size estimate is the computational time. The biggest the dataset, the slower the procedure of establishing the appropriate configuration. Therefore, a trade-off has to be made between the length and accuracy of the dataset in terms of considering the low and high fluctuations. In order to define a representative year, the yearly examination of wind speeds and comparison with the characteristics of the wind of the ten-year period is required. The time-restricted dataset that will significantly limit the computational time should still hold the attributes of the ten-year wind.

For the analysis of the wind speeds, the weekly average is established for every year, in order to ensure the preservation of the hourly wind fluctuations. Figure 2-5 presents the monthly averaged wind speeds for the years in question to provide insight into the wind resource evolution of the location. As can be seen, the wind is strongest in the summer and winter months, while the lowest wind speeds are recorded in the autumn and spring. This suggests that the system's capacity should be chosen such that the range of wind speeds may be harvested to the greatest extent feasible. However, crucial peaks impacting the system selection may be missed if the wind speeds are averaged monthly. As a result, the evaluation of the representative year will be based on both weekly and monthly wind values. The monthly average of each year is averaged further for the ten years in order to establish the trend of the data. In Figure 2-5, the black line represents the monthly average wind speed over the period in question. It is apparent that the high values found in the monthly averages of the discrete years are absent from the overall averaged wind. Consequently, the proper dataset should consider the peaks that each year presented in order to ensure that the algorithm will not overlook the high wind speeds due to fluctuations.
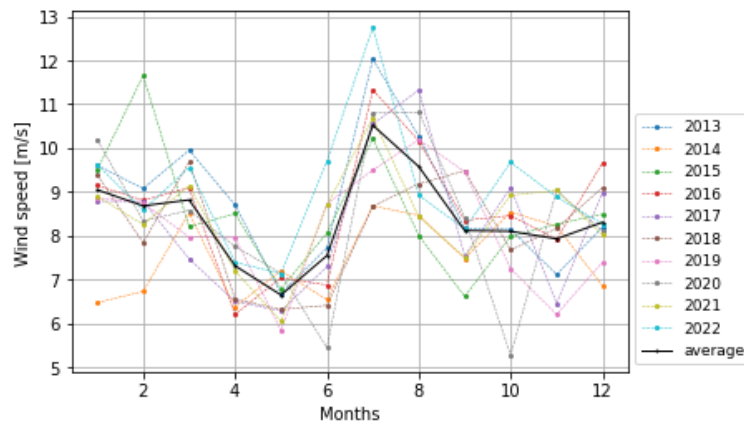
Figure 2-5: Monthly average of wind speeds for a ten-year period.

The representative year will follow the total average and preserve the weekly lowest and highest wind speeds, as shown in Figure 2-6. The maximum and minimum weekly values observed in the entire dataset will be recorded to ensure their inclusion in the representative year of wind speeds. More specifically, for the year following the total averaged trend, the weekly averages will be checked to include the highest and lowest values with short acceptable errors, as depicted in the following figure. It has to be noted that the yearly data consist of hourly wind speeds, which indicates that the system will calculate the water and power production hourly.
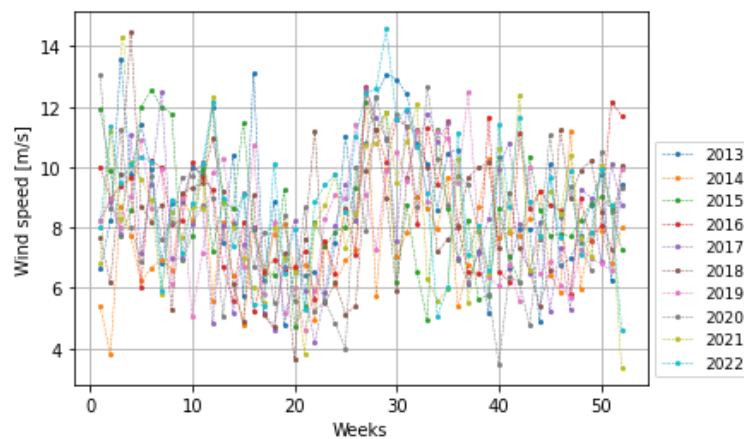
Figure 2-6: Weekly average of wind speeds for a ten-year period.

According to the evaluation of the annual winds, the monthly average wind speed of 2021 follows the total average trend with a minimum deviation. The weekly highest and lowest values of the entire period are included in the abovementioned year, rendering it adequate to represent the wind speeds of the examined ten-year period. The following table shows the abovementioned wind speeds occurring both in 2021 and the entire dataset, as well as the season in which they are observed. The season at which the highest wind speeds occur in the representative year indicates the demand to be covered, namely the winter or summer water requirements. The summer demand is the highest due to tourism seasonality; therefore, the corresponding wind speeds ought to be considered.

Table 2-4: *Highest wind speeds observed in the entire dataset compared to the values of the representative years.*

Dataset	Highest wind speed [m/s]	Season of occurrence
Total (all years)	22.80	Winter
2021	21.75	Winter
Error	4.6%	-

As seen in Table 2-4, the highest wind speeds of the representative year have a negligible deviation from the ones of the entire dataset. Additionally, as the comparative parameters were recorded during the same season, it can be deemed that the greatest values of the year 2021 will be accounted for the corresponding water demand, just as they would for the complete dataset. Consequently, the wind speed recorded in 2021 will be used to define the best combination of spear valve opening and reverse osmosis unit for Agios Efstratios island. The hourly wind data will be converted into the rotation of the high-pressure pump and then pressures and flows, specifying the hourly water production for every combination of the simulation parameters. The hourly permeate production will be translated into daily and weekly to check whether the seasonal water demand is reached.

Chapter 3

Principle of the Delft Offshore Turbine

As the capacity of offshore wind turbines is constantly increasing, all of its components have to scale up, increasing the weight of the nacelle and the support structure. This translates into additional required material and increased total cost of the wind turbine. Hydraulic drivetrain approaches have previously been investigated in an effort to reduce turbine weight, maintenance needs, complexity, and ultimately the levelized cost of energy (LCOE) for offshore wind. Various full hydraulic concepts have been developed and evaluated since 1967 when the first wind turbine with a hydrostatic power transmission was built. These concepts aimed to eliminate power electronics from the turbine for the use of a synchronous generator and utilised a mechanism to vary the hydraulic gear ratio ([13],[33],[27],[34]).

The hydraulic concept of DOT requires an open-circuit drivetrain with seawater as a hydraulic medium. In the open circuit, prefiltered seawater is circulated, eliminating the need for a cooling device as the hydraulic medium has a constant supply. The configuration of the system consists of a high-pressure pump directly connected to the rotor shaft and thus replacing the gearbox. The DOT concept requires a low-speed, high-torque seawater pump, which is not yet commercially available. However, DOT is designing this pump, allowing for the implementation of the design in subsequent phases of the project [35]. In order to speed up the development and evaluation of the original idea, different setups have been adopted using off-the-shelf components to replace the required – but not yet available – pump. The components selected for this design result in a reduced overall efficiency compared to the ideal concept with only a high-pressure pump but allow for faster development.

3.1. DOT Hydraulic Drive-train Evolution

3.1.1. DOT Closed-loop Set-up

The initial configuration of the hydraulic transmission aimed to contain as few components as possible [13], with a positive displacement radial piston pump located in the nacelle and directly connected to the rotor shaft. The high-pressure pump was connected with a high-pressure line to a hydraulic motor at the base of the turbine, which converts the flow into mechanical power. In order to test and evaluate the feasibility of this configuration, the microDOT 10kW project was successfully done. This was one of the initial set-ups that were tested for their efficiency and operation and is presented in Figure 3-1. The system consisted of a small Pelton turbine, an open-loop freshwater circuit and a closed-loop hydraulic circuit. An electric motor operating an oil pump was used to imitate the wind turbine rotor and a nozzle regulating the flow towards the Pelton turbine was used as means of pressure control to the system. By controlling the pressure in the system, the counteracting torque from the pump to the rotor could be controlled.

The experimental results of this setup proved the concept and set the base for various research to be conducted in order to expand the capabilities of the system. The overall efficiency of this set-up was around 48%, which indicates that the system was strongly damped. However, it was estimated that the total efficiency could be improved up to 60% by changing the design of the nozzle which acted as a passive torque controller for the system [11]. Moreover, the possibility of implementing the DOT concept in a wind farm or combining it with other production units requires different control strategies for each turbine [36].
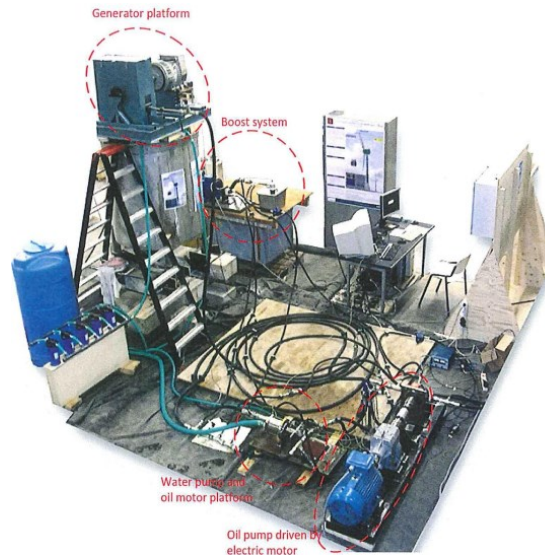
Figure 3-1: MicroDOT experimental setup [11].

The prototype testing of the abovementioned concept was implemented in DOT500 with an in-field 500 kW hydraulic wind turbine – a project that aimed to evaluate the initial idea in a full-scale demonstration, which is presented in Figure 3-2. This set-up consisted of an oil motor at the base of the tower, which was driven hydraulically by an oil pump that was connected to the rotor low-speed shaft in the nacelle. The closed oil circuit between the rotor and water pump functioned as a hydraulic gearbox. The water pump, which was located at the bottom of the setup, created a pressurized water flow and was mechanically connected to the motor. Spear valves transformed the flow into high-velocity water jets and a Pelton turbine-generator setup converted the hydraulic energy into electricity.
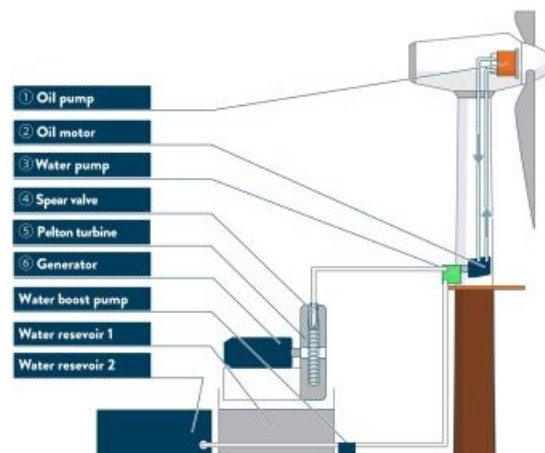
Figure 3-2: DOT500 intermediate hydraulic wind turbine configuration overview [34].

With this hydraulic drivetrain concept, Mulders et al. [34] considered an alternative torque control implementation, where fluid pressure was regulated to vary the system torque. The utilized pitch control

was designed and adapted from [37], to optimize the fine-pitch angle by an extremum-seeking controller. In this intermediate version of the ideal DOT concept, the generator was mechanically decoupled from the drive train, which did not allow for instant generator torque control (active control). Thus, the system torque control was performed using a spear valve that restricted the water flow to the Pelton turbine, changing the pressure and torque at the rotor, as tested by Diepeveen [38]. The desired variable speed operation of the rotor was achieved by sizing the nozzle area of the spear valve in order to change the pressure and torque of the system. The idea was to create a system that can match the hydraulic transmission torque and speed with the rotor's torque-speed operation characteristics for optimum aerodynamic performance.

According to test results of this configuration at nominal operation, it was established that below-rated wind speeds, a passive torque controller could be used to adequately vary the speed of the turbine drivetrain, by reasonably tracking the optimal tip-speed ratio and power coefficient $C_{p,max}$. Above rated wind speeds, a pressure relief valve had to be activated in order to limit the pressure and the drive train torque. Shutting down the turbine was also possible by gradually cutting off the flow rate in the high-pressure line using a valve. Except for that, the energy efficiency in the below-rated region, which was calculated as the ratio between the generator power output and the measured rotor power, ranged from 8 to 22%. However, by eliminating the intermediate oil loop and installing the in-house created high-pressure water pump, the overall performance would be much enhanced.

By expanding the aforementioned concept, the incorporation of more than one turbine into the hydraulic network has been examined by Laguna [39]. It was observed that the passive control strategy was limited by the use of independent lines and nozzles for each turbine. Moreover, from numerical simulations, it was reported that the hydraulic wind farm had an overall energy efficiency of around 68% – 81%, depending on the utilized control scheme. This overall efficiency is lower than that of reference wind farms using conventional technology, with an overall efficiency between 82% – 84% [39].

3.1.2. DOT Pilot Reverse Osmosis (PRO)

Besides electricity, the DOT hydraulic wind turbine could be used to produce fresh water by implementing a reverse osmosis unit to its configuration, as originally proposed by Diepeveen et al. ([17],[23]). The desalination unit can be located in parallel to the Pelton turbine-generator setup, in order for the potential of separate production of water or power, depending on the demand. The RO unit uses a pressure-based desalination technique, which is beneficial as the feed water has already been pressurized by the high-pressure pump [41]. The pressurized water enters the RO unit, which produces permeate (clean water) and brine (high concentration of dissolved salts). The part of the water that is not purified (brine/concentrate) has high energy and pressure that can be reused in order to minimize the losses and energy consumption of the system.

Wind resource is characterised by its stochastic nature which contradicts the operation requirements of a reverse osmosis unit for a short range of varying conditions. The effect on the behaviour of the RO membranes under variable conditions has been examined in literature ([42], [43]). A numerical model was constructed and simulated by Supper [44], to define the integration technique of a RO system to the DOT turbine, as well as to propose control strategies to achieve high efficiency and avoid membrane damage for different operation regions. For that purpose, the microDOT was used for sizing and determining the equipment needed for the experimental setups, but not for dynamic tests. Moreover, fluctuating pressures and flows, as well as two different wind speed regions, were taken into account to test several control strategies for water production

The research conducted by Supper [44] yielded results regarding the RO membrane implementation in a hydraulic wind turbine drive train. More specifically, varying pressures and flows (varying loads) resulting from varying wind speeds induced a membrane performance very similar to the one induced by constant pressures and flows (constant loads). This means that the system was able to deliver constant power to the grid with minimal dynamic variations. A combination of variable speed control and pitch control achieved the neutralization of the high frequent wind turbulence creating a constant power output to the grid, in the above-rated region. The research by Supper focused on the RO unit in combination with a line that was assumed to lead to a Pelton turbine and generator, without examining the direct effect of the Pelton turbine-generator combination on the system. In this context, the pilot DOT500 PRO project was developed, to test the hydraulic turbine for both water and electricity production.
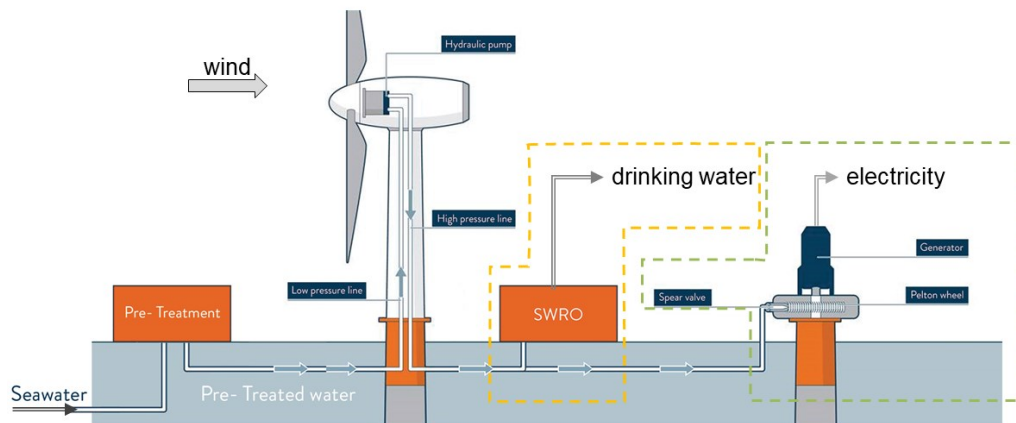
Figure 3-3: Schematic showing the main components of the DOT500 PRO project (DOT B.V.).

As already mentioned, reverse osmosis units have high energy consumption due to the required high-pressurized flow to desalinate seawater. Having acquired the knowledge of combining the DOT hydraulic drivetrain with a seawater reverse osmosis unit, Smits et al. [45] examined the integration of an energy recovery device (ERD) into the desalination unit. This device transfers the energy of the high-pressurized concentrate flow to low-pressurized seawater (see Figure 3-4). One of the features of a system with an ERD is that the flow rate at which permeate is generated is almost the same as the flow rate delivered by the high-pressure pump, as opposed to a system without ERD where this flow rate is dictated by the system's recovery rate. In order to operate the wind turbine at its maximum aerodynamic performance, the author proposed to implement the combination of the RO unit and ERD to the already examined DOT500 PRO concept with the Pelton turbine and generator unit. This would allow for both higher water production due to the ERD and control of the wind turbine's operation using the spear valve in the line leading to the electricity production system.
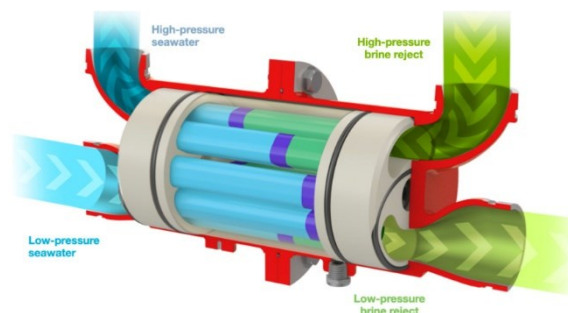
Figure 3-4: Schematic of pressure exchanger operation as an energy recovery device [46].

Following that, the research conducted by Greco et al. [27] examined the combined system of the DOT turbine with a RO unit-ERD setup and a Pelton-generator setup and defined the required settings for maximum water production. This research examined a series of operating points for different constant values of wind speed, within the limits and constraints of each component. By taking into account the operational window of the involved units, a control strategy was found for achieving maximum water production. By using an ERD, an increase in the produced water can be achieved, under the assumption that the booster pump can provide an adequate amount of seawater [33]. The system configuration remained the same as the latest-at-date developments, but the RO unit was modified to contain six RO vessels, which hosted six RO spiral wound membranes in series. The more the pressure vessels connected in parallel, the higher the capacity of the system.

The research by Greco et al. concluded that the proposed system could provide up to 300 kW of electricity and could desalinate water up to 25 m^3/h, at rated operating conditions. It was also found that, except for its role in water production, the ERD could contribute to the control of the system. When it comes to control design, the settings were adjusted to develop pressure as quickly as possible and reach the rated pressure as soon as water production started. Finally, it was found that the use of an ERD could enhance the water production for each operating point by improving the recovery rate, while the combination of active and passive control through the use of a spear valve allowed for the safe production of water and energy over a larger range of wind speeds.

The DOT500 PRO concept was further examined for optimization of water and electricity production. Goveas et al. [14] extended the literature investigation of such a system to a numerical model which could control and optimize power or water production based on different wind conditions. The developed numerical model used the spear valve as the main control mechanism to optimize the operation of the system. Only the below-rated discrete values of wind speeds were considered and combined with a certain number of possible nozzle positions. The parameters of the system were the pressure and flow rates from the high-pressure pump to the Pelton nozzle and RO system, as well as the rotational speed and torque of the rotor and Pelton turbine. For different wind speeds below rated, the system was simulated and its performance was assessed based on different demand scenarios (water or power production).

As regards the control method for the DOT PRO concept, van Hanswijk [47] examined the possibility of integrating a Learning-Based Model Predictive Control framework to the existing control scheme of the system. This research took into consideration the dynamics of the three major subsystems which are the wind turbine, the power production system and the reverse osmosis unit. It was found that the examined control scheme could handle multivariate systems. However, since the interaction of the individual system controls has unknown effects, the implementation of the proposed control may cause the subsystem states to exceed the imposed constraints and damage the overall system. The Learning-Based Model Predictive Control seems promising and capable to replace the existing control strategy but research is still needed to validate and expand the possibilities of applying it to the DOT PRO system.

Concluding the research that has been conducted over the years on the DOT concept, the examination and optimization of the system for discrete values of wind speeds is a very useful tool for the evaluation of the components and the establishment of the limiting parameters of the sub-units of the system. The control of the system is mostly based on passive torque controllers, while active controls are utilised only in specific wind regions. The behaviour of the system and its operation points are yet to be examined as a function of the wind climate and real water and electricity demands. In order to maintain constant operation at rated conditions, pitch control is activated together with the passive control of the spear valve. Systems that employ multiple controllers for the same purpose have more specifications for

design and limiting criteria, such as additional components and maintenance requirements. Therefore, one of the main goals is to determine a robust and simple operating strategy for the DOT500 PRO system with a constant spear valve and pitching as the main control to maintain constant operation at rated conditions. On top of that, it is of interest to develop a tool that will define the minimum required RO unit for a specific location, according to site-specific wind and water requirements.

3.2. DOT PRO Sub-systems

The three main subsystems that compose the whole DOT500 PRO setup are the hydraulic wind turbine, the electricity production system consisting of a Pelton turbine combined with a generator and the water production system which uses a reverse osmosis unit combined with an energy recovery device. A theoretical overview of the Reverse Osmosis (RO) technique and its integration with an energy recovery device (ERD) for water desalination is presented in Appendix A.

3.2.1. Design Criteria and Limits

The design criteria and constraints of the three subsystems can be established from the operation and type of their components. The desalination units are usually operated under constant flow rates with only small allowable deviations from their selected operating conditions [48]. The high-pressure pump has a flow rate proportional to its rotational speed, which is a function of the rotor rotation and therefore a function of the wind profile. As a consequence, the high-pressure pump delivers a variable flow rate to the reverse osmosis unit, which contradicts the constant flow requirement for the desalination operation.

As regards the safe operation of the wind turbine, two wind regions are identified which require different operational approaches [12]. From cut-in to rated wind speed, the wind turbine increases the rotational speed, the produced power and its torque. The operation of the wind turbine needs to be in the stable region and thus the high-pressure pump is acting as a load, exerting the required torque to counteract the aerodynamic torque and drive the system to an equilibrium point [27]. Above rated wind speed, pitching maintains the rotational speed and power constant and therefore the high-pressure pump is kept in stable operation. The constraint that defines the operation of the high-pressure pump is its maximum rotational speed which is related to a maximum feed flow.

Regarding the seawater reverse osmosis unit, the working limitations ensure its smooth operation and failure prevention, as well as the normal maintenance of its components. In order to start the operation of the desalination unit, pressure has to reach a certain level at which the reverse osmosis can take place. In case the desalination unit is operated with lower pressure than required, there will be no permeate produced and there is a chance of normal osmosis to occur and damage the membranes, which are not intended for reversed flow. In order to prevent mechanical failure of the membranes, the safe operation is additionally constrained by an upper limit pressure (around 83 bar) [48]. As mentioned above, the SWRO unit is combined with an energy recovery device, whose operation is limited by its minimum and maximum flow rates. In the ideal situation, an energy recovery device runs at variable speed according to the inlet flow of the desalination unit, in order to maintain a constant recovery rate. However, at this stage of concept development, the energy recovery device is operated at a constant speed, providing a fixed amount of seawater into the reverse osmosis unit, leading to a variable recovery rate according to the feed flow from the high-pressure pump.

3.2.2. Reference System

In the present thesis, the DOT PRO concept and additional sub-systems will be employed and examined for its installation configuration on a Greek island. In order to achieve this goal, some parameters of the system that directly influence the control and water production will be scaled accordingly to provide the necessary configuration for the supply of a specific water demand. However, DOT PRO employs several specific characteristics and components which will constitute the reference parameters and values for the system. The following table presents the key parameters that will be maintained in the present thesis as reference components of the system. The parameters to be scaled will change in accordance with the operation and constraints of the reference ones and will be analysed further.

Table 3-1: List of the main system parameters and constants used for modelling.

System Parameters	Value/Type
Wind Turbine Components	
Rated power	500 kW (redesign from Vestas V44/600)
Rotor radius	22 m
Moment of inertia	$6.6 \cdot 10^5$ kg·m^2
Nominal rotational speed	28 rpm
High-Pressure Pump Characteristics	
Model	Kamat Quintuplex Plunger Pump K 80000-5G
Rated flow	2394 l/min
Rated rotational speed	1500 rpm
Nominal pressure	160 bar
Volumetric displacement	1.61 l/rev
Mechanical efficiency at nominal conditions	90%
Volumetric efficiency at nominal conditions	93%
Electricity Production Components	
Spear valve nozzle diameter	25 mm
Maximum spear valve opening	39.4 mm
Spear valve angle	35 deg
Discharge coefficient	0.87
Generator nominal power	200 kW
Water Production Components	
ERD Type	Danfoss iSave 40
ERD flow rate range	21-41 m^3/h
ERD maximum rotational speed	1200 rpm
Rated membrane pressure	70 bar
Constants	

ρ_{air}	1.225 kg/m^3
ρ_{water}	1025 kg/m^3
Ideal recovery rate (γ)	40% (in practice it varies with the feed flow)
Water temperature	15-25 °C
Gearbox efficiency	90%
Generator efficiency	95%
Gearbox ratio	52.5
Intake feed concentration	39100 ppm

3.3. Analysis of Possible Components' Adjustment

As evident from the detailed description of the DOT500 PRO, the system consists of numerous components that interact with each other for optimal control. Each of the three sub-systems has components that directly or indirectly influence water production and are independent or interconnected with the operation of components in the same or other sub-systems.
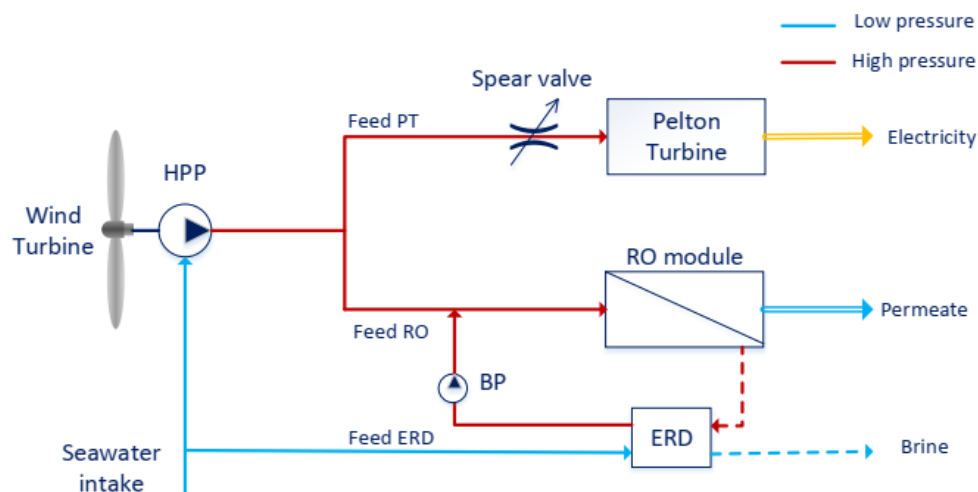
Figure 3-5: Schematic of the DOT500 PRO showing the sub-systems and their connections. Seawater flow is represented by solid lines while brine flow is depicted with dashed lines. The double lines depict the permeate production (in blue) and electricity production (in yellow) [27].

This research aims to develop a robust and yet simple operating strategy of the DOT500 PRO and create a model that will provide the minimum required size of the reverse osmosis unit to serve a certain water demand under a given offshore climate. For this purpose, the reverse osmosis module has to be scaled in size and integrated with the operating strategy, which utilises a constant spear valve opening throughout the operation. This translates into several combinations of desalination unit sizes and spear valve positions, which will be simulated and investigated for their performance and the new rated conditions they impose to the system.

The size of the reverse osmosis unit is defined as the number of RO membranes and pressure vessels contained in the module. Each membrane has a certain capacity, also known as flux rate, which is affected by several factors, such as the type of membrane, the temperature and the concentration of contaminants in the water being treated. Thus, the required number will be based on the capacity of the high-pressure pump that transfers the water to the reverse osmosis unit. Another parameter that limits

the number of membranes is the wind climate which drives the wind turbine and subsequently the high-pressure pump. In order to economically harvest the maximum water feasible, the number of RO membranes will be chosen, depending on the wind profile which directly influences the volume of pressurized water that can be fed to the RO unit.

Looking into the reverse osmosis membranes' characteristics, the active area of the membranes is a parameter that is proportionally connected to the number of membranes in the reverse osmosis unit and therefore, it cannot be considered as a separate varying parameter. However, research in varying the active area of the membranes could give additional insight into the effects that the variation of the number of membranes would have in the system. It has been observed that as the membrane active area grows (resulting from a larger number of membranes), the rated wind speed reduces, meaning that the turbine's blades must be pitched at lower wind speeds to maintain consistent power and water output at rated conditions [14]. This does not influence the wind speed at which the water production can begin because the size of the active area does not directly influence the operating point of the turbine [14]. Moreover, as the active area decreases (resulting from fewer membranes), the feed flow from the high-pressure pump decreases and therefore the operation has to be kept constant at lower wind speed due to the attainment of the maximum allowable pressures. This may translate to not fully harvesting the available wind speeds of the location, as the blades will be pitched accordingly to respect the pressure limits.

By utilizing the spear valve that jets the flow into the Pelton turbine, the pressure output can vary according to the opening of the valve. Several but constant throughout the operation spear valve openings will be examined in terms of pressure and flow rate ranges in the system. By moving the nozzle from the fully open to the closed position, the pressure in the high-pressure pump increases while the flow rate from the pump reduces. Thus, the available area of the nozzle (spear valve nozzle diameter) plays an important role in the pressure output and the flow that enters the Pelton turbine.

The pressures, flow rates and rated conditions of the system under the proposed operating strategy for several combination of the abovementioned parameters will be investigated. Based on the observations, the tool for defining the minimum required RO size with its associated spear valve opening will be developed for the specific case of Agios Efstratios island.

Chapter 4

Numerical Model of the DOT500 PRO

In this Chapter, the numerical model of the DOT wind-powered desalination system will be described based on the components shown in Figure 3-5. The DOT500 PRO consists of three sub-systems, namely the wind turbine-hydraulic transmission, the electricity generation and the desalination unit. The following diagram shows the system configuration and the connection between its sub-systems.
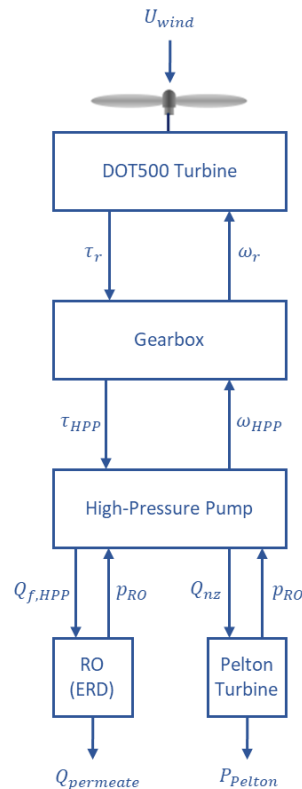
Figure 4-1: Flow chart of connections between the DOT500 PRO sub-systems [14].

The system consists of a 500kW redesigned wind turbine directly connected to the low-speed shaft of a gearbox with a reduction factor, G, equal to 52.5. The high-speed shaft of the gearbox is connected to a high-pressure pump that circulates seawater, which is supplied by the booster pump and has been subjected to prefiltration. The high-pressure pump is connected to the electricity and water production units. There is a parallel connection between these two subsystems that allows for controlling both with only one spear valve located just before the electricity production.

The electricity production system consists of a spear valve that regulates seawater flow into a Pelton wheel, which drives a generator with a nominal capacity of 200kW. The spear valve can regulate the flow into the electricity and water production units as it allows for dictating the pressure and flow rate

on the outlet of the high-pressure pump. The water production system consists of a reverse osmosis unit with parallel vessels that contain 6 to 8 membranes in a row. An isobaric pressure exchanger ERD is connected in parallel to the reverse osmosis unit to extract the energy of the high-pressurized brine stream and transfer it to the seawater feed flow that will be supplied to the RO. The main boost pump feeds the required low-pressure saltwater to both the high-pressure pump and the isobaric ERD.

4.1. Model Steady State Equations

The DOT500 PRO system is governed by aerodynamic and hydraulic formulas, that describe the operation and the connections between the three sub-systems. Wind energy is captured by the wind turbine and transformed into mechanical energy. The amount of electricity extracted is determined by several factors, the most important of which are the height and geometry of the wind turbine as well as the wind climate. Wind activates the DOT system and allows for the conversion of kinetic energy into electricity and freshwater utilizing its hydraulic transmission. The following equations were used to build the numerical model of the system and simulate its operation under different wind conditions and RO configurations.

4.1.1. Assumptions

One of the key pieces of information that has to be given in research is the list of assumptions that were made for the research to reach its conclusions. Most of the assumptions are usually made to simplify the required work and to ensure that the results are valid and credible. Therefore, it is important to go through some key assumptions that were made for the sake of this research. The assumptions that will be discussed refer to the high-pressure pump operation, as well as to the interaction between the sub-systems of the concept. Some of the most important assumptions are listed below:

1. The seawater fluid medium is assumed to be incompressible, meaning that the density of seawater remains constant throughout the system.

2. The pressure from the booster pump at the inlet of the high-pressure pump is significantly lower than that discharge pressure in the line after the pump that is directed to the Pelton turbine and reverse osmosis unit. Therefore, the pressure difference over the high-pressure pump is assumed to be equal to the discharge pressure on the output side of the pump.

3. For the sake of simplicity, the mechanical and volumetric efficiencies of the system components are assumed to be constant throughout the operation.

4. In an ideal pressure exchanger, where the speed could be controlled, a fixed recovery rate could be achieved for permeate production. However, in the investigations carried out, the pressure exchanger is kept in constant rotation providing a fixed amount of water to the reverse osmosis system. As a consequence, the recovery rate of the desalination changes according to the pressure and flow fed into the desalination.

5. The salinity of the Aegean Sea is considered fixed within the range of 39100 and 39200 ppt. The same applies for the temperature of this area, which was assumed constant within the range of 15-25 °C.

4.1.2. Aerodynamic System

The first subsystem consists of the 500kW redesigned wind turbine, which is connected to the Kamat pump through a gearbox. The performance of the wind turbine depends on the power and torque coefficients, which are a function of the tip speed ratio. The tip speed ratio, λ, is defined as the ratio between the speed of the tip of the rotor blade and the wind speed, U and is calculated as:

$$\lambda = \frac{\omega_r \cdot R_r}{U} \qquad (4.1)$$

Where ω_r is the angular velocity or angular rotational speed of the turbine in rad/s and R is the radius of the turbine which is equal to 22m. The power, C_P, and torque, C_τ, coefficients of the wind turbine as a function of the tip speed ratio follow the pattern presented in Figure 4-2.
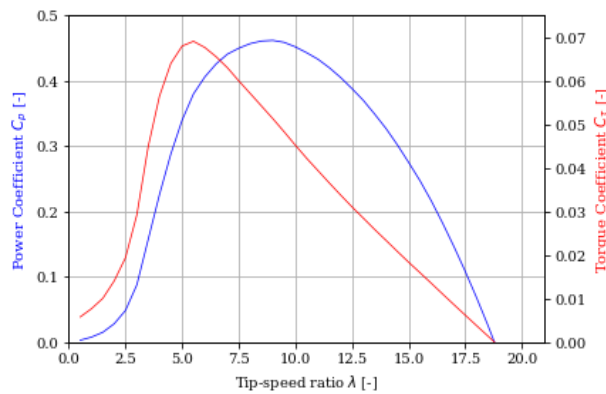
Figure 4-2: Power and torque coefficients as a function of the tip speed ratio for the DOT turbine.

At a tip speed ratio of zero, the wind turbine does not rotate and therefore no power can be extracted from the wind, meaning that the power coefficient is zero. The power extraction is also not possible at a tip speed ratio higher than 18.75 as the blades rotate too fast. The maximum power coefficient is equal to 0.462 and occurs at the optimal tip speed ratio equal to 8.6. At a lower tip speed ratio, equal to 5.5, the maximum torque coefficient occurs with a value of 0.0692.

The following figure presents the torque curves as a function of the rotational speed of the wind turbine. As evident, the torque line that corresponds to the maximum power coefficient is lower than the one corresponding to the maximum torque coefficient, implying that the torque required to extract the optimum power is less than the maximum for stable operation. The torque line that corresponds to the maximum torque coefficient indicates the stable region, as an operational curve above the red line would result in undesired effects on the wind turbine operation.
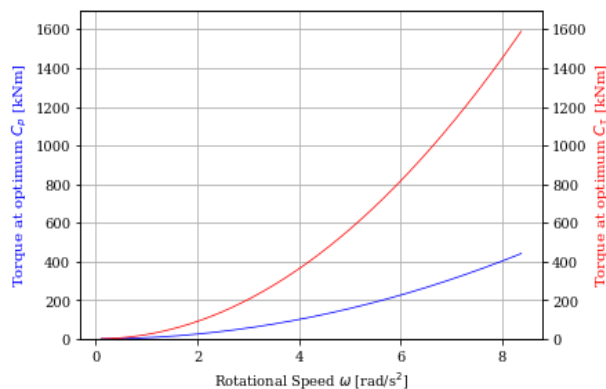
Figure 4-3: Torque curves as a function of rotational speed for the DOT turbine.

According to the tip speed ratio, the torque coefficient C_τ can be found in order to define the torque of the low-speed shaft as follows:

$$\tau_r = \frac{1}{2} \cdot \pi \cdot \rho_{air} \cdot C_\tau \cdot R_r^3 \cdot U^2 \tag{4.2}$$

The torque characteristics as a function of the rotational speed for different wind speeds can be seen in Figure 4-4. The wind speeds shown in the figure belong to the range between the cut-in and rated of the DOT500 wind turbine.
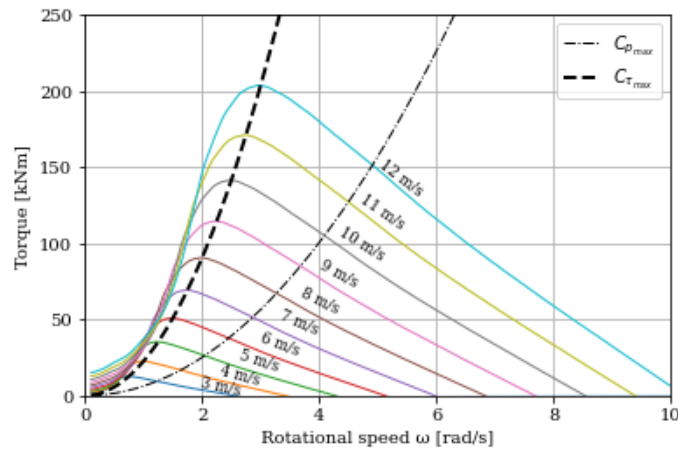
Figure 4-4: Torque – Rotor speed curves of DOT500 for different wind speeds at constant pitch angle.

In terms of stability, the turbine operation will be stable as long as the torque-speed curve of the combined pump-nozzle system intersects with the envelope curves of the rotor that have a negative slope ($dT/d\omega < 0$). When the wind speed increases, the rotor exerts more torque than the pump-nozzle torque, and the rotor speed increases. Increasing rotor speed induces lower aerodynamic torque for a given wind speed and higher torque from the pump, leading to a new equilibrium point. On the other hand, the region where the slope of the rotor torque curve is positive ($dT/d\omega > 0$) will cause instability in the turbine operation [13]. As a result, it's critical to design the nozzle appropriately so that the system can operate in the rotor's stable area.

For every wind speed between cut-in and rated, the C_τ and λ values of the red line from Figure 4-2 were used to obtain the corresponding rotational speed and torque using the abovementioned equations and a fixed pitch angle. The dotted lines indicate the torque curves for maximum torque and power coefficients, as accordingly depicted in Figure 4-3. The power harnessed by the wind turbine is a product of the rotational speed and the power coefficient that is selected for the operation based on the desired output.

4.1.3. Hydraulic Sub-system

The wind turbine is connected to the high-pressure pump through the gearbox with a gear ratio G equal to 52.5, which implies that the high-speed shaft rotates 52.5 times faster than the low-speed shaft.

$$\omega_{HPP} = \omega_r \cdot G \tag{4.3}$$

In equation (4.3), ω_{HPP} is the rotational speed of the Kamat high-pressure pump. With the acquisition of the low-speed shaft torque, the torque on the high-speed shaft, τ_{HPP}, can be calculated by taking into account the mechanical efficiency of the gearbox, $\eta_{g,mech}$.

$$\tau_{HPP} = \frac{\tau_r}{G} \cdot \eta_{g,mech} \qquad (4.4)$$

The high-speed shaft is directly connected to the shaft of the Kamat pump translating the high-speed torque into pressure. This pressure refers to the pressure of the seawater medium that can be provided by the pump and is defined as follows:

$$\Delta p_{HPP} = \frac{\tau_{HPP}}{V_{HPP}} \cdot \eta_{HPP,mech} \qquad (4.5)$$

Where V_{HPP} is the volumetric displacement of the Kamat pump and is equal to 1.61 L/rev, while the mechanical efficiency of the pump is referred to as $\eta_{HPP,mech}$. The discharge pressure on the outlet of the high-pressure pump must account for the pressure of the booster pump, p_{bp} , that supplies seawater. The positive displacement pump rotates at a certain speed with a fixed volume, supplying a certain flow independent of the pressure it operates at. This pressure is substantially lower than the pressure difference across the pump (3 bar) and thus it has a negligible contribution to the total pressure that is supplied to the systems following the pump. Therefore, the pressure on the outlet of the high-pressure pump, p_{HPP}, can be found as follows:

$$p_{HPP} = \Delta p_{HPP} + p_{bp} \qquad (4.6)$$

The rotational speed of the high-speed shaft that drives the pump can be translated into seawater flow rate [m^3/s] in the outlet of the pump with the following expression:

$$Q_{HPP} = \omega_{HPP} \cdot V_{HPP} \cdot \eta_{HPP,vol} \qquad (4.7)$$

Where $\eta_{HPP,vol}$ is the volumetric efficiency of the high-pressure pump and is equal to 93%. The torque of the high-pressure pump can be directly connected to the flow rate on the outlet as well as to the rotation of the rotor with the following equation:

$$\tau_{HPP} = \frac{Q_{HPP} \cdot \Delta p_{HPP}}{\omega_r} \qquad (4.8)$$

The torque produced by the high-pressure pump acts as a counter torque to the rotor rotation allowing for the direct regulation of the latter according to the desired operational points. The aerodynamic torque and rotor rotation can be translated into pressure and flow, respectively, by correlating the characteristics of the sub-systems. Figure 4-5 depicts the flow-pressure envelope curves of the system for different wind speeds below rated, as well as the stable limit as indicated by the maximum torque coefficient. The operating curve that could theoretically yield the highest power production is represented by the maximum power curve, $C_{p,max}$. Additionally, the nominal operating values of the pump and RO are presented in the graph. The dotted red line limits the operation of the high-pressure pump as it depicts its maximum flow rate while the yellow line represents the nominal pressure on the membranes. Therefore, the stable operational window is limited to the area fenced by the optimum torque curve and the two nominal pressure and flow values
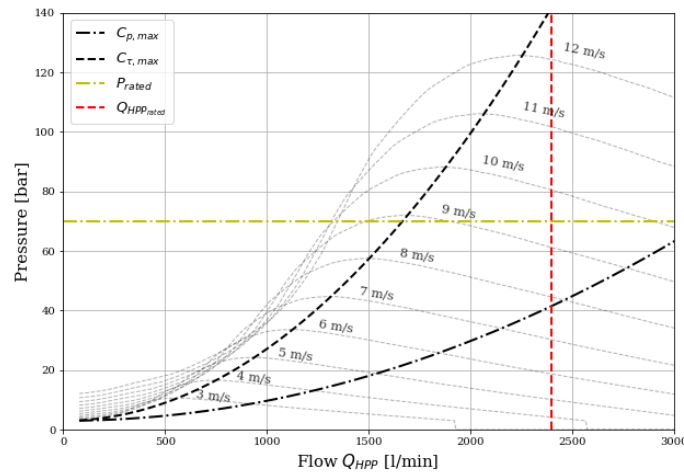
Figure 4-5: *Turbine rotational speed and torque translated to pressure and flow from the high-pressure pump.*

4.2. Volumetric Flow Rates

A schematic of the division of the flows from the high-pressure pump to the rest of the module is presented in Figure 4-6 below, where the electricity and water production units follow the pump in a parallel connection.
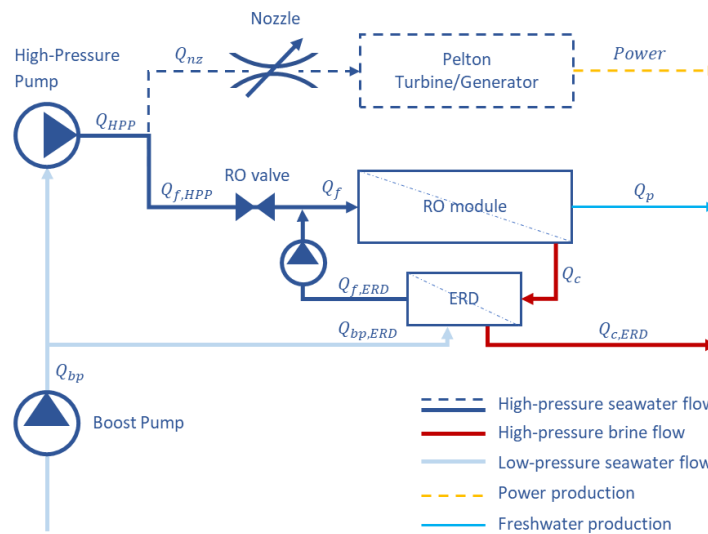
Figure 4-6: *Schematic representation of the flows from the high-pressure pump* [14].

The flow from the high-pressure pump is divided into two streams to the Pelton turbine and RO module. The stream $Q_{f,HPP}$ represents the high-pressurised seawater flow rate to the reverse osmosis membranes, while the Q_{nz} represents the input jetted flow to the Pelton turbine through the nozzle. The pressure of the fluid medium at all three streams is assumed equal and controlled by the position of the spear valve.

$$p_{HPP} = p_{RO} = p_{nz} = p \tag{4.9}$$

$$Q_{HPP} = Q_{f,HPP} + Q_{nz} \tag{4.10}$$

Where p_{HPP} is defined in equation (4.6) as the pressure at the outlet of the high-pressure pump. The pressures described with p_{RO} and p_{nz} indicate the pressures entering the desalination module and power production module, respectively.

4.2.1. Flow Rate in the Pelton Turbine

As mentioned before, DOT uses a spear valve as means of controlling the pressure and flow of the Kamat pump. The relation between the pressure fed to the nozzle and the flow travelling through it is defined as follows:

$$Q_{nz} = \sqrt{\frac{2 \cdot \Delta p_{nz}}{\rho_w}} \cdot C_d \cdot A_{nz}(s) \tag{4.11}$$

Where Δp_{nz} is the pressure drop across the nozzle, ρ_w is the seawater density and C_d is the discharge coefficient of the spear valve, which is assumed to be equal to 1. The pressure at the outlet of the nozzle is assumed equal to the atmospheric pressure. The effective area of the nozzle is notated as $A_{nz}(s)$ and is a function of the spear valve position, s, which measures the opening from the fully open position until the tip of the spear. The spear valve design incorporated in the DOT500 PRO system is shown in Figure 4-7 below.
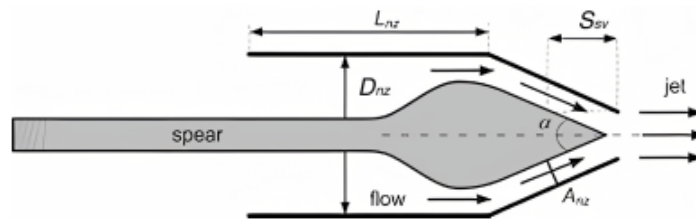
Figure 4-7: Schematic representation of the cross-section of the spear valve [39].

According to the spear valve cross-section design, the coning angle, a, is equal to 35° and the diameter of the spear, D_{nz}, is equal to 25 mm. The spear is allowed to slide through its casing in order to regulate the flow into the Pelton turbine and dictate the required pressure from the high-pressure pump. The effective area of the nozzle can be derived from the cross-sectional schematic as follows:

$$A_{nz}(s) = \frac{\pi}{4} \cdot D_{nz}{}^2 - \left[\left(s \cdot \tan\frac{a}{2} \right)^2 \cdot \pi \right] \tag{4.12}$$

The range of the nozzle positions varies from 0 to s_{max}, indicating the fully open and fully closed positions, respectively. The effective area is maximum when the valve is fully opened ($s = 0$), while it reaches zero at the fully closed position ($s_{max} = 39.65$ mm). Opening the valve results in an increase in the effective nozzle area and therefore a rise in the flow rate with a decrease in pressure. Similarly, when the decrease in flow rate and rise in pressure are of interest, the valve should move towards the closed position to limit its effective area.

4.2.2. Flow Rate in the Reverse Osmosis Unit

As regards the flow directed to the reverse osmosis module, it is a summation of the flow supplied by the high-pressure pump and the flow recovered from the pressure exchanger isobaric ERD. The flow rate at the stream starting from the outlet of the pump to the RO membranes is indicated as $Q_{f,HPP}$, while the flow rate provided by the ERD is shown as $Q_{f,ERD}$.

$$Q_f = Q_{f,HPP} + Q_{f,ERD} \tag{4.13}$$

The total mass balance and salt mass balance of each membrane element are expressed below, where Q represents the flow rate, while C is the salt concentration. The subscripts p, f and c indicate the permeate, feed and brine production, respectively.

$$Q_f = Q_p + Q_c \qquad (4.14)$$

$$C_f \cdot Q_f = C_p \cdot Q_p + C_c \cdot Q_c \qquad (4.15)$$

In the previous chapter, the main operating losses in the ERD were mentioned and briefly discussed. The transfer of the energy trapped in the brine flow is achieved without a physical barrier, which leads to a small amount of mixing between the saltwater and brine, also known as volumetric mixing (VM). In order to limit this, an excess of water has to be supplied from the booster pump to the ERD, to ensure the cleaning of the remaining salt in the chambers of the ERD. This procedure is called overflush (OF) and it is an operational loss that cannot be avoided. Finally, there is leakage (L) within the chambers of the ERD, which can be compensated with a higher water supply from the boost pump. As it is evident from the abovementioned losses, the amount of pressurized seawater provided by the ERD to the RO unit is lower than the input to the ERD by a factor of ($OF \cdot L$). Therefore, in order to provide the required flow rate to the desalination unit, the input feed flow from the boost pump to the ERD has to increase by the same factor ($OF \cdot L$).

A numerical model of the reverse osmosis desalination system is built under several assumptions. To begin with, the saltwater fluid medium is believed to be incompressible, leading to a consistent seawater density throughout the system. The head height of the entire system is deemed trivial, hence the change in potential energy of the liquid at any point in the system is 0. The fluctuating salinity of the feed has no impact on the fluid medium's density. The friction losses owing to any type of valve or pipeline resistance in the system are considered to be insignificant.

The main parameters used to calculate the flow and pressure through the membranes are defined below. These include the water flux, J_w, osmotic pressure, p_{osm}, and pressure differences $\Delta\pi$ and Δp. The water flow through the RO membranes can be expressed as a function of the permeability coefficient, K_w, the osmotic pressure difference, $\Delta\pi$, and the hydrostatic pressure difference, Δp.

$$J_w = (\Delta p - \Delta\pi) \cdot K_w = \frac{Q_p \cdot \rho_w}{A_m} \qquad (4.16)$$

Where Q_p is the permeate flow (the produced freshwater) and A_m is the membrane area. The term ($\Delta\pi - \Delta p$) is defined as the net driving pressure, which drives the water through the reverse osmosis vessel. The salt concentration of the inlet seawater increases as it travels towards the end of the RO pressure vessel, consequently increasing the osmotic pressure required to drive the fluid further. Usually, the osmotic pressure rise over the length of a vessel is in the order of a few bar. The osmotic pressure in the system can be calculated as follows:

$$p_{osm} = n \cdot C_{eff} \cdot \delta \cdot \frac{T}{M} \qquad (4.17)$$

Where C_{eff} is the effective average concentration at the surface of the membrane in ppm, n is the number of ions in the fluid (seawater includes two major ions), δ is the gas constant, which is equal to 8.314 J/mol·K, T is the temperature in Kelvin and M is the molarity of salt water. The Aegean Sea has a high salt concentration, equal to 39100 ppm and a temperature that varies between 10 and 25°C. In

order for the desalination unit to produce water, the pressure in the system has to be greater than the osmotic pressure at the end of the pressure vessels, which is influenced by the number of membranes and length of the pressure vessels.

The calculation of the pressure on the reverse osmosis module can begin with the determination of the permeate flow [49]. This is a function of the membrane permeability, effective area and osmotic pressure. It is assumed that the pressure of the permeate is equal to the atmospheric and therefore the pressure drop over the membranes is equal to the inlet pressure.

$$Q_p = (p_{RO} - \Delta\pi) \cdot \frac{K_w \cdot A_m}{\rho_w} \qquad (4.18)$$

An important parameter that characterizes the membrane performance is the rejection rate, R, which describes the amount of salt that is captured by the membrane and prevented to pass through the freshwater. Nowadays, membranes can reach a rejection rate up to 97-99%, meaning that only 1-3% of the salt remains in the permeate [27].

$$R = 1 - \frac{C_p}{C_f} \qquad (4.19)$$

An additional parameter, which indicates the amount of water produced with respect to the seawater fed to the desalination module, is the recovery rate γ which is defined as the ratio between the permeate (Q_p) and feed flow rates (Q_f).

$$\gamma = \frac{Q_p}{Q_f} \qquad (4.20)$$

The recovery rate is the one intended to be kept constant at optimum by the pressure exchanger, which feeds the required amount of pressurized seawater to the desalination unit. Assuming that the losses of the ERD are covered by the excess of feed flow from the boost pump, the output of the ERD to the RO unit is equal to the amount of brine entering the ERD chambers.

$$Q_{f,ERD} = Q_c \qquad (4.21)$$

The most significant consequence of the ERD implementation to the RO system is that the permeate flow Q_p is equal to the flow fed to the desalination unit by the high-pressure pump $Q_{f,HPP}$.

$$Q_{f,HPP} = Q_f - Q_{f,ERD} = Q_f - Q_c = Q_p \qquad (4.22)$$

More specifically, the permeate produced is only a function of the feed flow from the high-pressure pump and the recovery rate is affected only by the total feed flow to the RO unit. Therefore, given the flow from the Kamat pump, this configuration allows for the regulation of the recovery rate by continuously adjusting the output of the pressure exchanger ERD. In case the ERD rotation speed and consequently its output flow remain constant, the recovery rate varies according to the flow rate supplied by the high-pressure pump. It is, also important to note that the maximum permeate production is limited by the size of the RO module as well as the capacity of the high-pressure pump. More specifically, the maximum flow that the membranes can withstand is multiplied by the number of vessels and membranes installed in order to define the highest permeate production that the desalination unit can reach.

As regards the maximum operating pressure, the limit is set by the higher pressure allowed to be applied at each membrane. By substituting the permeate flow rate with its equivalent flow from the high-pressure pump, the pressure in the reverse osmosis unit can be formulated as:

$$p_{RO} = Q_{f,HPP} \cdot \frac{\rho_w}{A_m \cdot K_w} + \Delta\pi \qquad (4.23)$$

Substituting the formulations of flow rates entering the two production systems in Equation (4.10), the total flow rate from the high-pressure pump can be obtained as:

$$Q_{HPP} = \sqrt{\frac{2 \cdot \Delta p_{nz}}{\rho_w}} \cdot C_d \cdot A_{nz}(s) + (p_{RO} - \Delta\pi) \cdot \frac{K_w \cdot A_m}{\rho_w} \qquad (4.24)$$

By expressing the flow rates of the high-pressure pump as a function of the spear valve position, the correlation of the rotational speed on the high-speed shaft with the nozzle position has been achieved. For pressures below the osmotic pressure, the desalination unit cannot produce fresh water and therefore the RO valve is closed. This indicates that the flow from the high-pressure pump is exclusively delivered to the power generation system through the spear valve.

4.2.3. Boost Pump Flow

As mentioned above, the boost pump is located at the base of the tower of the wind turbine and supplies low-pressurized water to the high-pressure pump and the pressure exchanger ERD. According to that, the flow on the outlet of the boost pump forms as follows:

$$Q_{bp} = Q_{HPP} + Q_{bp,ERD} \qquad (4.25)$$

Where $Q_{bp,ERD}$ is the low-pressure seawater flow entering the ERD, which can be obtained from the amount of produced brine.

$$Q_{bp,ERD} = \frac{Q_c}{\eta_{ERD}} \qquad (4.26)$$

The efficiency of the boost pump accounts for the losses during the operation of the ERD and ensures that the output flow of the ERD is equal to its brine inflow.

4.3. Power Production

The second goal of the DOT500 PRO project is to generate electricity, which in this thesis will not be prioritized. According to the current configuration, electricity can be generated by jetting the high-pressure flow via the nozzle into a Pelton turbine wheel. The high-pressure seawater impulse hits the wheel's vanes (buckets), which are attached to a shaft that is forced to rotate. To produce power, the turbine wheel shaft drives a generator, which in the case of DOT500 PRO has a nominal power capacity of 200kW. This capacity dictates the optimal and actual produced power, even though the wind turbine was redesigned to reach a capacity of 500kW. As the generator has a lower capacity than that of the wind turbine, the rated power production is reached at lower wind speeds. Another factor that reduces the wind speed at which pitching is enabled is the pressure and flow limits of the RO module.
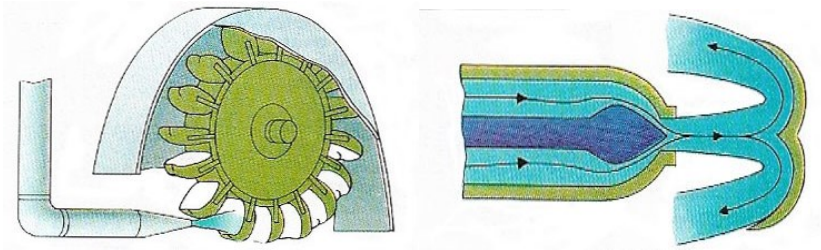
Figure 4-8: *Schematic of the Pelton turbine operation (left) and cross section of the jet flow provided to its buckets from the spear valve nozzle (right)* [50].

In Figure 4-8, the flow from the nozzle to the Pelton buckets that enables the rotation of the wheel shaft is shown. The hydraulic power contained in the water jet, P_{hyd}, is given by the product of flow and pressure at the nozzle, as follows:

$$P_{hyd} = Q_{nz} \cdot \Delta p \qquad\qquad (4.27)$$

The generator coupled to the turbine shaft converts the mechanical energy (rotation of the shaft) into electrical energy, accounting for the mechanical and electrical efficiencies, η_p and η_{el}, respectively.

$$P_P = P_{hyd} \cdot \eta_P \cdot \eta_{el} \qquad\qquad (4.28)$$

The produced power can be transferred to the electricity grid, while it can also cover the electricity requirements of the desalination system, which have been significantly limited by the implementation of the energy recovery device. Therefore, allowing for minimum electricity consumption by the system components, the DOT500 PRO can deliver most of its generated power to the electricity grid. Reverse osmosis has a significantly higher energy requirement than other desalination methods. The experimental model developed by Smits [45] concluded that a system with an ERD would consume 18% of the energy required to generate the same quantity of permeate without an ERD. This estimate did not take into account the electricity used by auxiliary parts, such as feed pumps and monitors. In Table 4-1 the energy consumption of the RO units with and without ERDs is depicted.

Table 4-1: *Power consumption per produced unit of permeate* [45].

System configuration	Value
Power consumption with ERD (Danfoss iSave 21 Plus)	3.23 kWh/m^3
Power consumption without ERD	18.62 kWh/m^3

Chapter 5

Operating Strategy for the Desalination System

5.1. Current Control Schemes

As the system aims to cover diverse operating purposes, various controls have been used and proposed to obtain the required system performance under different working conditions. The effectiveness and applicability of these will be discussed, and an operating strategy that will allow for constant spear valve opening will be suggested and assessed for implementation at an offshore location.

Three crucial limits on this system dictate the position of the spear valve and the pitch controller. The first limit is set by the membranes' rated – or maximum operating – pressure, while the others depend on the nominal flow from the Kamat pump and the uppermost flow that the membranes can handle. Each controller respects these limits and accordingly adjusts the spear valve opening and the blades' pitching.

5.1.1. Existing Control for Maximum Water Production

The existing control of the DOT500 PRO system aims to reach maximum water production for each wind speed. This can be achieved by applying the appropriate counter torque on the wind turbine through the high-pressure pump. In Figure 5-1, the coloured lines depict three spear valve openings which represent three of the system's load curves and dictate the flow and pressure of the pump. The green line represents an open valve, while the blue depicts the system operation for a smaller valve opening. Water production can begin when the pressure reaches the osmotic at the end of the RO pressure vessels. It is evident that with a smaller valve opening, the system attains osmotic pressure at lower wind speed (around 6.5 m/s) compared to the case of an open valve (around 7 m/s). Based on this observation, a smaller valve opening allows for faster water production in terms of wind speed.

The existing control used to maximise water production comprises selecting the control line that ensures attaining osmotic pressure at the lowest wind speed while still operating in the stable area to the right of the optimal torque curve of the wind turbine. Furthermore, the present control specifies that the valve will remain in the same position until the pressure limit in the membranes is achieved, and pitching will be engaged after additionally reaching one of the flow restrictions.

More specifically, a control line just right to $C_{\tau_{max}}$ is selected, which is dictated by a smaller valve opening. In the water production phase, when the rated pressure of the membranes is reached, the controller is activated to alter the spear valve opening and keep the system in constant operation. As soon as the flow limit of the high-pressure pump or the membranes' is attained, the pitch controller is activated to maintain the flow at the desired level.

5.1.2. Theoretical Control for Maximum Water Production

The control strategy proposed by Greco et al. defines the operation points of the sub-systems for increasing wind speed in order to reach stable operation for desalination as fast as possible. In Figure 5-1, the mapping of the proposed steady-state operation is presented, considering the limiting areas for stability and the constraints of the sub-systems. The letters A, B, C and D define the points at which the control changes to different modes in order to respect the system limits [27].
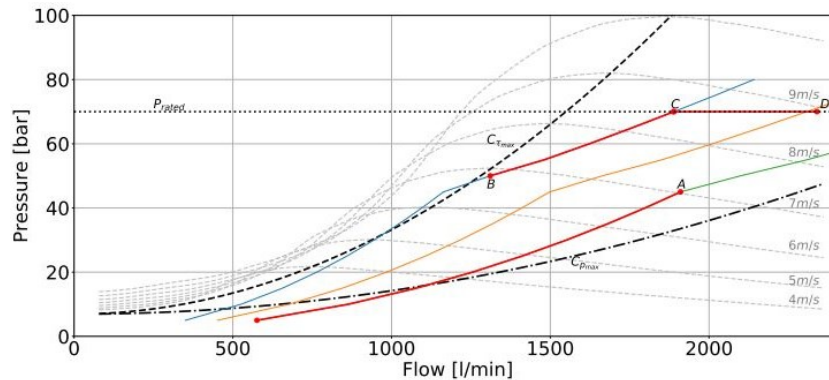
Figure 5-1: *Flow-Pressure lines of the rotor for different wind speeds and fine pitch angle are presented in grey. The load curves (SWRO, spear valve and ERD) are shown in coloured lines for different spear valve settings (green: large, orange: medium, blue: small). The proposed control follows the red lines* [27].

Starting with path 0-A, the system pressure is below the osmotic pressure at which the desalination can begin. Hence, the pumped water is directed to the power production unit, while the valve that allows water to the RO is closed. The passive torque control, as examined by Diepeveen et al. [40] is implemented to set the spear valve in a fully open position to extract as much power as possible. This path is followed until the wind speed reaches a value at which the osmotic pressure can be acquired with a change in the spear valve position. This point is defined by the letter A, where the osmotic pressure could be reached only by closing the spear valve to the maximum allowed without proceeding to the unstable region (above the $C_{\tau_{max}}$ curve). Therefore, the valve is closed until the operating point B at which the osmotic pressure is achieved for the given wind speed. As the wind speed increases with constant spear valve position, the flow and pressure increase until the rated pressure of the reverse osmosis unit is reached (point C). At this point, the valve gradually opens, allowing a higher flow rate to the power and water production systems. Letter D indicates the point at which the spear valve is fully open and either the maximum allowable flow of the RO unit or the ultimate rotational speed of the pump is reached. From this point forward, the control method dictates the pitching of the blades to keep the pump running continuously. More specifically, as soon as the flow limit is reached, the pitch controller is activated in addition to the passive one to maintain the flow at the desired level.

However, the simultaneous operation of these controllers which have the same ultimate goal of maintaining the system operation at rated conditions requires additional design aspects and trade-offs between water production and operating components using a reference RO unit. In order to limit the components subject to continuous motion, that are used to maintain constant operation with respect to the pressure and flow rate limits, the present thesis proposes an operating strategy that allows for maximization of water production under a constant valve opening.

5.2. Proposed Operating Strategy

The new scheme will have to maintain the system in the stable region with as few changes in the valve position as possible to avoid the necessity for additional design aspects and operating guidelines. This translates into a location-based selection of a specific valve opening for the whole operation, considering the site-specific wind conditions and water production requirements. Compared to the existing control, the new strategy will eliminate the step of arbitrarily selecting a control line only according to the wind turbine characteristics.

The new method will be implemented in this master's thesis in order to assess its operation under an offshore wind climate, which exceeds the range of the wind speeds examined by the authors of the ideal control. According to a specific wind profile and predetermined water demand, the appropriate control line will be selected to operate the system to meet the requirements. As the wind conditions will be acquired in the form of a dataset of discrete values over a year, the control and water production is expected to vary in every time step of the dataset according to the system constraints.

5.2.1. Operation for Maximum Power Production

In the previous sub-chapters, the aerodynamic and hydraulic connection was presented and explained in order to provide insight into the hydraulic conversion procedure. The aerodynamic torque and rotor rotation were translated into pressure and flow, respectively, by correlating the characteristics of the sub-systems. To solve the equations of the system operation, an algorithm was created in Python that provides the operating pressures and flows for each wind speed and spear valve opening. The working principles of the algorithm are presented in the following figures. Figure 5-2 and Figure 5-3 illustrate the sole operation of the power production system, while Figure 5-4 and Figure 5-5 present the combined operation of the RO and Pelton-generator unit.

As regards the sole power production, the valve leading to the RO unit is constantly closed. Therefore, the pressure limit of the RO does not influence the operation and the only flow limit derives from the maximum rotation of the pump. In Figure 5-2, the coloured solid lines represent the pressure-flow relation for every spear valve opening, with the slope of the curves increasing as the valve opening decreases. As already mentioned, the valve opening counts from the fully opened position (s = 0) to the fully closed position (s = s_{max}) and is represented as a percentage of the maximum distance, s_{max} that the spear can travel. The range of spear positions was divided into steps, with the final step indicating the completely closed position (100% · s_{max}), which is not depicted in the graph since it enables no flow from the nozzle to the Pelton wheel. The dashed black lines indicate the torque curves for optimum torque and power coefficients, as translated into pressure and flow of the high-pressure pump from Figure 4-3.

The graph presents the case of a closed RO valve, meaning that no water is produced and the pressurised water is directed to the Pelton turbine generator module. Therefore, the flow of the high-pressure pump, Q_{HPP}, is equal to the flow through the nozzle, Q_{nz}. As expected from Equation (4.11), the flow through the spear valve is higher with increasing pressures for each spear valve opening. The graph's upper limit corresponds to the Kamat high-pressure pump's maximum flow rate at 2394 l/min.

Given a fixed flow from the high-pressure pump, the pressure increases for decreasing valve opening due to the compression experienced by the fluid at the inlet of the nozzle. This opposing torque acts as a load on the turbine, forcing it to rotate at the speed dictated by the pump. Additionally, the pressure-flow curve of the high-pressure pump for turbine operation with maximum torque coefficient, $C_{\tau,max}$,

sets the upper limit for stable system operation. This indicates that only the curves below it reside in the stable region, while the ones exceeding it should be avoided. Therefore, the spear valve position is limited to a maximum of 68% of s_{max}, as this is the minimum effective area and highest operational curve that can hold the stable operation of the turbine.
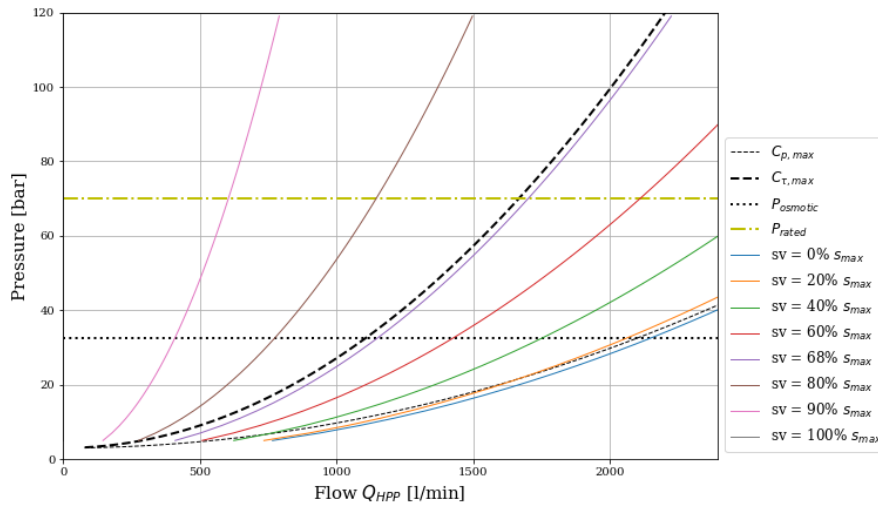
Figure 5-2: Pressure – Flow relation of the electricity production system, developed from different spear valve positions with constantly closed RO valve.

In Figure 5-3, the load lines are plotted on top of the envelop curves of the wind turbine and high-pressure pump for different wind speeds. The pressures related to the flows from the high-pressure pump are depicted in grey dotted lines for each wind speed. From this graph, the intersections between the load curves and the operational curves of the wind-pump system indicate the pressure and flow in the system for a given valve opening and wind speed. The power extracted by the generator may be established based on the flow and pressure entering the valve at each wind speed. By doing so, the optimum valve opening for maximum power extraction can be proposed for the specific operation. For ultimate power production, a load curve closest to and above the optimum power curve of the turbine would be selected to ensure flow build-up at a relatively low wind speed. The point is to reach maximum flow at the lowest wind speed, which can be achieved by utilising an open valve. As evident from the graph, such a curve is limited by the nominal flow from the high-pressure pump and requires direct pitching of the blades to maintain it. Therefore, the passive control is only engaged for the selection of the appropriate valve opening which in not changed throughout the operation.

Figure 5-3: Pressure – Flow relation of the DOT500 PRO for different wind speeds and spear valve positions with constantly closed RO valve.

5.2.2. Operation for Maximum Water Production

Having formulated and described the system for exclusive power production, the next step was the extension of the Python algorithm with the RO module combined with the pressure exchanger ERD. The total system operation accounts for the limits of the DOT500 PRO subsystems and is depicted in the figures below. As evident from Figure 5-4, only the load curves laying in the stable region are preserved and further limited by the rated pressure of the membranes and the maximum flow of the high-pressure pump. The case presented below corresponds to the simulation of a 6x6 RO unit.

Figure 5-4: *Pressure – Flow relation of the DOT500 PRO, developed from different spear valve positions with operational desalination unit.*

Compared to the case of sole power production, the RO valve opens as soon as the osmotic pressure required at the end of the pressure vessels is reached. This can be seen just above the area limited by the osmotic pressure, where the slope of the curve is decreasing owing to the RO valve opening. As the stream to the desalination unit opens, the flow from the high-pressure pump is divided between the RO module and the Pelton wheel while the system experiences relief in pressure. As regards the limits of the system, the operation of the RO unit is limited by the osmotic and rated pressure on the membranes at 35 and 70 bar, respectively. The flux constraints include the maximum flow rate supplied from the high-pressure pump and the nominal flow on the membranes. If the nominal flow of the high-pressure pump is higher than the nominal flow into the RO module, then an additional flow constraint is accounted for in the system, to ensure that the flow driven to the RO will not exceed the nominal of the membranes. In the case of a reverse osmosis module with six vessels containing six membranes each, the allowable flow through the membranes is greater than the nominal flow provided by the pump; hence the latter is the sole flow constraint of the system. Figure 5-5 depicts the load curves of the wind turbine-pump system for every wind speed while the values of pressures and flows for each combination of valve opening and wind speed can be established from the intersection of the envelop curves to the pump-nozzle curves.

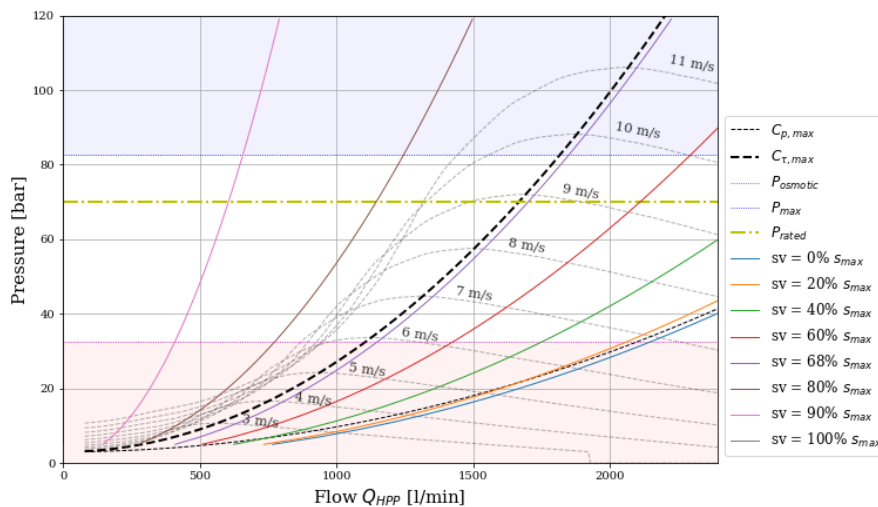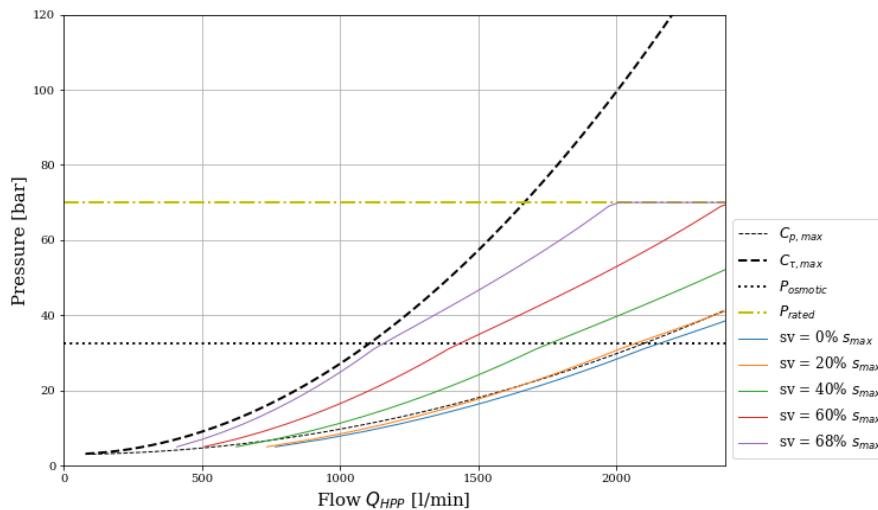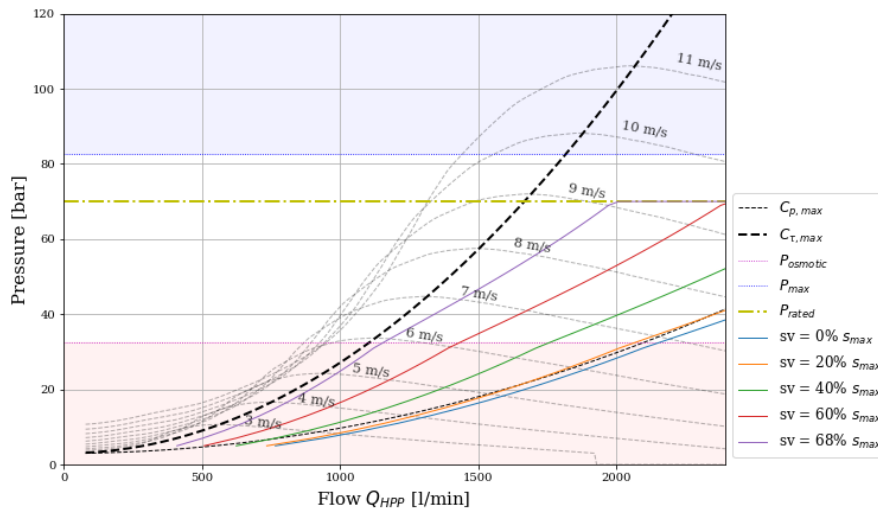*Figure 5-5: Pressure – Flow relation of the DOT500 PRO for different wind speeds and spear valve positions with operational desalination unit.*

The pitching of the blades cannot be restricted since it is required for turbine function; hence the passive controller operation must be confined to a constant valve opening. However, the arbitrary selection of a restricted valve for maximum water production is not a viable solution due to the inevitable variation in the valve opening to dodge pressure exceedance. Therefore, it is proposed to determine the valve opening for which the pressure and flow limits are reached at the same wind speed. By doing so, the pressure limit that dictates the maximum operating point with a constant valve opening will be met simultaneously with the flow constraint at the highest wind speed. As a result, a trade-off is made between the valve opening that allows for the highest permeate production and the one that drives the system to reach all of its limits simultaneously. The reason behind the intention of attaining the system constraints at the same wind speed is that it enables the pitch controller alone to maintain the operation without the requirement for a bigger nozzle opening.

Compared to the theoretical control of the system for maximum water production, the method proposed in the present thesis dictates that the system will operate at constant valve opening, which serves the requirements of the location. According to the site-specific offshore wind climate, the optimum spear position and required RO size will be provided to cover the freshwater demand. The RO size influences the appropriate valve opening selection, as depending on the number of parallel vessels, the maximum flow rate in the RO is determined.

A range of spear valve positions was examined, and their effect on pressure build-up in different sizes of RO units was evaluated. An algorithm was developed to conduct this evaluation with water demand and wind speed as input. The objective was to identify the ideal spear opening and RO size for the area of interest. The optimum combination of the system's setup is assumed to consist of a spear valve opening and the minimum RO size that can fully cover the requirement for water production under the specific spear position. The RO size can be further limited by implementing buffer storage according to the water requirement. A suitable control line can be chosen to operate the system in accordance with a predefined wind and water demand. Water production is anticipated to fluctuate at each time step in accordance with the system sizes and limits since the wind conditions are acquired as a discrete value dataset over the course of a year.

Chapter 6

DOT500 PRO Model Simulation and Results

The equations and proposed operating scheme described above were used to develop an algorithm for solving flows and pressures in the DOT500 PRO system. This algorithm simulated static scenarios of different wind speeds, spear valve positions and RO sizes, the results of which are presented and analysed in the present chapter.

6.1. System Operation

The algorithm developed in Python aims to provide insight into the steady-state behaviour of the system and the possibility of implementing the proposed operating scheme. The behaviour of the system will be established by investigating the pressures and flows developed by different wind speeds, spear valve opening and reverse osmosis sizes. The wind speeds bins belong to the range between the cut-in and rated wind speeds of the 500kW wind turbine. According to Figure 5-5, only the system load curves that belong to the stable region are taken into consideration in order to avoid the undesired operation of the wind turbine.

The system has to respect the operational and manufacturing limits of its components with the hydraulic ones being the maximum pressure limit of the membranes and the nominal flow rate of the high-pressure pump. These limits will determine the wind speed at which the pitching will start. As mentioned before, the principle that will be followed dictates the constant spear valve opening throughout the whole system operation. The intention is to attain the system constraints at the same wind speed to enable the pitch controller alone to maintain constant operation without the requirement for a bigger nozzle opening.

In the following figures, the operation of the system will be presented in terms of pressures and flows in order to understand its behaviour and assess the performance of the operating strategy. A reference RO unit of six pressure vessels containing six membranes is used for the following analysis. As regards the system operation under discrete variable winds, two nozzle positions are presented for the sake of understanding the influence of the spear valve opening to the system with increasing wind speed. This will provide insight into the developed pressures and flows in the system for every combination of wind and valve position that consequently will set the key criteria based on which the proposed operating scheme will select the optimum opening according to site-specific input. Figure 6-1 shows the pressure curves along the examined wind speed range for the fully open spear valve ($s = 0\% \cdot s_{max}$) and for the one that produces a load closest to the stable operational curve of the turbine without exceeding it. Therefore, two limits of the spear valve are presented in the following analysis, with the nozzle at $s = 68\% \cdot s_{max}$ indicating the maximum allowable positioning of the spear. It is important to note that the valve opening counts from the position s = 0 mm, indicating a fully open valve while the fully closed valve is achieved at $s_{max} = 39.5$ mm.
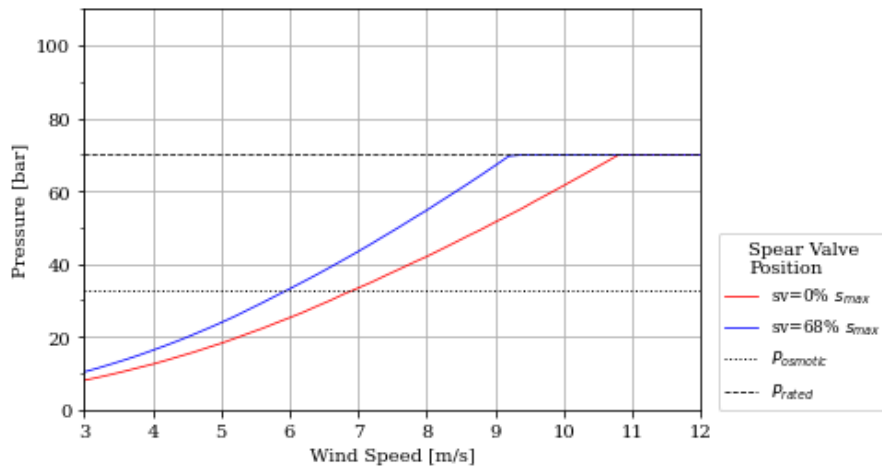
Figure 6-1: *Pressure on the system corresponding to fully opened and 'stably closed' position of the spear valve.*

As seen in Figure 6-1, the red curve shows the pressure evolution for increasing wind speed with a fully open spear valve, while the blue one depicts the closed valve at $s = 68\% \cdot s_{max}$. The pressure build-up of the system with the smaller opening is higher than that of the system with the open valve. This derives from the fact that for the same wind speed, the open valve allows for more flow to travel through its nozzle. As we restrict the effective area of the spear valve, the flow entering the Pelton turbine decreases and therefore the pressure on the line before the nozzle increases. As the pressure increases faster with the wind in the case of the restricted opening, the osmotic pressure is reached at a lower wind speed (6 m/s). The same applies to the rated pressure limit on the membranes (70 bar), which is reached at lower wind speed in the case of the closed valve at $s = 68\% \cdot s_{max}$. The pressure behaviour per wind speed and spear position indicates that water production can start at a lower wind speed when engaging the maximum allowable spear positioning ($s = 68\% \cdot s_{max}$). This translates into achieving the rated pressure of the RO membranes at a lower wind speed compared to the case of an open valve.

This behaviour provides the first indicator regarding the pressure operational window of the water production system. The examined strategy will define the optimum spear valve position that will be implemented for the required operation as a trade-off between the pressure operational window of the RO module, taking into consideration the wind speed of the location and the RO size that will cover the water demand. The pressure limit of the RO module is not influenced by the size of the unit, which is defined by the number of membranes. This is due to the parallel connection between the RO vessels that dictates equal pressure in the connected lines. However, the more the pressure vessels, the higher the maximum flow allowed to travel through them. Hence, the RO size, may not influence the pressure limit but it directly affects the flow that is allowed to enter the RO module and the remaining flow that will be driven to the Pelton turbine. The interaction of the flow variations with the pressure built-up for each spear valve position and size of RO unit is accounted for and evaluated for the induced water production by the proposed operating strategy in order to define the appropriate combination of the examined parameters.

The flow rates of the system consist of the total flow produced by the high-pressure pump which is divided into two flow streams driven to the RO module and electricity production unit. The system flow rates are presented per spear valve opening and wind speed in Figure 6-2 below.
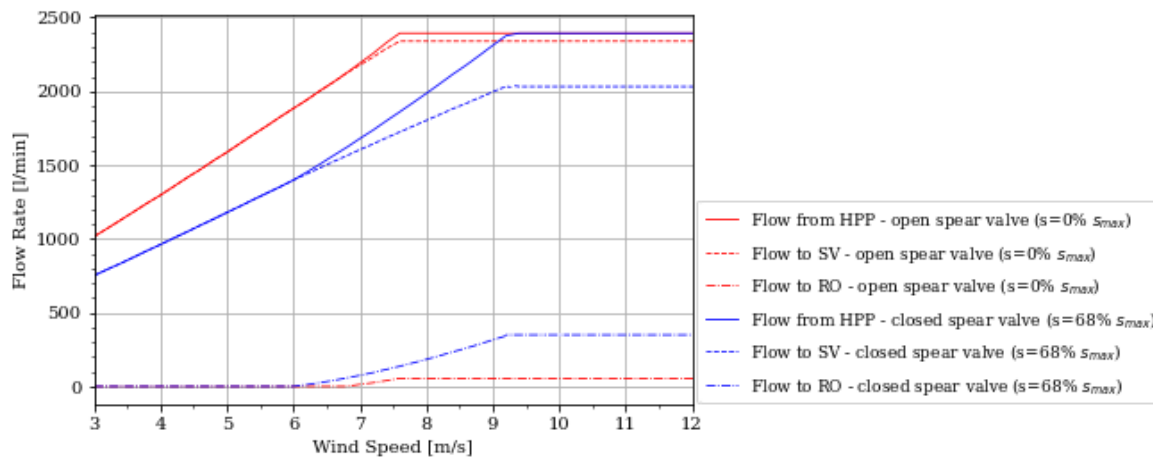
Figure 6-2: Flow rates corresponding to fully opened and 'stably closed' position of the spear valve.

The red lines indicate the flow rates developed in the system by maintaining the spear valve in open position. The solid lines correspond to the total flow provided by the high-pressure pump and reach a plateau at the maximum flow rate of the Kamat pump at 2394 l/min. Before this limit is reached, the flow rate from the HPP exhibits linear behaviour since the positive displacement pumps provide constant flow at fixed wind speeds. A positive displacement pump transfers a fluid by periodically enclosing a fixed volume and mechanically moving it through the system with the use of seals or valves. As the wind speed increases, the rotor rotates faster, which increases the rotational speed of the wind turbine and the high-pressure pump, according to Equation (4.3). The flow rate produced by the high-pressure pump is linearly related to its rotational speed and therefore is linearly rising with increasing wind speed. Opposite to the pattern of the pressure over the wind speed range for the two spear positions, the flow rate from the HPP is lower for the closed valve. This derives from the fact that the pump is forced to operate at higher outlet pressure due to the restricted flow at the nozzle. Before the water production can start, the high-pressure pump is forced to deliver a flow rate equal to the amount allowed to flow through the nozzle. Therefore, if the nozzle is restricted, the pressure in the line after the pump increases and the flow provided by it has to reduce to fit through the area of the nozzle.

Regarding the flow through the RO unit, the valve with the smallest effective area ($s = 68\% \cdot s_{max}$) reaches the required pressure at a lower wind speed and water production can start faster (at 6m/s). This indicates that the pump is freed to have a higher flow rate at its outlet to feed the RO membranes. The rate of change (slope) of the flow entering the RO is the same for both valve positions, owing to the RO unit size. The flow through the nozzle for a given wind speed follows the same rate of increase as the one before water production, meaning that the flow entering the Pelton turbine is only dictated by the spear valve opening and system pressure. The flow through the RO unit increases until the flow limit of the RO is reached and is added to the HPP flow. For the wind speed at which the pressure or flow limit is reached, pitching is activated to maintain constant operation. For the system with the open valve, the flow limit of the Kamat is reached at 7.5 m/s according to Figure 5-5. Therefore, the system is forced to maintain its operating points at low wind speed which results in low water production. For the system with the restricted valve opening, the membranes' rated pressure is reached at a higher wind speed (9.2 m/s), which allows for an enlarged water production window between 6 and 9.2 m/s. However, none of the above-presented nozzle openings drives the system to reach its limits simultaneously, which would happen at higher wind speed, according to Figure 5-5. This indicates that there is an ideal operational curve between the lowest and greatest valve openings, which allows for water production to occur over a wider range of wind speeds.

6.2. Operating Conditions

6.2.1. Influence of Nozzle Area

In order to reach a conclusion regarding the effectiveness and the benefits of selecting a curve that attains the hydraulic limits at the same wind speed, the behaviour of the system at different conditions has to be compared. Pressures and flows of the DOT500 PRO are plotted against a range of nozzle positions from fully open at $s = 0\% \cdot s_{max}$ until the closed position at $s = 68\% \cdot s_{max}$, for wind speeds between the cut-in and rated. Figure 6-3 presents the pressure developed in the system at all nozzle positions and wind speeds.

The bottom curve represents the cut-in wind speed and the top one represents the rated wind speed of the wind turbine. It can be observed that for increasing wind speeds, as the nozzle moves to the 'stably closed' position at $s = 68\% \cdot s_{max}$, the pressure built-up is higher. The pressure in the system for the wind of 3 m/s is low for all valve openings, due to the intersection of all pump-nozzle curves with the turbine-pump curves at low-pressure points, as shown in Figure 5-5. As the wind speed increases, the pressure-flow curves of the turbine-pump system capture a bigger area allowing for the above-mentioned intersections to occur at higher pressure.
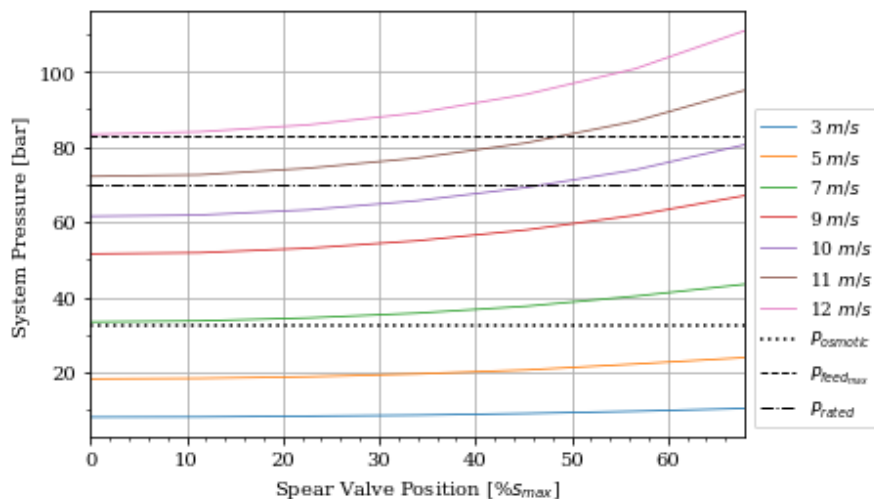
Figure 6-3: System pressure at all nozzle positions and different discrete wind speeds.

The graph is limited to the maximum allowable restriction in the effective area of the valve in order to avoid the unstable operational region of the system. This region is depicted by the pressure-flow curves of the pump-nozzle system that exceed the optimum torque line, as seen in Figure 5-3. At that region, the aerodynamic torque increases with increasing rotational speed and consequently system pressure gets higher as the flow in the HPP rises. Moreover, the intersection points occur at very low pressure for low wind and there is no intersection point for higher wind speeds. This would cause a sudden drop in the pressure and consequently halt the operation of the RO unit.

As regards water production, the osmotic pressure can be reached by an open valve at 7 m/s while the more restricted valve allows for the operation of the unit at lower wind speeds. Additionally, the rated pressure at 70 bar is reached at a lower wind speed for a restricted nozzle, as followed by the pressure development seen in Figure 6-1. The RO is recommended to operate at constant high pressures close to the rated to avoid damage in the membranes due to sudden pressure fluctuations causing exceedance of the maximum allowable pressure (82.7 bar). Following, the flow rates of the high-pressure pump are presented for different nozzle positions and wind speeds.
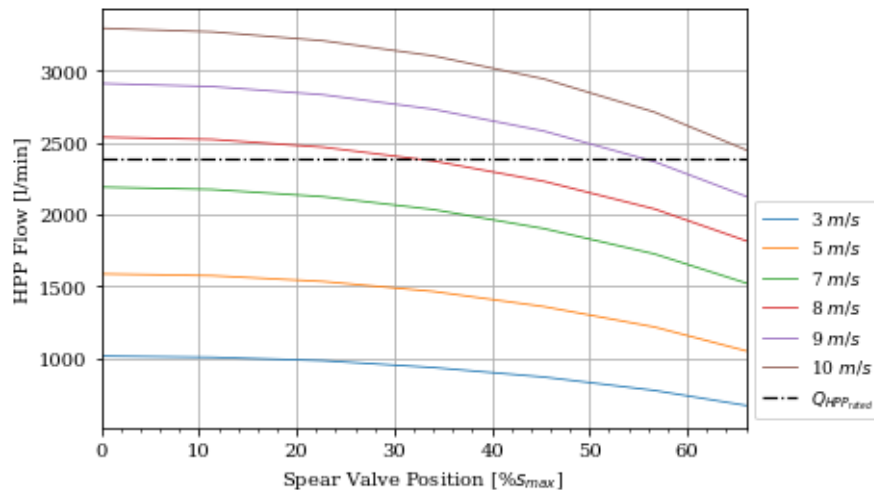
Figure 6-4: *Flow from the HPP at all nozzle positions and different discrete wind speeds.*

The flow rate of the high-pressure seawater pump is directly proportional to the rotational speed of the high-speed shaft of the hydraulic drive train, which is connected to the rotor. The higher the rotational speed of the rotor, the higher the rotational speed of the high-pressure pump, which leads to a higher flow rate from the pump to either the RO unit or the Pelton-generator module. In Figure 6-4, the fully open position of the valve allows for the maximum flow that the pump can produce at each wind speed. This derives from the fact that the intersection of this nozzle curve occurs at the highest rotational speed of each fixed wind speed. The delivered flow reduces as the valve travels towards the restricted valve position, reaching the minimum amount of water that the pump can deliver for each wind speed. This explains the decreasing trend in the flow rates of each wind speed for decreasing the effective nozzle area.

It can be observed that the flow produced from wind speeds above 7 m/s may exceed the flow limit of the high-pressure pump. For a fully open valve, the flow limit of the pump is reached at 7.5 m/s, while for the closed valve the limit is reached at around 10 m/s. If the exceedance of the flow limit occurs before the rated membranes' pressure is reached, then this wind speed represents the rated of the system and pitching is activated. By comparing the wind speeds at which the limits are reached for all nozzle openings, the one that drives the system at the required point of attaining the constraints simultaneously was recorded. For the spear position of $58\% \cdot s_{max}$, the flow limit is reached at 9.44 m/s which is the same wind speed at which the pressure limit is reached.

Table 6-1 presents the wind speeds at which the pressure and flow constraints are attained for different spear valve openings. Most valve openings drive the system to reach the flow limit of the pump at a lower wind speed than that of the rated pressure resulting in representing that wind speed as the system's rated. The closed valve at $s = 68\% \cdot s_{max}$ produces an operational curve that reaches the pressure limit of the membranes faster than the nominal flow from the pump, setting the lowest wind speed as the rated of the system. As for the curve derived from an opening of $58\% \cdot s_{max}$, the limits are reached at the same wind speed, indicating that this opening is required for the proposed strategy for the specific RO size (six vessels with six membranes). Moreover, the rated wind speed dictated by that opening (9.44 m/s) is higher than all the rated wind speeds set by the smaller and bigger nozzle openings. Consequently, this opening and its corresponding pump-nozzle curve appears to be the one that allows water production over a broader range of wind speeds. The extended table for all valve openings is included in the Appendix B.

Table 6-1: Wind speeds at which water production begins and the hydraulic limits are reached for specific valve openings.

Spear valve opening [% of s_{max}]	Wind speed at which water production may occur [m/s]	Wind speed at which the membranes' rated pressure is reached [m/s]	Wind speed at which the nominal pump flow is reached [m/s]
s = 0%	6.92	10.62	7.61
s = 20%	6.76	10.50	7.96
s = 40%	6.28	10.08	8.45
s = 58%	**6.01**	**9.44**	**9.44**
s = 68%	5.88	9.25	10.62

For a fully open valve, the system can produce water for wind speeds above 6.92 m/s, while for the closed valve above 5.88 m/s. Water production is not possible at wind speeds below the abovementioned for the corresponding nozzle openings. As the wind increases, water can be produced for a broader range of spear valve positions. This is explained due to the intersection of more pump-nozzle curves with the envelop pressure-flow curves above osmotic pressure for increasing wind speed. Between the 'stably closed' and fully closed valve positions, water production is not possible due to the operation of the turbine at very low tip speed ratios. This results in turbine operation at low rotational speeds, leading to low torque and pressures below the osmotic.

The flow in the reverse osmosis unit is equal to the permeate flow, as explained in Equation (4.22) due to the presence of the energy recovery device. Permeate flow is a function of the pressure entering the RO module, the characteristics of the membranes and the osmotic pressure. System pressure rises as the valve moves closer to the closed position, increasing the quantity of freshwater the RO unit can generate. Consequently, the flow entering the RO module increases with the same trend as the one followed by the pressure in Figure 6-3 (see Figure B - 1). In this instance, a six-by-six RO unit is considered, resulting in a RO flow limit higher than the high-pressure pump's limit. The flow from the high-pressure pump is divided into streams to the RO and the Pelton-generator unit. The flow to the RO unit is significantly lower than the total provided by the pump, and therefore the remaining flow driven to the Pelton turbine follows the pattern of the total flow. The flow through the nozzle is a function of system pressure and nozzle opening. Even though the pressure in the system increases with decreasing nozzle area, the nozzle area effect on the flow to the Pelton turbine is much higher. The pressure and flow rate of seawater through the spear valve can be converted into torque and rotational speed of the Pelton wheel. The power extracted by the generator is a function of the torque and rotational speed of the wheel and is limited by the capacity of the ge6nerator at 200 kW.

6.2.2. Influence of RO Size

One of the main parameters that may influence the flow limit of the system is the size of the RO unit. As the number of membranes and vessels employed decreases, the flow allowed to enter the desalination unit decreases and the system's flow constraint is reduced even further than the nominal flow of the high-pressure pump. Therefore, the appropriate valve opening that ensures the achievement of the hydraulic boundaries at the same wind speed depends on the size of the desalination unit connected to

the system. The following figures present the rated wind speed, maximum water production, power generation and consumption of the system for different RO sizes and spear valve openings.

The reverse osmosis unit consists of spiral-wound membranes enclosed in series inside the RO vessels, which are connected in parallel to each other. The stream combining the ERD flow is divided into parallel-connected lines leading to the vessels. Each vessel may contain six to eight membranes with their connection pieces. The RO size is measured by the total number of membranes contained in the module. The following table mentions the number of vessels and membranes considered for the evaluation of the proposed operating strategy.

Table 6-2: *Number of RO vessels and membranes for the numerical evaluation of the proposed method.*

Parameter	Range [-]
Number of RO Vessels	1 … 10
Number of RO Membranes	6 … 8

The range of vessels was selected arbitrarily to include the lowest possible RO module that could be implemented in the system. The number of membranes contained in each vessel has to account for the desired recovery rate and permeate production. An optimal recovery rate can be achieved with more than six membranes in a series. However, this parameter is limited by the recovery rate and the pressure build-up inside the membranes. As the number of membranes inside a pressure vessel increases, the recovery rate achieved rises, leading to higher salt concentration. According to Figure 6-5, a recovery rate of 50% induces double salt concentration. Therefore, if a high recovery rate is achieved before the vessel's outlet, salt deposits may occur and damage the membranes. Besides, as more membranes are placed in series, the pressure build-up at the end of the container is higher, leading to higher pressure requirements at the inlet of the unit to ensure that reverse osmosis can occur across the whole length of the vessel. This indicates that higher wind speed is required for water production, and the available range of operational wind speeds for permeate production is reduced. Due to these, the maximum number of membranes in series is limited to eight in each RO vessel, while a further rise in the RO size would require additional pressure vessels [51].
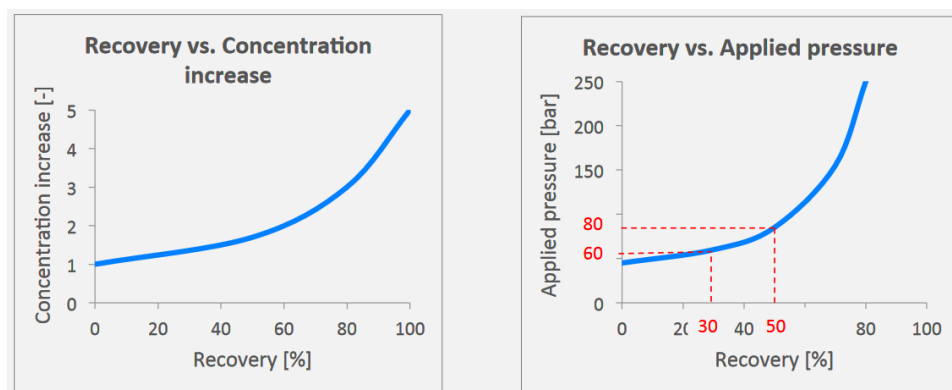
Figure 6-5: *Salt concentration and pressure build-up in the membranes against the recovery rate.*

The internal layout of the reverse osmosis unit is an important parameter that can be chosen while designing the system to modify the model according to the requirement of a particular location. The effect of different RO sizes and their associated flow rates will be considered to analyse the influence on the proposed operating strategy. Given that the membranes are connected in series inside the vessels,

the maximum allowable flow through a single container is defined as the nominal flow in each membrane. The vessels are connected in a parallel layout, which indicates that the maximum flow through the whole desalination module is defined as the maximum flow through the membranes multiplied by the number of vessels. Therefore, the highest allowable flow in the RO system depends on the number of vessels and not the number of membranes contained in each vessel. Figure 6-6 depicts the increase in the allowable flow for increasing the number of RO vessels in comparison with the flow limit of the high-pressure pump.
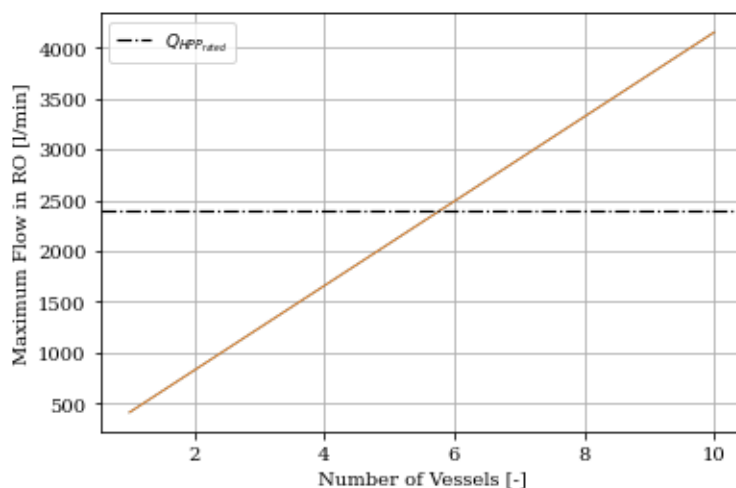
Figure 6-6: Maximum flow allowed in the RO unit for different number of parallel RO vessels.

The amount of water allowed to enter the RO unit is directly proportional to the number of vessels that are part of the RO layout. This explains the linearly increasing nature of the maximum flow in the RO for an increasing number of vessels. Moreover, the number of RO containers defines the general flow limit of the system. For a system containing more than six RO vessels, the flow limit is represented by the ultimate flux of the pump. For a system containing less than six RO vessels, the membranes pose an additional limit to the system with their maximum flow rate. If the flow allowed in the RO decreases further and is reached before the rated pressure or the total flow from the pump, the corresponding wind speed will be considered as the rated of the system.

The wind turbine has a rated wind speed of 12 m/s, which alters according to the operational limitations set to the system. This strategy imposes that the rated wind speed will be represented by the wind at which one of the two hydraulic limits is reached. It is evident that this concept will decrease the original rated wind speed of the turbine according to the system parameters, such as the RO size and spear valve position. According to the previous analysis of the spear valve positions, the optimum valve opening is the one that drives the system to reach both of its limits at the same wind speed. This approach will allow the system to operate for a wider range of wind speeds and extend the point at which it reaches its limits.

In Figure 6-7 (a), three valve openings are depicted, which correspond to the operational curves that reach the flow limit of the Kamat pump before the rated pressure of the membranes. For nozzle openings between $0 - 50\%$ of s_{max}, the rated wind speed reduces with increasing RO size due to the decreasing slope of the pump-nozzle curve, as seen in the qualitative Figure 6-7 (b). Increasing RO size allows for a higher flow rate at a given pressure or a fixed wind speed, implying that more permeate production is possible as soon as the osmotic pressure is achieved. As the curve negatively inclines, the nominal flow of the pump is reached at a lower wind speed, therefore reasoning the drop of the rated wind of the system. Further increase in the RO size could lead to pump-nozzle curves with slighter slopes, which

would indicate that the nominal flow of the pump would be reached at pressures just above the osmotic. Such a behaviour would not be realistic or efficient as it would significantly limit the range of wind speeds at the value for which water production is starting. This must be accounted for when increasing the RO unit, as it may promise higher inlet and outlet flows, but these may never be achieved. The algorithm, aiming to provide the appropriate RO setup for a particular location, accounts for the system's behaviour at increasing RO size to ensure that the demand is covered with the available wind resources.
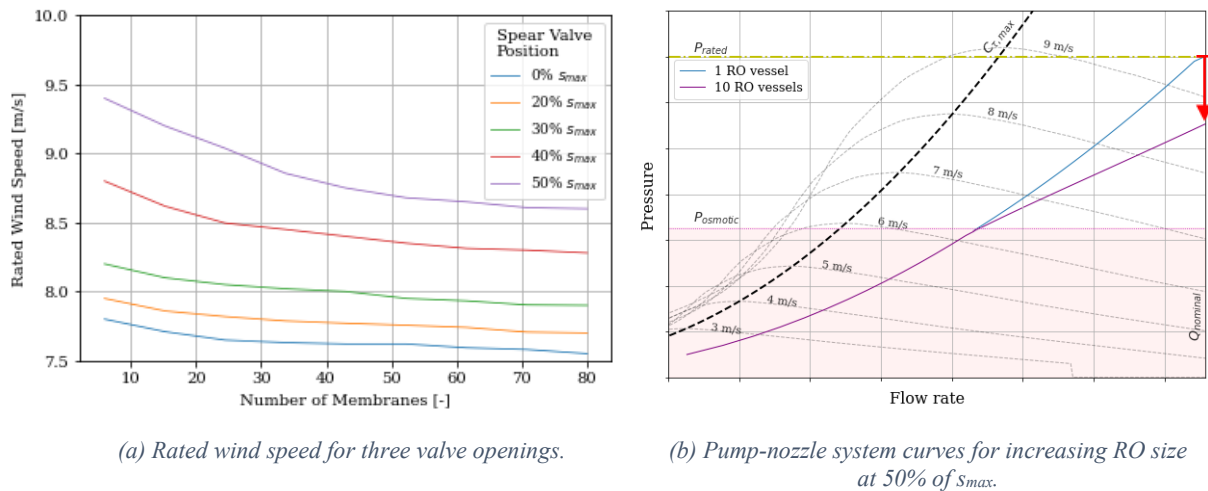

(a) Rated wind speed for three valve openings.   *(b) Pump-nozzle system curves for increasing RO size at 50% of s_{max}.*

Figure 6-7: *Rated wind speed for spear valve positioning between 0% – 50% of s_{max} for different RO sizes.*

The abovementioned behaviour is met only in the spear valve openings that force the system to reach the flow limit of the pump before the rated pressure on the membranes. For further closing the valve, the system attains the rated pressure on the membranes, with the pump performing below its nominal capacity. The case of $58\% \cdot s_{max}$ is examined due to its performance for the 6x6 RO configuration. At this setup, closing the valve at $58\% \cdot s_{max}$, drove the system to reach its flow and pressure limits at the same wind speed, corresponding to the highest rated wind speed of that RO setup. With a closer look at the reason behind this behaviour, Figure 6-8 (a) shows the evolution of rated wind speed for the specific valve opening, while its corresponding curve path is depicted in Figure 6-8 (b). By following the pump-nozzle system curves, the addition of pressure vessels decreases the slope of the flow-pressure relation above the osmotic pressure. Regarding the RO unit with one sole pressure vessel, the spear valve opening drove the integrated system to reach the rated pressure of the membranes before the Kamat provided its nominal flow. Therefore, by putting additional parallel RO vessels, the slope decreases until the nominal flow of the pump is also reached. At that point, both limits are attained at a higher wind speed (9.44 m/s), which corresponds to the optimal point of the proposed strategic scheme for the specific RO setup. This behaviour is explained due to the parallel connection of the RO pressure containers that dictate a single pressure and cumulative flow rate throughout the unit. Further addition of RO vessels leads to the behaviour described in Figure 6-7, where the rated wind speed decreases as the flow limit of the pump is attained first. Hence, for each RO size, the highest operational wind speed corresponds to the point at which both hydraulic limits are obtained simultaneously. The peak in Figure 6-8 (a) corresponds to the RO setup of 6x6, which confirms that the specific opening is the one allowing for a wider range of wind speeds to develop before pitching is activated for this desalination unit size.
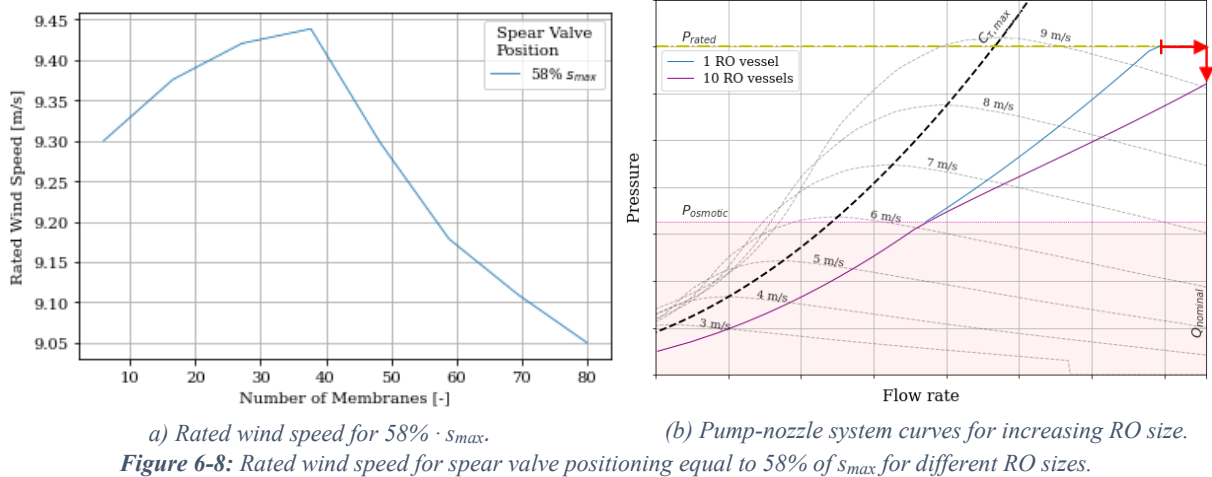
a) Rated wind speed for 58% · s_max.

(b) Pump-nozzle system curves for increasing RO size.

Figure 6-8: *Rated wind speed for spear valve positioning equal to 58% of s_max for different RO sizes.*

As regards the valve that corresponds to the positioning of $68\% \cdot s_{max}$, an increase is observed on the rated wind speed that is adopted by the system, as seen in Figure 6-9 (a). This spear position dictates that the system is operated as it would have been under the influence of the optimum torque coefficient of the wind turbine. Therefore, the sole electricity production would follow the path defined by $C_{\tau,max}$ with an offset to ensure turbine stability. The implementation of one RO pressure container would lead to a small inclination of the curve towards higher flows, therefore slightly diverging from the relative approximation of the $C_{\tau,max}$ curve. This results in attaining the rated pressure at a relatively high wind speed with a flow rate below the nominal flux from the pump. The implementation of ten RO pressure vessels will only increase the flow through the membranes and the wind speed at which the rated membrane pressure is met. More specifically, the point at which the limits are attained for the same wind speed will not be reached for the simulated range of RO pressure containers for the specific valve opening. Therefore, according to the curves' path and increasing flows, an ascending course of the system's rated wind speed can be observed.
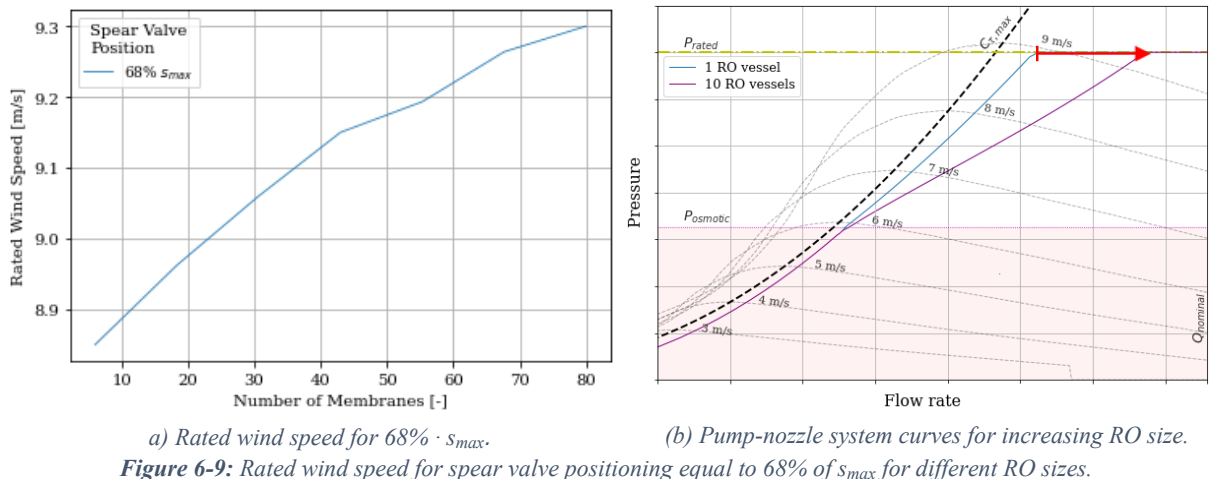
a) Rated wind speed for 68% · s_max.

(b) Pump-nozzle system curves for increasing RO size.

Figure 6-9: *Rated wind speed for spear valve positioning equal to 68% of s_max for different RO sizes.*

According to the paths of the pump-nozzle system curves for increasing RO size, the spear positions that force the system to firstly reach the flow limit of the pump will develop decreasing wind speed. On the contrary, the spear positions, which allow rated membrane pressure to be succeeded before the nominal pump flow, lead to increasing rated wind speed for increasing RO size. Every spear position in between results in an evolution of the rated wind speed that matches the pattern shown in Figure 6-8 (a), including the most suitable spear positioning for the simulated RO configurations. In Figure 6-10, the rated wind speeds of the system are depicted for spear positions above $40\% \cdot s_{max}$, for the sake of comparison. As can be seen, the spear positioning between 0 and 40% of s_{max} dictate pitching at lower

wind speeds compared to the more restricted nozzle openings. For the RO module containing one vessel with six membranes, the opening of $50\% \cdot s_{max}$ corresponds to the most appropriate of the system, as it reaches the highest rated wind speed compared to a wider and more restricted nozzle. The rated wind speeds dictated by the openings of $58\% \cdot s_{max}$ and $68\% \cdot s_{max}$ intersect when 56 membranes are utilized. From that RO size, the 'stably closed' valve allows for a wider range of wind speeds to develop before pitching is activated.
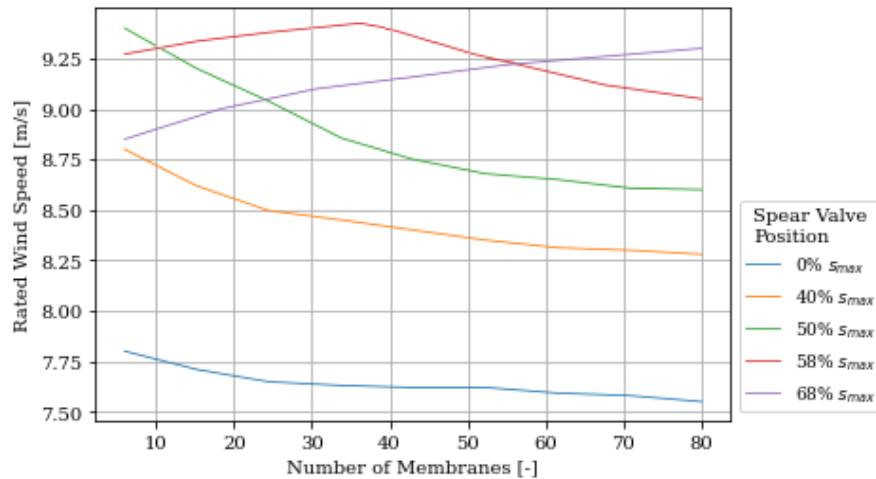
Figure 6-10: *Rated wind speed as defined from the wind at which the first hydraulic limit is reached for different number of RO vessels and nozzle openings.*

The rated wind speed behaviour depicted in Figure 6-10 confirms that for each RO size, a different spear positioning between 50% and 68% may be considered suitable regarding water production and wind speed harvesting range. This can be explained by the peak wind speed for every spear opening at the corresponding RO sizes. For the smallest RO unit with one vessel and six membranes, the valve put at 50% of its maximum travelling distance allows for a wider range of wind development. For the biggest RO unit examined (10x8), the 'stably closed' valve allows for a wider range of wind speeds to be extracted. For desalination units between the abovementioned magnitude, a spear positioning between 50% and 68% of the maximum distance can be considered the optimum for wind harvesting. For instance, the case of six vessels with six membranes has an optimum opening of $58\% \cdot s_{max}$.

As regards the amount of freshwater produced by each RO unit, Figure 6-11 presents the maximum permeate that can be produced at rated conditions for each spear positioning. The rated wind speed and the operational points it dictates will determine the pressure and flow into the Pelton-generator and RO units. The flow driven to the RO is equal to the permeate produced due to the existence of the energy recovery device. A restricted valve enables for higher pressure build-up at lower wind speed, leading to augmented permeate production. In Figure 6-11, as the valve travels towards the closed position, the maximum permeate produced at the rated wind speed increases.
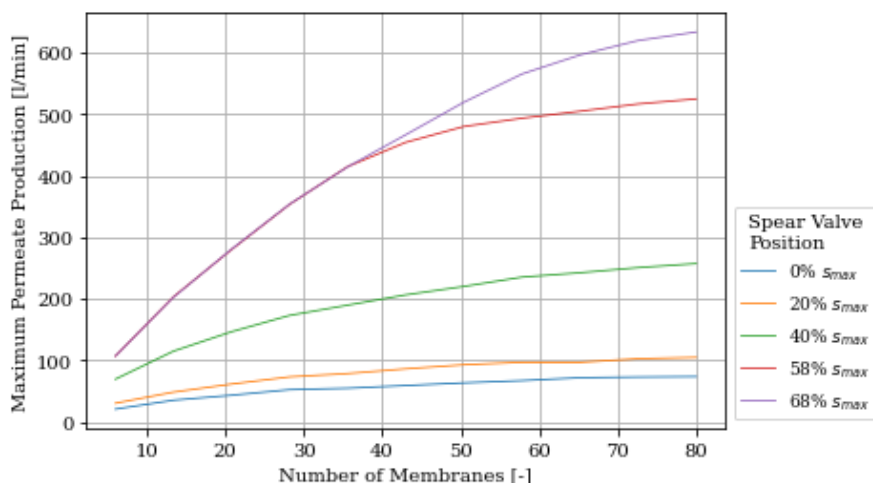
Figure 6-11: *Maximum permeate production for different RO sizes and nozzle openings.*

At rated conditions for the spear positions between $0 - 40\%$ of s_{max}, the flow entering the RO unit remains constant while the pressure is higher for the valve that has moved further. Therefore, it is anticipated that a system incorporating a restricted nozzle will deliver more permeate than a system with a fully open spear valve. Moreover, the cumulative number of membranes in the RO unit affects the amount of water in the module's inlet and the amount of freshwater delivered. Regarding the opening of $58\% \cdot s_{max}$, two regions are considered, defined by the RO size that forces the simultaneous attainment of the flow and pressure limits. For increasing RO sizes smaller than 6x6, the system has attained its rated pressure and increases its flow into the RO as more membranes and vessels are added. For RO sizes bigger than 6x6, as more membranes and vessels are integrated into the system, the same flow is achieved at a lower pressure. As a result, even if the desalination unit allows for more flow, the flow limit of the pump is reached at lower pressure. The increase in flow through the RO combined with the relatively slighter decrease in pressure explains the difference in the slope of the permeate production path. As the operational curve passes through the attainment of the rated pressure to the flow limit of the pump, the rising rate of produced freshwater reduces. This behaviour – a relatively lower growth rate – can be observed in the spear positions between $0 - 40\% \cdot s_{max}$, which firstly reach the pump's flow limit for all the examined RO sizes.

Concerning the opening of $68\% \cdot s_{max}$, the rated permeate production notes a sharp growth rate, as the membranes' rated pressure limit is firstly attained for all RO sizes considered. As evident, for RO sizes and valve combinations that allow for the sole attainment of membranes' rated pressure, the flow towards the RO unit depends only on the RO flow requirements and not the spear positioning. This explains the similar paths of the two closed valve positions described by 58% and 68% of s_{max}. At the point where the flow limit of the high-pressure pump takes the lead, permeate is produced at a slower rate than before. However, if the operational curve does not fall into the case of initially reaching the flow limit of the Kamat, the permeate production pace remains constant.

6.2.3. Discussion

The examined reverse osmosis sizes and spear positions raised the conclusion that the spear openings allowing the system to operate without pitching for the wider range of wind speeds lay between 50% and 68% of s_{max}. However, water production is not only depending on the wind speed at which the system operates without pitching, because even after that value of wind, the system is operated at constant flows and pressures, producing fixed amount of freshwater. Therefore, the appropriate RO size

has to be combined with the freshwater production enabled by each opening not only during rated conditions but also during the site-specific wind speed.

The developed algorithm takes into account the wind speed of the location and adjusts the system such that the produced permeate can cover the demand even though a higher amount of freshwater could be delivered with a different RO size. The proposed configuration is a function of both the capabilities of the system dictated by its RO size and valve opening and the required demand. One of the goals is to find the minimum RO module that will allow for the coverage of specific water requirements. The algorithm compares the performance of each system setup and proposes the minimum RO size and the corresponding valve opening that can cover the demand.

Finally, the algorithm accounts for both the operational range of wind speeds without pitching and the pressure build-up at each wind speed. These conditions have to be combined while deciding the suitable RO arrangement and its corresponding spear position, as a more restricted nozzle will allow for faster pressure increase at lower wind speed, even though the rated wind speed is lower. This trade-off has to is accounted for during the simulation of the case study, as the real offshore wind data may present extended periods with lower than the rated wind speeds. In these eventualities, water demand would be covered by a restricted nozzle that allows for the required pressures to be attained at lower wind speeds.

Chapter 7

Application on Agios Efstratios

The application of the DOT500 PRO system was examined in Agios Efstratios island, located in the North Aegean Sea. Agios Efstratios is expected to face water shortage shortly, as established by the National Operational Plan for Drinking Water in 2022. Moreover, due to the high wind resource availability, Agios Efstratios can accommodate wind turbines of various ranges. According to the analysis of wind characteristics, the wind speed recorded in 2021 is used to define the best combination of spear valve opening and reverse osmosis configuration for Agios Efstratios Island. The hourly wind data is converted into rotation of the high-pressure pump and then pressures and flows, specifying the hourly water production for every combination of the simulation parameters. The hourly permeate production is converted to daily and weekly to check whether the seasonal water demand is reached. The combination of RO size and valve opening that meets the freshwater requirements over a year will be considered suitable for the location.

The developed algorithm in Python provides the appropriate solution for the location according to the minimum amount of site-specific input data, namely the annual wind speed and seasonal freshwater requirements. The selection of the minimum desalination size that can cover the demand consists of a trial-and-error process, which calculates the water production per wind input. The wind input consists of hourly data translated to hourly produced permeate. The winter and summer water requirements of Agios Efstratios are obtained daily, and therefore the daily production is of interest. However, offshore wind is characterised by periods of extreme events with high or very low wind speeds, leading to consecutive days of wind speed inadequate for water production. In such a case, it is evident that the RO size would not influence the permeate production, and the demand would not be covered. To account for such occurrences, the daily output must be converted to weekly, which is then compared against weekly requests. The logic of the developed algorithm in Python (Spyder software) is presented in Figure 7-1.
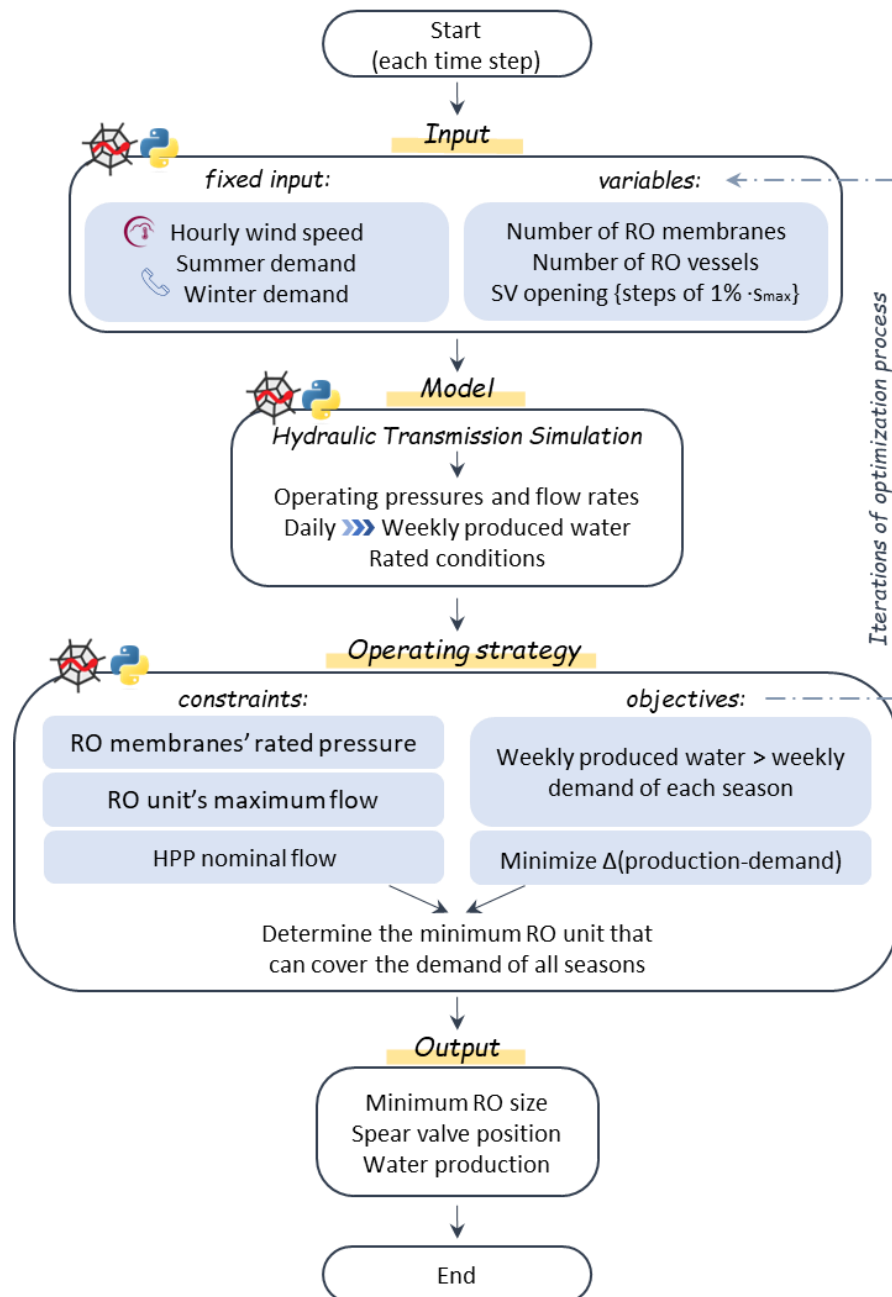
Figure 7-1: Schematic of the overall algorithm logic in Python.

The conversion of daily produced water to a weekly production will be referred to as weekly coverage period. This could be understood as an intermediate tank between the reverse osmosis module and the water grid. In this tank, the daily produced permeate would be collected for a week before its distribution to the network. In the case of a weekly coverage period, the size of the tank has to be equal to the amount of permeate produced in a week in order to account for the extreme event where only one day of the week allows for water production, which is such that can cover the whole demand. In this scenario, the RO size simulated is considered adequate, and the tank should be able to collect it and distribute it to the island's water grid. Consequently, the weekly permeate production by each RO size will be compared to the weekly freshwater demand of every season in order to define the minimum RO arrangement that can meet the water requisition. Each seasonal demand, as defined by the municipality of the island, will be compared to the water production of the wind speed corresponding to the respective period. The coverage period at which the algorithm converts the daily production and demand influences

the minimum appropriate RO configuration. The more the membranes included in the desalination unit, the more permeate is produced for each wind speed. The spear positioning is engaged to define the minimum RO size that can cover the demand, which has been converted to weekly. The spear valve openings count from the fully open position with an increment of 1% of s_{max} until the closed position that tracks the optimum torque operating curve of the turbine ($s = 68\%$ of s_{max}). The following figure shows a detailed schematic of the operating strategy and the iterations executed for the determination of the appropriate set of variables, which consists of the RO unit size and the spear valve opening.
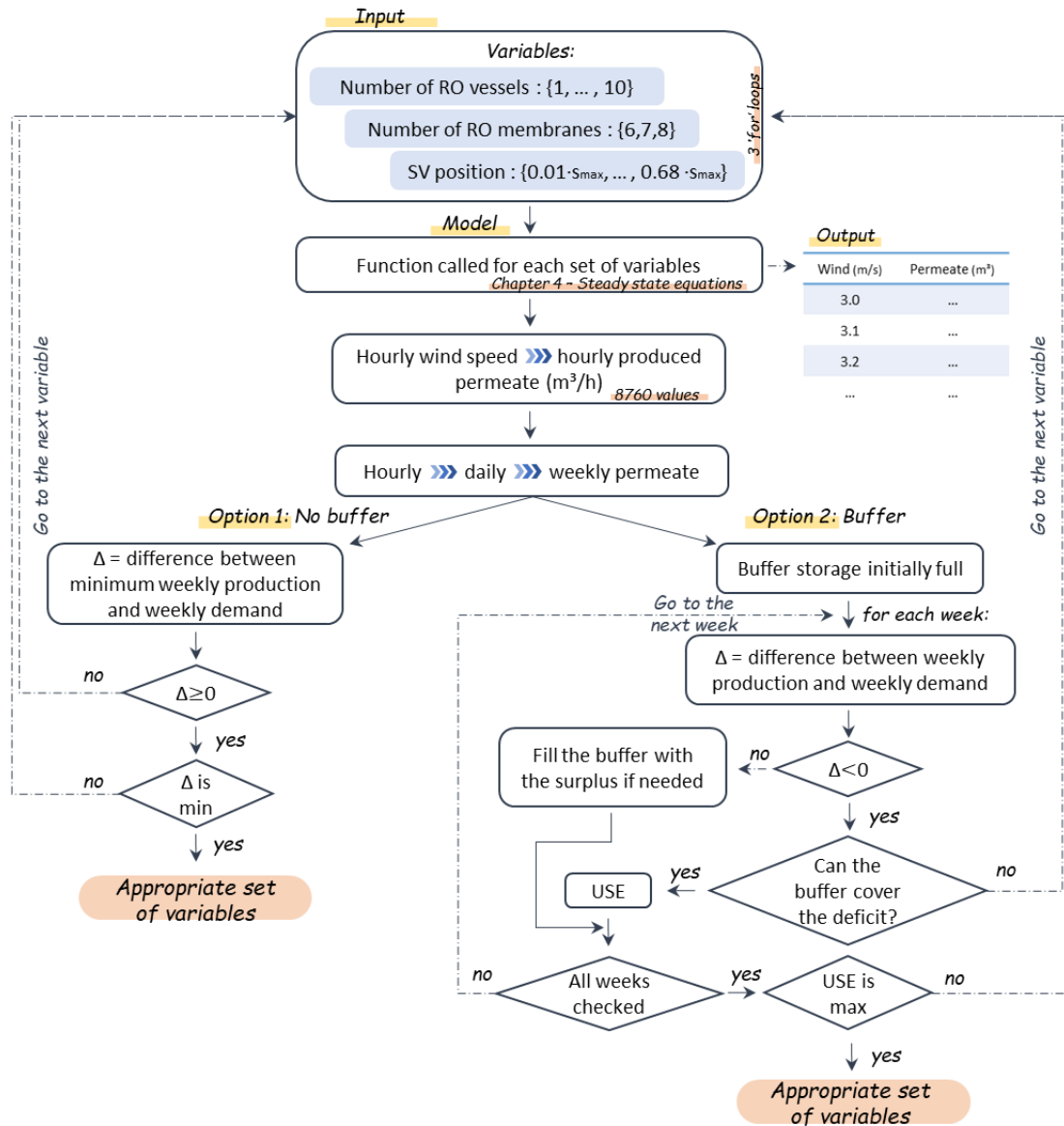
Figure 7-2: Detailed schematic of the operating strategy process that delivers the appropriate set of variables.

In order to decrease the required RO size, buffer storage could be implemented in the system between the unit and the grid. This buffer tank would save the excess produced water for a week or more to allow for a different RO size. By decreasing the RO unit, the produced permeate per wind speed declines, causing a daily deficit. However, due to the variability of offshore wind, there might be consecutive days with high wind speeds that enable daily water production to exceed demand. The tank is considered at its highest capacity in the beginning, while after its use, it is filled with the excess of the daily produced water, always to be loaded with the water requirement of the selected period according to its size.

Implementing buffer tanks will significantly reduce the required number of RO membranes and pressure containers while ensuring an adequate quantity of permeate with a safety threshold. The algorithm accounts for the inconsistency of wind speed by forcing the algorithm to select the RO size that closely tracks the water demand.

7.1. Determination of RO Size

Having formulated the Python algorithm, the site-specific input and the design parameters yield the proposed system size for Agios Efstratios. It is important to note that the following results specifically refer to the case of Agios Efstratios due to the site-specific input. However, the operating scheme explained in the previous sections generally holds and can be applied to any case study and location.

One of the interests of this thesis was to examine whether the application of DOT500 PRO could be adjusted as subject to an offshore wind profile and predetermined water demand. The first approach was to define the minimum required RO size for a coverage period of one week, meaning that the daily water production was converted to weekly and was compared to the weekly water demand of the island.

Regarding the combinations of RO sizes and spear positions, it is anticipated that the appropriate configuration will adhere to the guidelines outlined in Section 6.2. The abovementioned guidelines provide the maximum amount of water produced by each RO size while using particular spear positions. The objective of Agios Efstratios' case study is to identify the smallest RO size that can meet the demand while considering all alternatives. As a result, the most suitable setup may be suggested with a RO size that isn't operating at its maximum capacity. This may be justified if the size-preceding unit could not meet the demand at its ultimate capability for the particular wind speeds and all considered spear positions. According to the proposed operational strategy, the ultimate capacity of a RO size can be reached in combination with the spear position that drives the system to reach its hydraulic limits simultaneously; therefore, allowing for operation in the widest range of wind speeds without pitching. Figure 7-3 depicts the proposed solution in terms of water and electricity production, as well as the suitable combination of spear position and RO size.

Figure 7-3: *Production of permeate and power accompanied by the proposed RO size and spear position for a coverage period of one week.*

The proposed size of the reverse osmosis module for the weekly coverage consists of seven pressure vessels with seven membranes each. The corresponding spear position is suggested to be set at 59% of the maximum spear distance, in order to allow for the maximum water production of that unit. As can be seen, water production begins at 6.2 m/s and reaches its rated at 9.44 m/s, which indicates that the

opening of 59% of s_{max} is the ideal opening for the specific RO setup. The term 'ideal opening' refers to the spear position for which the pressure and flow limits are reached simultaneously at the highest wind speed, leading to the widest operational wind speed range without pitching for the specific RO. According to Table 6-1, for each RO size, there is only one spear position that allows for the abovementioned attainment of the limits at a maximum wind speed of 9.44 m/s, while all other spear positions dictate a lower rated wind speed. As regards the power generated by the system, there is an additional limit imposed by the nominal capacity of the generator at 200 kW. Even though the flow and pressure are allowed to increase until the wind speed reaches its rated value, the generated power has a maximum value set by the generator's capabilities. Therefore, a plateau in power is attained at 9 m/s, while permeate production keeps increasing.

Another approach would be to implement a bi-weekly comparison with the water requirements, meaning that the daily output would be converted to bi-weekly production. This is expected to reduce the number of RO vessels and membranes required to cover the demand. The following figure shows the proposed system configuration for a coverage period of two weeks, as well as its corresponding spear position.

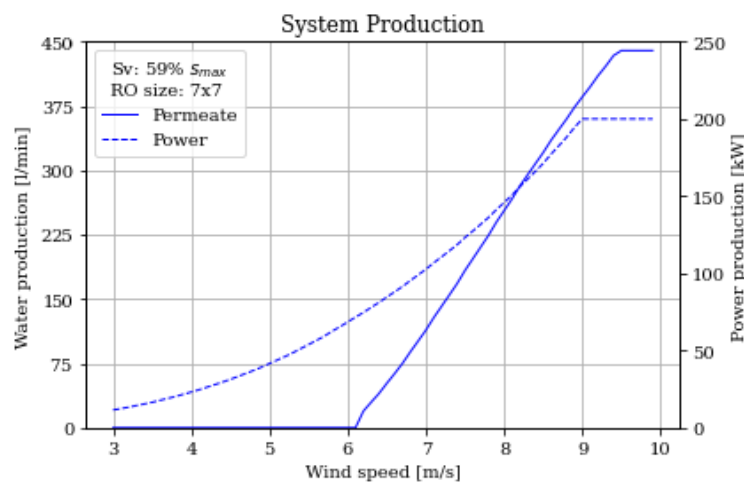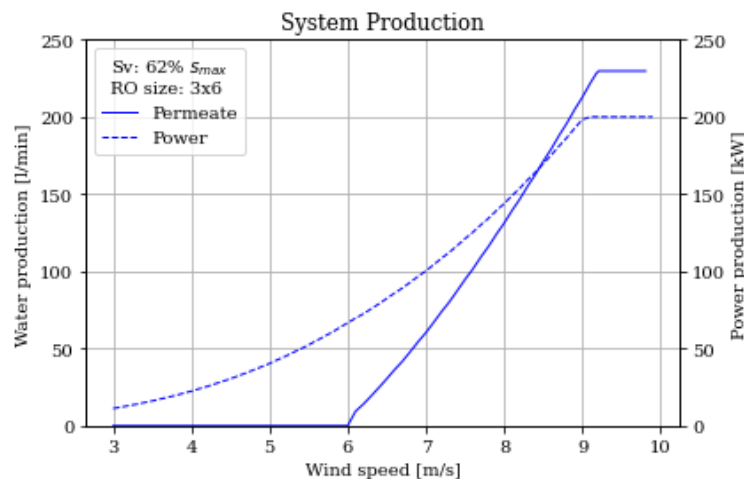*Figure 7-4: Production of permeate and power accompanied by the proposed RO size and spear position for a coverage period of two weeks.*

As evident from Figure 7-4 for a bi-weekly coverage period, the most suitable size for desalination consists of three pressure containers with six membranes each, at a spear valve position of 62% of the maximum spear distance. Water production begins at 6.1 m/s and reaches its rated conditions at 9.1 m/s, indicating that the proposed valve opening is not optimum in terms of harvesting wind speed range without pitching. By attaining lower wind than the maximum of 9.44m/s, as indicated for every RO size with their optimum corresponding spear position, it is evident that one of the two hydraulic limits is met first (see Table 6-1). The proposed spear position is above 50% of s_{max}, implying that the pressure limit is initially attained. This could be reasoned due to extended periods of below-rated wind speeds at which the required pressure had to be succeeded in order to meet the water demand. It can be concluded that for an increasing coverage period, the required RO unit reduces significantly in size, while the amount of permeate produced is a product of the RO characteristics, wind speed and pressure build-up.

7.2. Coverage Period

In order to define the appropriate RO size, several steps towards its reduction can be considered. The first step consists of the timeframe selected for the comparison between the required and the produced freshwater. Figure 7-5 presents the influence of the coverage periods between one and five weeks on the

total number of membranes of the desalination module. The total number of membranes has been produced by multiplying the number of pressure vessels by the number of membranes they contain.

Figure 7-5: Influence of coverage period on the total number of membranes of the RO unit.

As can be seen from the graph, the RO size significantly reduces with increasing coverage period while it reaches a plateau at the RO configuration of 2x6 (two pressure vessels containing six membranes each). The reduction rate is sharp as the coverage period passes from one to two weeks, due to the summation of weeks that have low permeate production owing to low wind speeds. A reduction of 67% in the tot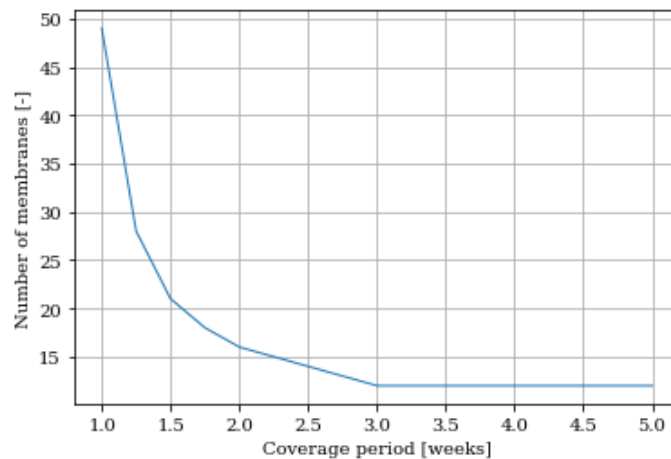al number of membranes is noted with the adoption of a bi-weekly coverage period, instead of a weekly one. The effect of accumulating the inadequate weeks – in terms of freshwater production – diminishes as more weeks are added with an increasing coverage period. This explains the gradual decrease of 25% in the RO size for coverage periods between two and three weeks, and the minimum RO size that is reached for higher coverage intervals. The specific system reduction in size and the associated values are based on the individual input of the location. The wind speed and water requirements of Agios Efstratios produced that relation between the RO size and coverage period, although in general a proximate behaviour would be expected for different comparison periods between the produced and required water from the location. Therefore, the RO size reduction rate against the coverage period is site-specific and must be determined for each research area.

7.3. Buffer Storage

Another step towards the size reduction of the desalination module is the integration of a buffer storage. The algorithm is initiated by having the buffer tank full while – in case of utilisation – filling it with the excess recorded by the site-specific wind speeds. Figure 7-6 depicts the reduction course drawn by the RO size against the coverage period in weeks for two distinct sizes of buffer storage relative to the original scenario of no buffer storage.

As expected, the implementation of buffer reservoirs contributes to the further reduction of the suitable RO unit for the location. As regards, the rising coverage periods for each system configuration, the setup integrated with a buffer of one week notes a decline of 65% in the number of membranes required. The system engaging a buffer reservoir with a capacity of two weeks presents 75% fewer membranes when examined under a bi-weekly coverage interval instead of a weekly interval.
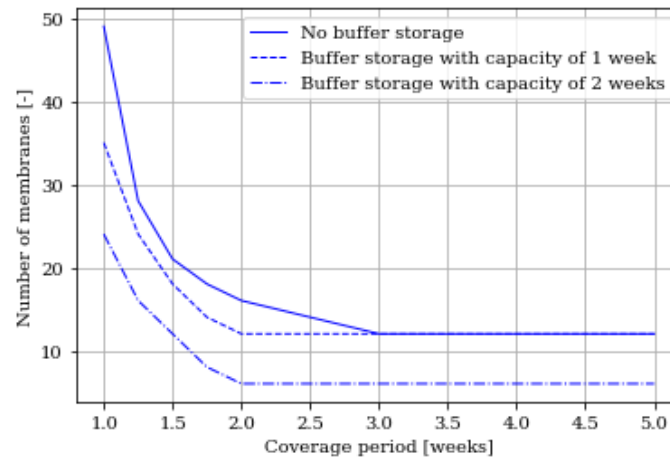
Figure 7-6: Influence of coverage period and buffer storage on the total number of membranes of the RO unit.

For the weekly coverage period, the minimum suitable size of RO reduces by 29% when a buffer reservoir with a capacity of one week is integrated, while a system with a buffer of two weeks will allow for a drop of 51% from the originally determined RO size. In the case of buffer storage with a capacity of one week, the aforementioned effect of summing the weeks with low production is recorded at the coverage period of two weeks with a minimum RO unit of 2x6 (total of twelve membranes). The coverage period of two weeks induced 25% decline in the total number of RO membranes compared to the corresponding ones for a system with no buffer storage. Additionally, is evident that by engaging a coverage period of more than two weeks, there is no benefit in the RO reduction and therefore this would be the appropriate combination of RO, buffer and collector tank sizes.

The implementation of bigger-sized buffer storage would lead to a greater decrease in the required RO unit, reaching the minimum arrangement of one pressure vessel with six membranes at a coverage period of two weeks. At that coverage period, the required RO size is lower than its respective for the case of no buffer storage, by 62.5%. As a consequence, the buffer implementation enables a significant reduction in the RO unit to the minimum setup, which would be extremely beneficial in the case of a location with a large number of citizens and extremely high freshwater demand. More specifically, this integration would allow for meeting considerable water requirements with a reasonable RO size, which would be huge in the original scenario of no buffer tank.

The capacity of the buffer storage is translated into the amount of produced freshwater that it can store. Therefore, the container with one-week capacity has the appropriate dimensions to store the amount of freshwater that covers the requirement of one week for the summer season, which is the most demanding. This corresponds to approximately 850 m^3 of storage for the buffer tank with capacity of one week. Table 7-1 presents the cumulative water demand according to every considered coverage period, which will define the size of the buffer tanks.

Table 7-1: Cumulative water demand for the touristic season for different coverage periods.

Coverage period	Summer demand [m^3/coverage period]
One week	833
Two weeks	1666
Three weeks	2499

7.4. Coverage Prediction

Having formulated the algorithm for proposing the appropriate RO size and accompanying spear valve position for the island in question, the redundancy of the proposed system has to be figured. As mentioned above, the appropriate RO covers the water requirements of all seasons with a safety threshold, to account for extreme weather events. This safety threshold is translated into the fact that the produced freshwater is constantly higher, but as proximate as possible to the water demand. Moreover, the system is examined under the wind speed of one year, which is not the case when designing for an offshore wind concept that is expected to last for approximately 25 years. Therefore, it is important to establish the rise in demand that can be handled by the system for every proposed RO size. This would provide insight into the redundancy of the system and its ability to account for future increase in population.

Table 7-2: Percentage of increase in water demand that the system is able to cover.

Coverage period	Increase in water demand [% of the original demand]
No buffer storage	
One week	18%
Two weeks	36%
Three weeks	49%
Buffer storage of one week	
One week	66%
Two weeks	68%
Three weeks	71%
Buffer storage of two weeks	
One week	70%
Two weeks	71%
Three weeks	75%

As both permanent and seasonal demands have to be covered, the one resulting in the lowest tolerance rate was considered as critical. Table 7-2 presents the percentage of increase in the original water request that each system setup can accommodate. For the system with and without a buffer storage, the ability of the system to meet additional freshwater requirements increases with increasing coverage period. As regards the case where no buffer storage is accounted for, the redundancy depends only on the effect of adding the permeate produced by inadequate weeks before distributing it to the grid. The percentage of water produced doubles as the coverage period rises by a factor of two. In the setup implementing buffer reservoirs, the percentage of increase that the system can handle is significantly higher than in the case of no buffer, while for a higher demand, this reservoir is utilized more frequently. As expected, the bigger the buffer tank, the greater the amount of permeate it can store and the highest the water requirements it can cover.

By taking into account the water equilibrium of the Greek islands, drinking water constitutes only 44% of the total water requirements [52]. Agriculture makes up 54.5%, while industry and stockraising cover the remaining 1.5%. In case the coverage of the overall water requirements of the island is of interest,

the acquired simulated daily demand would approximately double, indicating an increase of more than 100%. In that case, the newly defined water demand requires new system size estimation in order to fully satisfy the overall water consumption.

Chapter 8

Conclusions and Recommendations

The main goal of this thesis was to assist in the research regarding the possibility of producing desalinated water using a wind turbine for supplying remote areas. This was done by focusing on the production of freshwater using a 500 kW DOT hydraulic drivetrain integrated with a reverse osmosis unit combined with an energy recovery device and a Pelton turbine generator (DOT500 PRO). The study aimed to investigate and simulate the performance of the combined system for maximal production of desalted water under offshore wind conditions and predetermined demand on Agios Efstratios island. A numerical model of the system was developed to assess the implementation of the operational strategy that adjusts the spear valve and RO size for maximum water production. The ultimate goal was to apply the DOT500 PRO on Agios Efstratios island in order to cover its drinking water requirements, under constantly varying wind speeds. The proposed strategy was applied in the case study of Agios Efstratios and the most suitable system sizes were determined and discussed for their performance and expandability.

8.1. Main Conclusions

The DOT hydraulic drive train turbine connected to a RO with ERD for desalination and a Pelton turbine to generate power might be the answer for developing nations along the coast where fresh water is limited and electricity is produced using conventional methods. The steady-state simulation of the operating strategy that utilizes constant spear valve opening yields encouraging results in regulating the system under offshore wind speeds and fixed water requirements. The main research question that characterizes the thesis project was formulated in Section 1.4 as:

How can the DOT500 PRO hydraulic drive train be adjusted and operated to meet a standard water demand under the influence of an offshore wind climate?

To answer the research question, five sub-questions were formulated, which assisted in the structure and organisation of the research and are answered below:

1. *What is a simple and robust operating scheme for the system that allows for maximum water production while ensuring stable operation?*

Chapter 5 describes the existing and theoretical ideal control of the system for maximum water production by utilizing the spear valve as means of passive torque regulation. Both control strategies regulate the permeate production by opening the spear valve as soon as the rated pressure on the membranes is reached, while activating the pitch controller when the nominal flow of the high-pressure

is attained. At that time frame, two of the main system controllers are operating with the same ultimate goal of respecting the pressure and flow rate limits defined by the sub-systems. This imposes additional design requirements, as well as more constantly varying components which affects the operating guidelines and the maintenance aspects of the system.

The proposed scheme maintains the system in the stable region with as few changes in the valve position as possible to avoid the abovementioned interaction between two control systems that work for the same goal. This was achieved by confining the spear valve to a constant position. Instead of arbitrarily selecting a restricted nozzle opening for maximum water production, it was proposed to determine the valve opening for which the pressure and flow limits are reached at the same wind speed while ensuring that the turbine operates in the stable region. By doing so, the pressure limit that dictates the maximum operating point with the same valve opening is met simultaneously with the flow constraint. The reason behind the intention of attaining the system constraints at the same wind speed is that it enables the pitch controller alone to maintain constant operation without the requirement for altering the nozzle opening. Additionally, it allows for the highest rated wind speed, while also providing an expanded range of winds for which freshwater may be produced.

2.   How does the spear valve position influence the pressures and flows in the RO unit?

The spear valve opening enables for passive control of the flow and pressure in the system by regulating the counter torque that the high-pressure pump applies to the wind turbine. The operating pressure window, at which reverse osmosis can occur, can be modified by the spear valve opening that dictates the operation of the pump. For different spear valve positions, the combination of pressures and flows from the high-pressure pump produce the operational curves of the pump-nozzle scheme, which intersect with the pressure-flow curves of the wind turbine-pump sub-system, providing the functional values for each wind speed. According to the pressure and flow evolution patterns against wind speed for different valve positions, water production was evaluated in accordance with the range of wind speeds at which permeate could be produced. The combination of these parameters influences the size of the RO unit, as maximum freshwater production is the ultimate goal of this research. A medium closed valve may guarantee the highest rated wind speed and allow for the highest simultaneously occurring pressure and flow into the system, leading to high distinct permeate production. On the contrary, the closed valve (at 68% of s_{max}) allows for faster pressure build-up at lower wind speed, leading to high cumulative permeate production, although the flow into the system is below the nominal of the pump. Therefore, the spear valve position determines the required RO size that needs to be implemented in the system to reach maximum water production. It is important to note that, although the basis of determining the RO size can be limited to an extent by the spear valve opening, the interaction of both is of interest when a predetermined demand is set.

3.   What is the effect of the combinations of different spear valve positions and RO sizes on the operating conditions of the system?

For the scope of this sub-question, several RO unit sizes were examined in combination with a range of spear positions. The rated wind speed and permeate flow rates were analysed for each combination, in order to examine their effect on the system production. The examined parameters yielded the conclusion that the spear openings allowing the system to operate without pitching for the wider range of wind speeds lay between 50% and 68% of s_{max}. Each spear valve position draws a unique operating path for the different RO sizes integrated to the system, due to the different pressure level that each RO unit allows for attainment at a specific flow rate. These unique operating lines define the wind speed at which

the hydraulic boundaries are reached, limiting the system operation and determining the cumulatively produced freshwater. The wind speed at which both limits are attained simultaneously marks the highest rated wind speed of the system. The implementation of the proposed operating strategy indicated that the highest rated wind speed of the system is 9.44 m/s for all RO sizes, which is lower than the rated wind speed of the reference wind turbine by 21.3%. A conventional wind turbine provides a rated wind speed at which the rated rotational speed of the rotor is reached and the blades start pitching. In the case of a hydraulic drivetrain connection, the nominal flow rate and consequently the rotation of the pump is the limiting parameter as it is reached at a lower wind speed than that of the rotor. Therefore, the operation of the wind turbine is altered in terms of the parameter based on which the blades start pitching.

4. *How can the required RO unit size and spear valve position be obtained under a predetermined water demand and an offshore wind profile?*

The developed algorithm in Python provides the appropriate solution for the location according to the minimum amount of site-specific input data, namely the annual wind speed and seasonal freshwater requirements. One of the goals was to find the minimum RO module that allows for the coverage of specific water requirements. This can be achieved with a trial-and-error process, which calculates the water production per wind input. The wind input consists of hourly data translated to hourly produced permeate. However, offshore wind speed is characterised by periods of extreme events with high or very low wind speeds, leading to consecutive hours or days of wind speed inadequate for water production. To account for such occurrences, the daily output was converted to weekly and bi-weekly, which was then compared against the corresponding requests. This conversion can be practically understood as an intermediate tank between the reverse osmosis module and the water grid. In this tank, the daily produced permeate can be collected for a week or more before its distribution to the network. Consequently, the permeate production from each coverage period was compared to the associated freshwater demand of every season in order to define the minimum RO size that can meet the water requisition. This approach was selected due to its cost-efficiency, as the adequate desalination module can be defined with a margin of redundancy.

5. *How can the system components be adjusted in order to reduce the required number of RO pressure vessels and membranes?*

The coverage period at which the algorithm converts the daily production and demand influences the minimum appropriate RO size. The spear positioning is engaged to define the minimum RO size that can cover the demand, which has been converted to weekly or bi-weekly. As evident from the simulation of the Agios Efstratios case under the additional storage components, an increase in the coverage period from one to two weeks could lead to a reduction in the minimum required number of RO membranes by 67%. To further decrease the required RO size, a buffer storage could be implemented in the system between the RO unit and the grid. This buffer tank would save the excess produced water for a week or more to allow for a smaller desalination unit. By decreasing the RO unit, the produced permeate per wind speed declines, causing a daily deficit. However, due to the variability of offshore wind, there might be consecutive days with high wind speeds that enable daily water production to exceed demand. The excess of daily produced permeate will be presumed upon by filling the buffer storage and utilising it in the case that the system cannot cover the water requirements. Implementing a buffer tank with a capacity of one week can reduce the required number of RO membranes by up to 29%. By integrating a buffer reservoir with a two-week capacity, the original number of membranes can be limited by 50% for all coverage intervals.

The overall conclusion that can be made from this thesis is that operating the system with a constant spear valve is a promising method for the DOT500 PRO, as regards its offshore application in remote areas. The combination of a constant nozzle opening and the size of the reverse osmosis unit can be determined to meet the freshwater requirements of the examined location under offshore wind speed while ensuring that the turbine operates in a stable region. The rated wind speed of the system is lower than the one corresponding to the conventional utilisation of the reference wind turbine. However, this does not pose any concerns for locations with an average wind speed proximate to the new rated value. The created numerical model provided insight into the system behaviour at different operating conditions and allowed for the development of an effective method for the establishment of the minimum appropriate number of RO pressure vessels and membranes. Finally, further reduction of the size of the desalination unit is possible by adjusting the coverage period and implementing a buffer storage. The integration of this additional component to the system reduced the RO size to the minimum possible, indicating that the application at greater water-demanding areas is more than feasible and redundancy can be achieved by modifying the additional components.

8.2. Future Research

As in every research, there are still questions to be addressed and methods to be implemented and improved. In this section, several of these topics for further research work are mentioned and briefly analysed.

Wind turbine control strategy

Further research and improvements on the simultaneous operation of the active pitch control of the turbine and the passive control of the hydraulic system are necessary to maintain the constant operation of the system at rated conditions for a wider range of wind speeds. A solution has to be provided for both controllers to work efficiently during the same time frame and ensure the stable operation of the system. The application of the improved strategy under an offshore wind climate will assist in the effort to maximize water production in real conditions.

Expansion of the proposed operating scheme

The proposed operating scheme requires further expansion in order to cover both the water and electricity requirements of a location. By implementing power as an equally important target, the behaviour of the system under different operating conditions would provide the required control strategy. The algorithm that proposes the appropriate system size would account for both requirements and would adequately adjust the parameters, the modification of which allows for the ultimate goal achievement.

Model components' extension

Further investigation on the parameters' sizing of the existing model would lead to different results in terms of water production and suitable system setup. Several components that were assumed constant for this research could be modified in terms of size and capabilities in order to investigate the performance of the concept. These components could include the wind turbine, the high-pressure pump, the nozzle diameter and the pipelines used for the high-pressure lines. By differentiating the sizes, losses and capacities of such components, the operating points of the system would alter and the final water output would be significantly affected, leading to a completely different proposed system setup. Finally, this would be an option in case of inability to cover the demand of an examined location, for which a cost-effective and reasonable solution is desired.

Wind farm implementation

Economic viability depends on scaling up the DOT concept from a single turbine to a wind farm and optimising its design for an exact location. Additional research on different control strategies is essential to optimise the operation of individual turbines in a wind farm while accounting for wind farm effects and wind variation within the park. To examine the viability and efficiency of implementing the complete DOT500 PRO concept offshore, numerous case studies may be carried out. This would allow for research into wind farm deployment using either high-pressure flow pipes from individual turbines to the onshore water and energy production facilities or shared pipelines to the offshore RO and Pelton-generator setup. Additionally, it is possible to investigate the system configuration and location requirements above which the entire offshore installation is cost-effective and feasible. Finally, it is possible to optimise the position of the RO and Pelton scheme within the farm in order to minimise pressure losses.

Financial analysis

To expand the notion of wind-driven desalination, particularly in developing nations, the generation of energy and water must be more cost-effective than conventional methods. This thesis provided a model to calculate the suitable system configuration for water demand satisfaction while theoretically accounting for the financial aspect in terms of determining the minimum required system setup. However, it is possible to implement the site-specific revenue for different operating conditions in the algorithm and set the financial aspect as a criterion to determine an appropriate RO size. Additionally, an extensive financial model is necessary to account for capital and operating expenditures in order to establish the levelized costs of energy and water based on realistic financial factors.

Investigation on the energy consumption

The current model utilizes an energy recovery device to cover for the energy losses by the reverse osmosis module, which led to a significant reduction in the energy consumption by the unit. Further energy conservation can be achieved by implementing different types of membranes or pressure exchanger characteristics in the system. This would also influence the overpressures at the end of the RO vessels that dictate different pressure handling at the inlet of the unit in order to produce water while respecting the limits. Detailed research on the RO model could be conducted in order to determine the most effective parameters and components of the unit for all operating conditions.

Appendix

A. Principle of Reverse Osmosis

This section presents theoretical information about the Reverse Osmosis (RO) technique and its combination with an energy recovery device (ERD). The scope is to understand the working principle and constraints of a Reverse Osmosis unit, as well as the combined operation with an ERD. The elaboration on the working parameters of the desalination unit will provide insight into its operational window in order to develop a reliable and efficient system. Desalination of water is considered to be the most important technique to produce clean water from a range of sources [4]. Desalination is the process of purifying brackish or seawater to render it suitable for human consumption as well as for industrial and residential use by removing salts and minerals (contaminants). Strict government requirements on drinking water quality have forced advancements in water desalination facilities and increase in their productivity. Thermal desalination technologies based on phase change processes, such as evaporation and condensation have traditionally been employed for producing fresh water. These processes, however, have substantial startup and operating costs and are regarded as being very energy-intensive due to their intrinsic dependency on thermal energy, which is mostly obtained from fossil fuels.

Membrane-based technologies are currently regarded as the most promising and effective desalination solutions due to their high energy efficiency [4]. These procedures have the benefits of reduced space requirements, compactness of the plant, ease of process automation, and operational simplicity. In pressure-driven membrane-based procedures, salts are rejected while water molecules flow through semipermeable membranes to cleanse water. For the treatment of brackish and seawater from various sources, several different membrane-based techniques have been used. The most popular techniques among these are membrane distillation (MD), nanofiltration (NF), and reverse osmosis (RO).

Reverse osmosis is currently the most trustworthy approach for saltwater and brackish water desalination and has been employed as an alternate source for providing clean water in order to reduce desalination-related expenditures. Nowadays, RO is employed to produce around 50% of the desalinated water that is accessible worldwide. Its efficiency is determined by a variety of factors, including operational settings, membrane type, and input water qualities [48]. Osmosis is a natural process in which water molecules move through a semipermeable membrane from a solution with a low solute concentration (low osmotic pressure) to a solution with a high solute concentration (high osmotic pressure). Due to the membrane's semi-permeability, only water molecules may travel through it, rejecting all other solutes (see Figure A - 1). When the chemical potentials across the membrane are equal, the osmosis process is said to have reached an equilibrium condition.
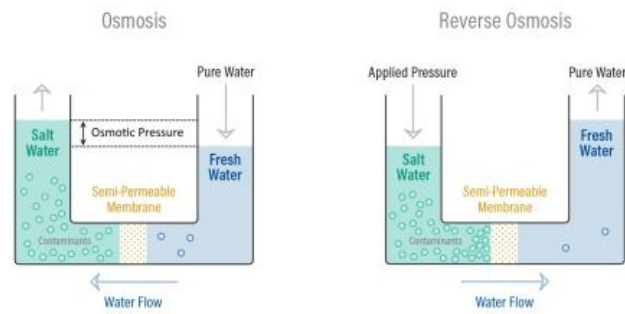
Figure A - 1: *Osmosis and reverse osmosis principle* [53].

The flow of water molecules can be halted or reversed by applying external pressure on the solution of higher concentration (feed solution). If the applied pressure difference is larger than the difference in osmotic pressure across the membrane, molecules are compelled to flow in the opposite direction from that of the natural osmosis process. Under this circumstance, the resulting process is referred to as reverse osmosis (RO). A reasonably high feed pressure is needed to overcome the feed side osmotic pressure. Typically, the range in seawater desalination is between 55 and 68 bar, while the operating pressures for the purification of brackish water are lower.

Diffusion and pore flow are the two fundamental mechanisms behind transport through membranes. The membrane pore diameter determines which of the two driving forces is more dominant [44]. Pore flow transfer is predominant in filtering techniques that use membranes with greater pore diameters, such as ultrafiltration and microfiltration. In the case of nanofiltration, pore flow and diffusion work together to convey the fluid medium through the membrane [54]. Transport across reverse osmosis membranes is entirely controlled by diffusion, due to the absence of open channels that may support pore flow [54].
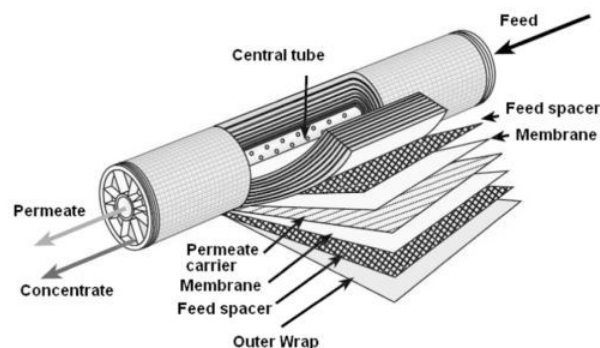
Figure A - 2: *Schematic representation of the inside configuration of a spiral wound membrane module* [55].

The polymer material employed in RO membranes allows for the rejection of particles up to 0.1 nm [53]. The typical methods for RO desalination employ crossflow filtration with spiral wound membranes. The crossflow method keeps the membrane surface free by generating enough turbulence in the flow to sweep away accumulated impurities. The semi-permeable membrane employed in the RO process is subjected to a stream of feed saltwater flowing over it at high pressures. Only fresh water may pass through the membrane, which prevents the passage of most dissolved salts, bacteria, alga, suspended particles, organic macromolecules, and pyrogens. Since its pores are smaller than one nanometre, the RO polymer filter rejects dissolved ions like Na^+ and Cl^- [53].

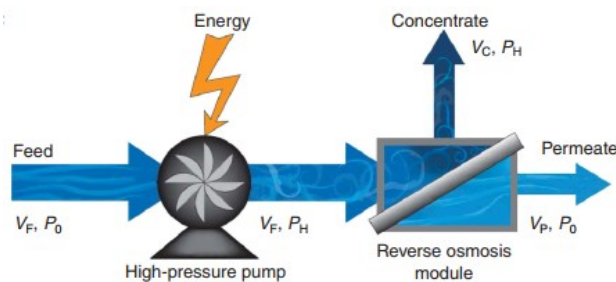***Figure A - 3:*** *Schematic diagram showing the configuration and flow streams of a reverse osmosis unit* [7]*.*

This crossflow concept, where input water is pushed over the membrane, is depicted in the previous simplified diagram. Two outflow streams are produced once the saline water has been driven through the barrier. One of them is referred to as the permeate (or freshwater stream), which has a low-pressure flow and contains very little to no pollutants and salts. The second is the reject stream, also known as the concentrate, which is a high-pressure flow that contains all impurities that failed to pass through the RO membrane. The concentrate is regarded as a desalination by-product, which can be supplied to either another desalination stage to recover the permeate even further or as an input to an isobaric pressure exchanger ERD to recover its energy [14].

A.1. Membrane Performance

The ratio of the permeate flow rate divided by the feed flow rate is known as the recovery ratio of a RO membrane. It is the percentage of feedwater that is converted to fresh water, which ranges between 35% and 85% [45]. The recovery ratio is affected by numerous aspects such as pre-treatment type, temperature, salinity and composition of input water, system operating pressure, and concentrate disposal depending on the location of the unit [56]. The performance of RO membranes is primarily determined by the kind of arrangement inside the pressure vessels: plate and frame, hollow fibre, and spiral wound, with the last being the most efficient and cost-effective. In the case of seawater reverse osmosis (SWRO), 30% to 50% of the permeate water may be extracted from the feed water [57]. Depending on the salt rejection rate of the membrane, the concentration of dissolved salts in the concentrate stream ranges from 98% to 99.8%. The quantity of salt removed from the feedwater stream is represented by the salt rejection rate, R. The amount of salt that permeates through the RO membrane and into the permeate stream is referred to as the salt passage.

To improve the recovery ratio, both the feed pressure and permeate flow rate must be increased. While permeate flow increases, permeate salinity drops owing to dilution [45]. However, this implies that the brine stream gets more concentrated, increasing the local osmotic pressure and salinity at the membrane surface, which can increase salt precipitation and fouling, leading to a degradation in membrane performance. Crossflow filtering enables water to wash away accumulated impurities to prevent their development. Moreover, it permits enough turbulence to maintain a clean membrane surface. The salt permeability is also affected by the temperature of the input water [51]. At temperatures below 30°C, increasing the temperature of the feed water leads to a lower feed pressure required to run the system. Nevertheless, further temperature rise causes a rise in osmotic pressure, which might impact the RO system's power requirements [51].

A.2. Energy Recovery Device (ERD)

As mentioned before, the concentrate flow can either be fed to an additional reverse osmosis unit or to a device that can extract its energy. One of the reasons RO systems have grown more efficient is the use

of Energy Recovery Devices (ERD) in the desalination process [45]. Depending on the ERD type utilized, a system's power consumption per generated volume of permeate – and hence expenses – can be reduced by up to 60% [58]. Energy recovery from the high-pressure concentrate stream is the fundamental tenet of an ERD [45]. The pressure in the concentrate stream will be almost as high as the intake pressure since there is still potential energy stored in this stream. A typical pressure drop through the RO membranes (pressure differential between the feed stream and the concentrate stream) is in the order of a few bar [58]. The Pressure Exchanger Energy Recovery Device, commonly known as PX or Isobaric ERD, is currently the most effective and extensively used ERD, which transfers the hydraulic energy using a spinning piston, as shown in Figure A - 4.
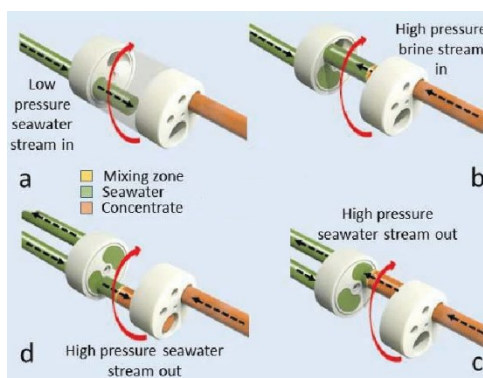

Figure A - 4: Schematic of pressure exchanger operation in steps [59].

The working principle of the Pressure Exchanger ERD is as follows:

1. The rotor cylinder (indicated in white) rotates in the direction depicted by the red arrow, with the use of an electric motor. The ideal situation dictates the adjustment of the rotor's rotational speed according to the concentrate flow. However, in the DOT500 PRO, the rotational speed of the ERD is kept constant throughout the whole operation, providing an additional fixed amount of water to the RO unit. While rotating, two flows enter the cylinder chambers, with the first being the low-pressure seawater provided by the boost pump and the second being the high-pressurized concentrate flow from the RO. An excess of seawater is fed into the ERD to ensure that the chambers are fully cleared from the brine flow [45].

2. While rotating, when the chamber containing seawater reaches the line carrying the brine, seawater is pushed out of the chamber due to the high pressure in the concentrate flow. As a result, the low-pressure seawater feed from the boost pump becomes a high-pressure feed to the RO unit (Steps b and c in Figure A - 4).

3. When the feed water is pushed out of the ERD, the chambers contain only low-pressure concentrate flow (Step d). Then the cycle repeats by pumping water from the boost pump to the rotor chambers.

Given the lack of a physical barrier separating the feed water and concentrate, a little portion of the concentrate will inevitably mix with the feed water, slightly raising the salt content of the high-pressure feed water stream. By supplying more saltwater than concentrate water, this mixing can be adequately addressed [45]. The proportion of the device's total energy output to its total energy intake is considered to represent the total efficiency. Depending on the rotor's length and concentrate flow rate, the rotational speed can reach up to 1500 rounds per minute (RPM).

As pressure exchanger ERDs are most effective when utilized in high-concentration flows, medium to large-scale desalination facilities often employ them. Nowadays, however, a growing number of small-scale PX ERDs are being created, allowing them to compete in small-scale operations, for instance, with

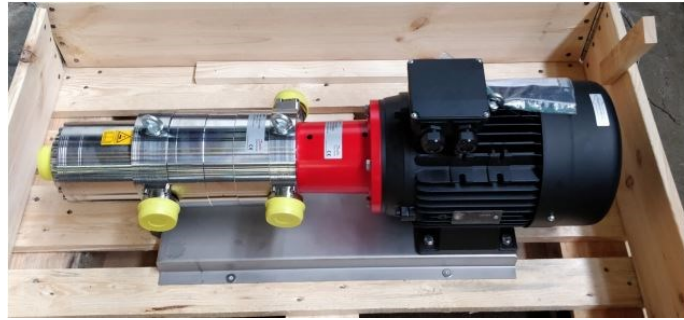turbocharger ERDs [57]. The DOT500 PRO concept employs the Danfoss iSave 21 Plus Energy Recovery Device.

Figure A - 5: *Danfoss iSave 21 Plus Energy Recovery Device used by DOT B.V. in DOT500 PRO* [45].

Hydraulic losses are the most crucial factor to consider when employing a pressure exchanger as an ERD since they have an impact on efficiency. Mixing, leakage, overflush, and differential head are some of these losses [16]. A brief explanation is provided for each loss below:

1. *Mixing*: Before the saltwater reaches the membranes, the concentrate stream taints the high-pressure feed seawater. Given that the concentration of the input water and osmotic pressure both rise with a faster mixing rate, the power consumption of the unit increases accordingly. A typical mixing rate is lower than 2.5%.

2. *Leakage*: It refers to the immediate release of high-pressure concentrate into the low-pressure concentrate stream. To compensate, the high-pressure pump must generate a higher flow, causing the RO to consume more power. A normal leakage rate is in the range of 1%.

3. *Overflush*: The seawater feed stream is immediately discharged from the low-pressure feed line to the low-pressure concentrate line. This is mostly done to remove the residual brine from the ERD before refilling it with feed water.

4. *Differential head*: A pressure drop between the feed and the reject stream causes a high-pressure differential, that the high-pressure pump must consider. There may be effects from this differential head on both the high- and low-pressure sides. When there is an excessive pressure gap between the brine outflow and feed input, a low-pressure differential occurs. As a result of the necessity to produce a higher pressure in this case, the feed pump will use more energy.

B. Operating Flows and Pressures

B.1.   Spear Positioning

According to the examined operating strategy, each spear valve opening indicates a unique operating curve for every RO unit implemented to the DOT500. This translates into various, distinct pairs of system pressures and flows developed by each wind speed for every parameter combination. These sets of operating values dictate the wind speed at which the hydraulic limits are reached, which is defined as the rated wind speed of the system. The following table presents the spear valve opening and the associated wind speeds that reach the hydraulic limits for the case of a 6x6 RO unit. The permeate production reached at each rated point is presented to support the claim of Table 6-1, at which the ideal valve opening for the specific RO size was detected.

Table B - 1: Wind speeds at which the hydraulic limits are reached for specific valve openings, as well as the corresponding rated permeate production (6x6 RO unit).

Spear valve opening [% of s_{max}]	Wind speed at which the RO rated pressure is reached [m/s]	Wind speed at which the nominal HPP flow is reached [m/s]	Pressure at rated conditions [bar]	Flow from the HPP at rated conditions [l/min]	Permeate production at rated conditions [l/min]
s = 0%	10.62	7.61	38.54	2394.09	54.55
s = 20%	10.50	7.96	41.26	2393.82	78.73
s = 40%	9.94	8.45	51.178	2394.01	190.51
s = 50%	9.71	8.80	57.59	2393.42	270.71
s = 52%	9.67	8.92	58.54	2394.48	340.84
s = 54%	9.63	9.03	60.58	2393.59	398.37
s = 56%	9.56	9.15	63.88	2394.47	410.68
s = 58%	***9.44***	***9.44***	***69.98***	***2394.10***	***432.17***
s = 60%	9.35	9.49	70.00	2388.73	432.95
s = 62%	9.33	9.61	70.00	2385.78	433.24
s = 64%	9.30	9.79	70.00	2302.73	433.99
s = 66%	9.29	10.33	70.00	2216.38	434.01
s = 68%	9.25	10.62	70.00	2127.71	434.32

As can be seen, for the specific RO setup (6x6), the valve opening of 58% of s_{max} provides the highest rated wind speed, as this is defined as the lowest at which one of the two hydraulic limits is reached. The permeate production for valve positioning above 58% of s_{max} is almost constant, as it is a function of the inlet pressure which is equal to the rated. Therefore, the combination of 6 pressure vessels containing six membranes with the 58% spear opening allows for the highest freshwater production and the wider range of wind speeds captured by the system. The negligible deviations from the nominal flow of 2394 l/min is owned to the discrete values of wind speed simulated which produced discrete sets of pressure and flow of the system.

B.2.   Flow to the Sub-systems

Following, the flow rate driven to the RO unit (6x6) is presented for different wind speeds and spear valve positions. As evident, the flow entering the RO unit follows the pattern of pressure under every specific valve opening (see Figure 6-1). As the valve travels towards the closed position at 68% of s_{max}, the pump provides higher pressure to the system, which in turn generates higher permeate production. According to Equation (4.18), permeate is a function of the inlet pressure, as well as the membranes' characteristics, and is considered equal to the flow driven from the high-pressure pump to the RO due to the existence of the ERD (see Equation 5.24). Water production is possible above 6m/s for the whole range of examined spear valve positions.
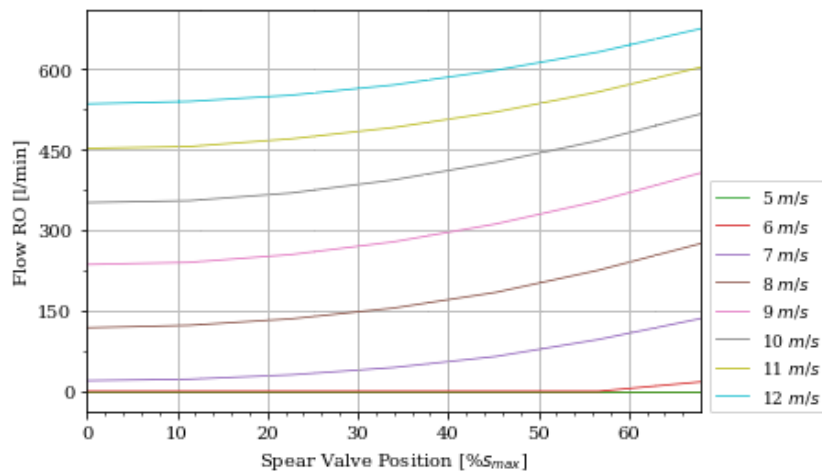

Figure B - 1: Flow through the RO unit for different wind speeds and spear valve positions.

References

[1] "Freshwater crisis. Competing for water has led to a clean water crisis.," 2020. https://www.nationalgeographic.com/environment/article/freshwater-crisis.

[2] A. Boretti and L. Rosa, "Reassessing the projections of the World Water Development Report," *npj Clean Water*, vol. 2, no. 1, p. 15, Dec. 2019, doi: 10.1038/s41545-019-0039-9.

[3] J. Eke, A. Yusuf, A. Giwa, and A. Sodiq, "The global status of desalination: An assessment of current desalination technologies, plants and capacity," *Desalination*, no. March, 2020, doi: 10.1016/j.desal.2020.114633.

[4] M. Qasim, M. Badrelzaman, N. N. Darwish, N. A. Darwish, and N. Hilal, "Reverse osmosis desalination: A state-of-the-art review," *Desalination*, no. February, 2019, doi: 10.1016/j.desal.2019.02.008.

[5] J. Kim, K. Park, D. R. Yang, and S. Hong, "A comprehensive review of energy consumption of seawater reverse osmosis desalination plants," *Appl. Energy*, no. July, 2019, doi: 10.1016/j.apenergy.2019.113652.

[6] D. Akgul, M. Çakmakci, N. Kayaalp, and I. Koyuncu, "Cost analysis of seawater desalination with reverse osmosis in Turkey," *Desalination*, Mar. 2008, doi: 10.1016/J.DESAL.2007.01.027.

[7] M. Elimelech and W. A. Phillip, "The future of seawater desalination: Energy, technology, and the environment," *Science (80-.).*, 2011, doi: 10.1126/science.1200488.

[8] E. Mathioulakis, V. Belessiotis, and E. Delyannis, "Desalination by using alternative energy : Review and state-of-the-art," no. May 2006, 2007, doi: 10.1016/j.desal.2006.03.531.

[9] F. Moreno and A. Pinilla, "Preliminary experimental study of a small reverse osmosis wind-powered desalination plant," *Desalination*, 2005, doi: 10.1016/j.desal.2004.06.191.

[10] F. Greco, S. G. J. Heijman, and A. Jarquin-Laguna, "Integration of Wind Energy and Desalination Systems: A Review Study," *Processes*, Dec. 2021, doi: 10.3390/pr9122181.

[11] N. F. B. Diepeveen, A. J. Laguna, and A. S. Kempenaar, "Water-Hydraulic Power Transmission for Offshore Wind Farms," *Dutch Fluid Power Conf.*, 2012.

[12] S. Paul Mulders, N. Frederik Boudewijn Diepeveen, and J. W. Van Wingerden, "Control design, implementation, and evaluation for an in-field 500 kW wind turbine with a fixed-displacement hydraulic drivetrain," *Wind Energy Sci.*, 2018, doi: 10.5194/wes-3-615-2018.

[13] N. F. B. Diepeveen, "On the Application of Fluid Power Transmission in Offshore Wind Turbines door," 2013.

[14] A. I. Goveas, "Simulation of a Wind Powered Freshwater and Electricity Production System. Numerical Modeling and Optimization," Master Thesis, Delft University of Technology, Sustainable Energy Technology, 2020.

[15] S. Wild, "Water in a loop: how to combat water scarcity on remote islands," 2022. https://ec.europa.eu/research-and-innovation/en/horizon-magazine/water-loop-how-combat-water-scarcity-remote-islands.

[16]   P. Triantafyllou *et al.*, "Optimum green energy solution to address the remote islands' water-energy nexus: the case study of Nisyros island," *Heliyon*, Sep. 2021, doi: 10.1016/J.HELIYON.2021.E07838.

[17]   P. Daskalaki and K. Voudouris, "Groundwater quality of porous aquifers in Greece: a synoptic review," *Environ. Geol.*, Apr. 2008, doi: 10.1007/s00254-007-0843-2.

[18]   J. K. Kaldellis, K. A. Kavadias, and E. Kondili, "Renewable energy desalination plants for the Greek islands—technical and economic considerations," *Desalination*, Oct. 2004, doi: 10.1016/J.DESAL.2004.01.005.

[19]   L. García-Rodríguez, V. Romero-Ternero, and C. Gómez-Camacho, "Economic analysis of wind-powered desalination," *Desalination*, May 2001, doi: 10.1016/S0011-9164(01)00235-1.

[20]   A. Al-Karaghouli and L. L. Kazmerski, "Energy consumption and water production cost of conventional and renewable-energy-powered desalination processes," *Renew. Sustain. Energy Rev.*, Aug. 2013, doi: 10.1016/J.RSER.2012.12.064.

[21]   O. Aristeidou, "How Greece is embracing offshore wind energy with EBRD support," *European Bank for Reconstruction and Development*, 2022. https://www.ebrd.com/news/2022/how-greece-is-embracing-offshore-wind-energy-with-ebrd-support.html#:~:text=Greece's National Energy and Climate,wind capacity by that time.

[22]   Wind Europe, "First Greek Offshore Wind Law seeks 2 GW by 2030," 2022. https://windeurope.org/newsroom/news/first-greek-offshore-wind-law-seeks-2-gw-by-2030/.

[23]   S. Spyridonidou, D. G. Vagiona, and E. Loukogeorgaki, "Strategic planning of offshore wind farms in Greece," *Sustain.*, 2020, doi: 10.3390/su12030905.

[24]   H. Republic, "National Operational Plan for Drinking Water," 2022.

[25]   Hellenic Statistical Authority, "Provisional Results of the Census of Housing for 2021," 2021.

[26]   D. Xevgenos, A. Vidalis, K. Moustakas, D. Malamis, and M. Loizidou, "Sustainable management of brine effluent from desalination plants: the SOL-BRINE system," *Desalin. Water Treat.*, 2015, doi: 10.1080/19443994.2014.933621.

[27]   F. Greco, D. De Bruycker, A. Velez-Isaza, N. F. B. Diepeveen, and A. Jarquin-Laguna, "Preliminary design of a hydraulic wind turbine drive train for integrated electricity production and seawater desalination," *J. Phys. Conf. Ser.*, 2020, doi: 10.1088/1742-6596/1618/3/032015.

[28]   "ERA5 hourly data on single levels from 1959 to present." https://cds.climate.copernicus.eu/cdsapp#!/dataset/reanalysis-era5-single-levels?tab=overview.

[29]   C. Jung and D. Schindler, "The role of the power law exponent in wind energy assessment: A global analysis," *Int. J. Energy Res.*, 2021, doi: 10.1002/er.6382.

[30]   TERNA ENERGY and GEK TERNA GROUP, "RENEWABLE ENERGY SOURCES: AI STRATIS ISLAND BECOMES ENERGY-AUTONOMOUS," 2023. https://www.terna-energy.com/restories-en/renewable-energy-sources-ai-stratis-island-becomes-energy-autonomous/.

[31]   FREEWORLDMAP, "GREECE PHYSICAL MAP." https://www.freeworldmaps.net/europe/greece/map.html.

[32]   V. Stergiopoulos, "The Good Life," *In.gr*, 2019. https://www.in.gr/2019/05/07/life/diakopes/idees-gia-taksidia/agios-eystratios-mia-plori-kontra-sto-voria-tou-aigaiou/.

[33]   A. Jarquin-Laguna, N. F. B. Diepeveen, and J. W. Van Wingerden, "Analysis of dynamics of fluid

power drive-trains for variable speed wind turbines: Parameter study," *IET Renew. Power Gener.*, 2014, doi: 10.1049/iet-rpg.2013.0134.

[34] S. P. Mulders, S. M. Jager, N. F. B. Diepeveen, and J. W. V. Wingerden, "Control design for the DOT500 hydraulic wind turbine," DOT B.V., 2017. [Online]. Available: http://resolver.tudelft.nl/uuid:594f9180-ad47-4c7e-b0e8-e8686677afeb.

[35] J. Nijssen, A. Kempenaar, and N. F. B. Diepeveen, "Development of an interface between a plunger and an eccentric running track for a low- speed seawater pump," 2018, doi: 10.18154/RWTH-2018-224521.

[36] N. F. . Diepeveen, "On the Application of Fluid Power Transmission in Offshore Wind Turbines door," 2013.

[37] Y. Xiao, Y. Li, and M. A. Rotera, "Experimental Evaluation of Extremum Seeking Based Region-2 Controller for CART3 Wind Turbine," San Diego, California, USA, 2016. doi: 10.2514/6.2016-1737.

[38] N. F. . Diepeveen and A. Jarquin-Laguna, "Wind tunnel experiments to prove a hydraulic passive torque control concept for variable speed wind turbines," no. Journal of Physics: Conference Series 555 (2014) 012028, p. 12, 2014, doi: 10.1088/1742-6596/555/1/012028.

[39] A. Jarquin Laguna, "Centralized electricity generation in offshore wind farms using hydraulic networks," 2017. doi: 10.4233/uuid:9a8812d1-d152-4a68-bd17-c88261f06481.

[40] N. F. . Diepeveen and A. Jarquin-Laguna, "Wind tunnel experiments to prove a hydraulic passive torque control concept for variable speed wind turbines," no. Journal of Physics: Conference Series 555 (2014) 012028, 2014, doi: 10.1088/1742-6596/555/1/012028.

[41] M. F. Supper, "Desalination Module part 1 : Reverse Osmosis model," 2016.

[42] W. Lai, Q. Ma, H. Lu, S. Weng, J. Fan, and H. Fang, "Effects of wind intermittence and fluctuation on reverse osmosis desalination process and solution strategies," *Desalination*, 2016, doi: 10.1016/J.DESAL.2016.05.019.

[43] F. J. García Latorre, S. O. Pérez Báez, and A. Gómez Gotor, "Energy performance of a reverse osmosis desalination plant operating with variable pressure and flow," *Desalination*, Jun. 2015, doi: 10.1016/J.DESAL.2015.02.039.

[44] M. F. Supper, "Fluctuating Flows on Reverse Osmosis Membranes: An Experimental Approach for Hydraulic Drive Train Wind Turbine Applications," Master Thesis, Delft University of Technology, Faculty of Mechanical, Maritime and Materials Engineering (3mE), 2017.

[45] R. A. G. Smits, "Analysis of a Wind Driven Reverse Osmosis Desalination System - Experimental Study Using a Pressure Exchanger Energy Recovery Device," Master Thesis, Delft University of Technology, 2019.

[46] Flowserve, "Flowserve FLEX™ Isobaric Energy Recovery Device." https://www.flowserve.com/en/products/products-catalog/energy-recovery-devices/isobaric-devices/flowserve-flextm-isobaric-energy-recovery-device/.

[47] D. van Hanswijk, "Learning-Based Model Predictive Control for a Wind-Powered Fresh Water Production Plant with Integrated Electricity Production," Master Thesis, Delft University of Technology, 2021.

[48] C. Fritzmann, J. Löwenberg, T. Wintgens, and T. Melin, "State-of-the-art of reverse osmosis desalination," *Desalination*, Oct. 2007, doi: 10.1016/J.DESAL.2006.12.009.

[49] A. R. Bartman, P. D. Christofides, and Y. Cohen, "Nonlinear Model-Based Control of an Experimental Reverse Osmosis Water Desalination System," *IFAC Proc. Vol.*, vol. 42, no. 11, pp.

892–897, Jan. 2009, doi: 10.3182/20090712-4-TR-2008.00146.

[50] D. Darling, "Pelton Turbine, David Darling Encyclopedias," *David Darling Encyclopedias*, 2016. https://www.daviddarling.info/encyclopedia/P/AE_Pelton_turbine.html.

[51] R. Bergman, *Reverse Osmosis and nanofiltration*. American Water Works Association, 2007.

[52] K. Kouloupsouzis, "Water resources in the Aegean islands: Current situation and evaluation of alternative methods of water supply," Athens, 2018.

[53] PURETEC Industrial Water, "What is Reverse Osmosis?," 2023. https://puretecwater.com/reverse-osmosis/what-is-reverse-osmosis.

[54] J. G. Wijmans and R. W. Baker, "The solution-diffusion model: a review," *J. Memb. Sci.*, 1995, doi: 10.1016/S0166-4115(08)60038-2.

[55] S. M. F. Hasani, A. S. Sowayan, and M. Shakaib, "The Effect of Spacer Orientations on Temperature Polarization in a Direct Contact Membrane Distillation Process Using 3-d CFD Modeling," *Arab. J. Sci. Eng.*, vol. 44, no. 12, pp. 10269–10284, 2019, doi: 10.1007/s13369-019-04089-x.

[56] VEOLIA Water Technologies and Solutions, "Spiral Wound Membrans," [Online]. Available: https://www.watertechnologies.com/products/spiral-wound-membranes.

[57] Y. Wang, S. Wang, and S. Xu, "Experimental studies on dynamic process of energy recovery device for RO desalination plants," *Desalination*, 2004, doi: 10.1016/S0011-9164(04)90008-2.

[58] Lenntech B.V., "Reverse Osmosis Desalination Process," 2017. https://www.lenntech.com/processes/desalination/reverse-osmosis/general/reverse-osmosis-desalination-process.htm.

[59] A. Jarquin-Laguna and F. Greco, "Integration of hydraulic wind turbines for seawater reverse osmosis desalination," *2019 Offshore Energy Storage Summit, OSES 2019*, 2019, doi: 10.1109/OSES.2019.8867343.